Université Mohamed Boudiaf - M'sila

FACULTE DE TECHNOLOGIE

DEPARTEMENT DE GENIE MECANIQUE

Numéro de série……

Numéro d'inscription : D. EN/3C/02/17

Thèse

Présentée pour l'obtention du diplôme de

DOCTORAT LMD

Filière : GENIE MECANIQUE

Spécialité : Energétique

THEME

Contribution à l'étude de la thermique des bâtiments en Algérie

Présentée Par
HADJI Feres

Soutenue le: 19/06/2023

Devant le jury composé de :

Nom & Prénom	Grade	Etablissement	Qualité
BENARIOUA Younes	**Professeur**	Univ. de **M'sila**	Président
IHADDADENE Nabila	**Professeur**	Univ. de **M'sila**	Encadreur
BELGHAR Nour Eddine	**Professeur**	Univ. de **Biskra**	Co-Encadreur
BEGHIDJA Abed El Kader	**Professeur**	Univ. **de Constantine**	Examinateur
BENDERADJI Razik	**Professeur**	Univ. de **M'sila**	Examinateur
ZERGANE Said	**MCA**	Univ. de **M'sila**	Examinateur
BENDERADJI Razik	**MCA**	Univ. de **M'sila**	Examinateur

Année Universitaire : 2021/2022

TITLE

Thermal conductivity of two kinds of earthen building materials formerly used in Algeria

F Hadji, N Ihaddadene, R Ihaddadene, A Betga, A Charick, PO Logerais

Journal of Building Engineering 32, 101823

Solar Energy in M'Sila (Algerian Province)

F Hadji, N Ihaddadene, R Ihaddadene, Y Kherbiche, M Mostefaoui, ...

2018 6th International Renewable and Sustainable Energy Conference (IRSEC), 1-5

Effect of building materials on temperature evolution inside the premises in Algeria

F Hadji, N Ihaddadene, R Ihaddadene, M Choudira, A Hami, M Bekkari

CHAPTER EIGHT THE EFFECT OF VARYING THE DISTANCE BETWEEN THE DOUBLE-GLAZING OF A SOLAR THERMAL COLLECTOR ON ITS FUNCTIONING

N IHADDADENE, R IHADDADENE, F HADJI

Advances in Renewable Energies and Power Quality 113

Solar Energy Potential Evaluation. Case of Study: M'Sila, an Algerian Province

Y Kherbiche, N Ihaddadene, R Ihaddadene, F Hadji, J Mohamed, A Hadi

Planning 16 (8), 1501-1508

Acknowledgements

First of all, I thank Allah, the Almighty, for giving me the strength to continue and complete this modest work, as well as the courage to overcome all difficulties. The work presented in this thesis was carried out under the supervision of ***Mrs. IHADDADENE Nabila, professor in the Department of Mechanical Engineering at the University of M'sila*** *My deepest gratitude goes to my supervisor for her availability and the trust she placed in me. I have benefited greatly from the knowledge and expertise gained through numerous discussions. I would also like to thank her for the autonomy he granted me and his valuable advice that allowed me to successfully complete this work.*

I express my sincere appreciation to ***Mr. BENARIOUA Younes, professor in the Department of Mechanical Engineering at the University of M'sila****, for kindly agreeing to chair the jury of this thesis.* May ***Mr. BEGHIDJA Abed Elhadi, professor at the University of Constantine****, find here my heartfelt thanks for agreeing to evaluate this work. May* ***Mr. BENDERADJI Razik and Mr. ZERGANE Said, lecturers at the University of M'sila****, find here my heartfelt thanks for agreeing to evaluate this work*

I would like to thank my small family. My parent, for their unlimited support and encouragement during these long years of study. I would like to express my deep gratitude to them. In order not to forget anyone, my heartfelt thanks go to all those who helped me in the realization of this modest thesis.

Tables of content

Table des matières

List of Figures and Tables

List of Figures

Lists of tables

Notations

D : Equivalent diameter

p : Percentage (relative to the mass of the test portion in the dry state) of particles with a diameter less than or equal to D

Vs: The volume of the suspension

m : The mass of dry soil taken from the sieve at 80m

ρs: The density of solid particles

ρw : The density of the distilled water at the test temperature conventionally

ρ: The density of the suspension at time t_t

$R c$: The corrected reading of the densimeter at time t

R : Reading of the hydrometer (top of the meniscus) at time t

$C t$: The correction due to temperature variations during the test

$C m$: The correction due to the meniscus

$C d$: The correction due to the deflocculant

g : The acceleration of gravity

μ: The dynamic viscosity of the solution at time t

H_t : Effective depth of push center at time t

t : Time

H_c : Displacement height of the solution due to the densimeter

V_d : The volume of the densimeter

A : The cross-sectional area of the test specimen

α : Constant is equal to 0.003368

β : Constant is equal to 0.00022

θ : The temperature expressed in degrees Celsius of the control specimen at time t

H : The distance separates the middle of the bulb of the densimeter

H_1 : The distance separating graduation 1 from graduation 1.010

W : The water content in %

m_d : The dry weight of the sample

M_w : The wet weight of the sample

V_s : The volume of the sample

m_2 : Waxed sample weight

m_1 : Wet weight of the

m_3 : Submerged weighing

ρ_{wax} : Density of paraffin (in

Introduction

Introdution

A building is a closed structure of various shapes and sizes, comprising a roof and walls that create a comfortable environment for living and working. However, this comfort often comes at the expense of excessive energy consumption, making the construction industry one of the most energy-intensive sectors globally. In fact, energy consumption in most countries is estimated to range between 25% and 40% of primary energy resources[1-4].

A significant portion of the energy used in buildings is dedicated to maintaining a comfortable indoor environment, which includes heating in the winter and cooling in the summer[5]. This is crucial for safeguarding occupants' health and enhancing their productivity[6]. In Algeria, the construction sector is responsible for 34% of the country's total final energy consumption, making it the largest electricity consumer. According to the National Agency for the Promotion and Rationalization of Energy Use, the average annual energy consumption of a house in Algeria from 2000 to 2012 was approximately 54.55 GJ[7]. This figure is projected to rise as the construction industry grows and living standards improve, as demonstrated by M'Sila, where electricity consumption in the building sector tripled between 2006 and 2018, marking an increase of 200%.

Moreover, the building sector's reliance on conventional energy sources during construction, use, and dismantling significantly contributes to environmental pollution through greenhouse gas (GHG) emissions, particularly CO2[8-9]. The construction industry is responsible for 23% to 40% of global GHG emissions[10-11], with Algeria accounting for 31% of the country's emissions. In 2004, CO2 emissions from the construction industry were estimated at 6.8 billion tons, and according to the International Panel on Climate Change, this number could rise to 15.6 billion tons by 2030[12-14].These greenhouse gases are crucial contributors to recent global warming, posing threats to life on Earth. If measures to mitigate these emissions are not implemented, the average Earth's surface temperature is predicted to increase by 1.1 to 6.4 degrees Celsius by the end of 2100[15].

Notably, the Swedish scientist Arrhenius first predicted in 1896 that industrial emissions would lead to global warming. Given these facts, the building sector bears significant responsibility for energy and environmental challenges. Thus, it is crucial to reduce energy consumption in buildings, adopting energy-efficient practices as a global policy aimed at ensuring a sustainable future.

There are various strategies available to decrease energy consumption in buildings, including the integration of renewable energies, emissions control, and improvements in energy efficiency. Thermodynamically, a building operates as an open system, exchanging heat and matter (including air and greenhouse gases) with its environment. Heat energy is absorbed during summer months and lost in the winter across the building's envelope due to temperature discrepancies between indoor and outdoor conditions.

Therefore, an energy-efficient building must minimize heat exchanges to reduce the energy required for maintaining comfortable indoor conditions. The exterior walls, which represent the largest heat exchange surface area, play a critical role in heat loss or gain[16]. Enhancing their thermal performance is one of the technical solutions aimed at reducing overall building energy consumption[17].

Additionally, utilizing solar energy through both passive and active methods presents another viable solution [18], which this study aims to explore in depth. The thesis is structured into three chapters: the first chapter introduces concepts related to solar energy and construction materials; the second chapter details the materials and methods employed; and the final chapter presents and discusses the results obtained. The study concludes with a general summary of the findings and their implications.

Chapter I

Building and Solar Energy

I.1 Introduction

In this chapter, we will present comprehensive definitions and explanations related to solar energy, drawing upon a variety of sources from the existing literature. We will explore fundamental concepts such as the nature of the Sun, its movements, and the various angles of solar radiation that impact energy collection. Additionally, we will delve into the intricate relationship between solar energy and building design, examining aspects such as passive and active solar techniques, the orientation of structures, and the role of solar energy in enhancing energy efficiency. By synthesizing this information, we aim to provide a thorough understanding of how solar energy can be effectively harnessed within the built environment, ultimately contributing to sustainable architectural practices

I.2 Building:

A common-sense building is a construction intended to serve as a shelter or habitat and to protect property and persons from outdoor weather conditions. This building construction is carried out by human intervention. Legally, the term “building” generally refers to build construction, whereas the adjective “building” refers to assets that cannot be moved, whether they are building or land.

Buildings are still the largest energy consumers, consuming 30% to 40% of primary energy in most countries [7]. This energy is intended primarily for the following purposes:

- Heating and/or cooling, to ensure an indoor climate comfortable,
- Circulation of fluids such as air (ventilation), water (hot water, heating),
- Transportation (elevators),
- The lighting,
- Communications (telephone, radio, television),
- The production of goods (factories, kitchens, sewing, etc.).

Algeria’s residential sector accounts for 35% of energy consumption final. The evolution of its energy consumption is in continuous increase, due to even the pace of growth in housing stock and household equipment rates in particular, electrical household appliances and heating air conditioning [20].

I.3 Energy consumption

I.3.1 Consumption of natural gas by sector

The graph below shows Natural gas total final consumption by sector from 1973 to 2019. While the industry sector consumption showed a slow and steady increase from during this time, the same cannot be said for the other especially residential sector .

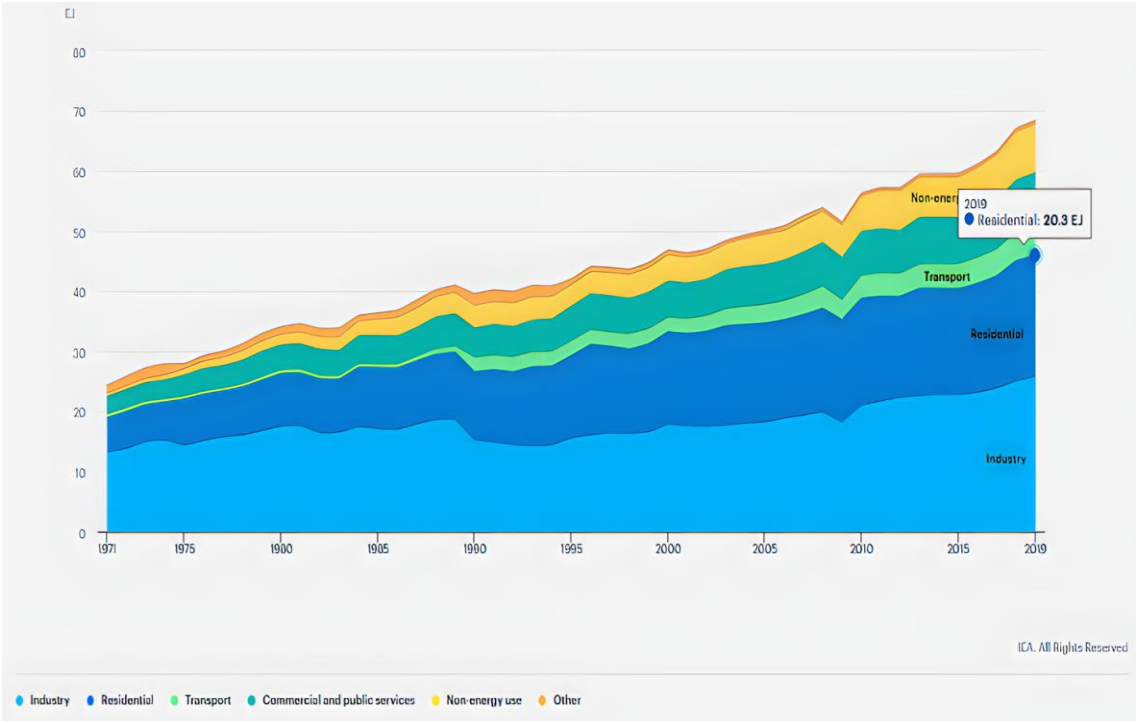

Figure I.1: Natural gas total final consumption by sector, 1971-2019 IEA

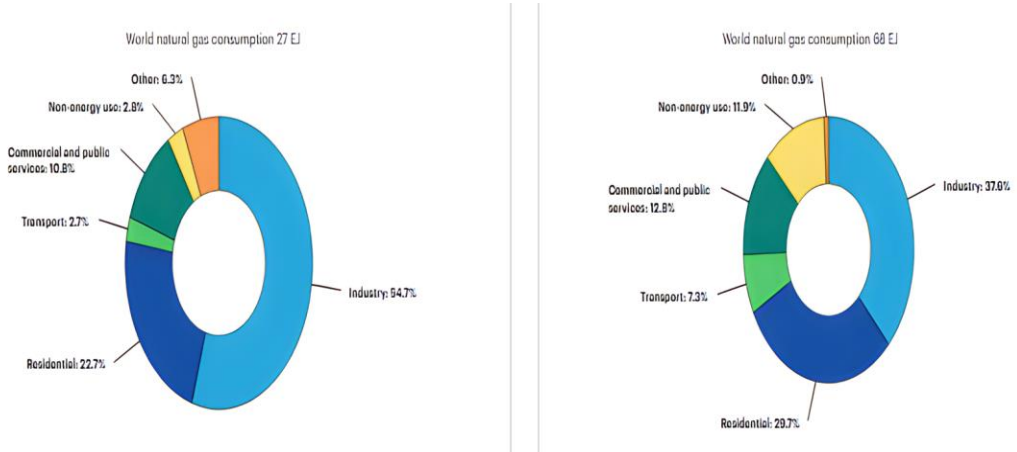

Figure I.2: Share of natural gas final consumption by sector, 1973left and 2019 right IEA

The two pie charts compare the percentages of share of natural gas final consumptions by sector in the world in the years 1973 and 2019. For six of the sectors, it is evident that over this time frame there was significant change in their proportion of energy consumption

At 54.7% we can see that industry sector accounted for the majority of consumption in 1973, but this percentage had dropped to 37.6% by 2019. During the same forty-six-year period, as an increasing number of consumptions of residential sector, we can see that transactions went from just 22.7% to 29.7%, making it near to industry sector. Several factors have contributed to this increase, including increased energy consumption for heating and cooling, as well as increased air-conditioner ownership and extreme weather occurrences. (IEA) in the same manner we can notes that other sectors increased during this period.

I.3.2 Consumption of electricity by sector

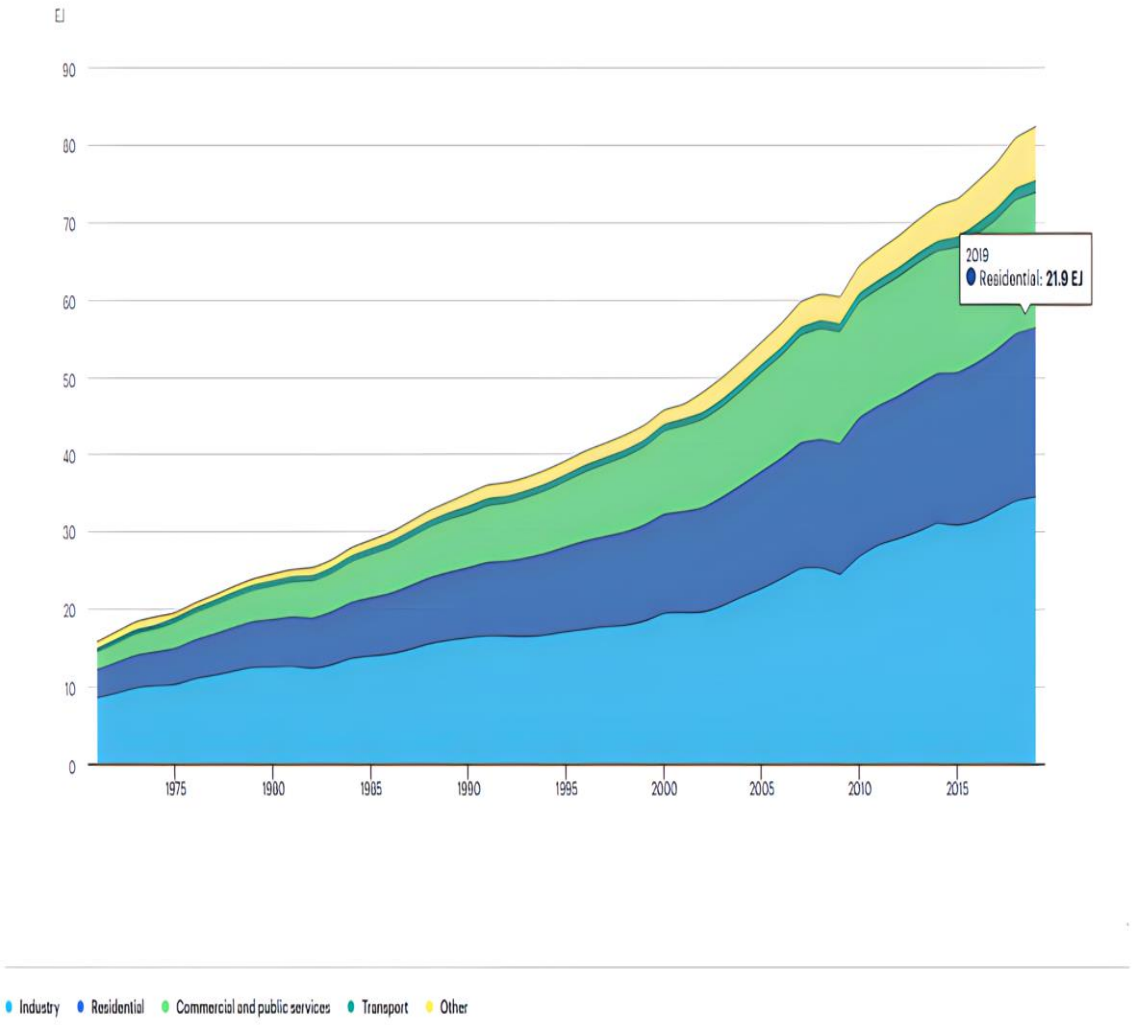

Figure I.3:Electricity total final consumption by sector, 1971-2019 IEA

According to the US Energy Information Administration's (EIA) International Energy Statistics, global electricity consumption continues to grow faster than global population, resulting in an increase in the average amount of power consumed per person (per capita electricity consumption). Buildings use electricity for lights and appliances, industrial processes use electricity to produce things, and transportation uses electricity to power rail and light-duty vehicles. Almost majority of the increase is due to rising energy use in developing nations that are not members of the Organization for Economic Cooperation and Development (OECD) [7].

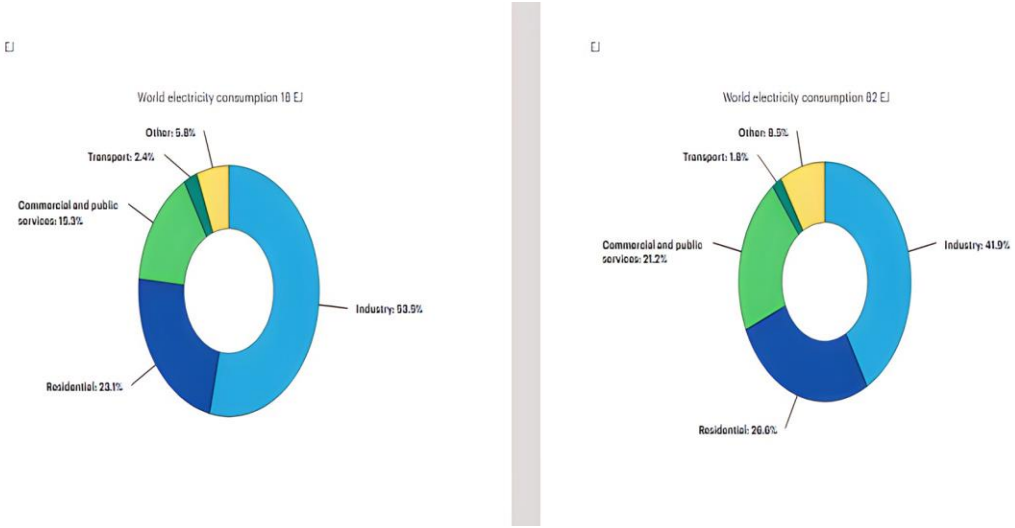

Figure I.4: Share of electricity final consumption by sector, , 1971left and 2019 right IEA

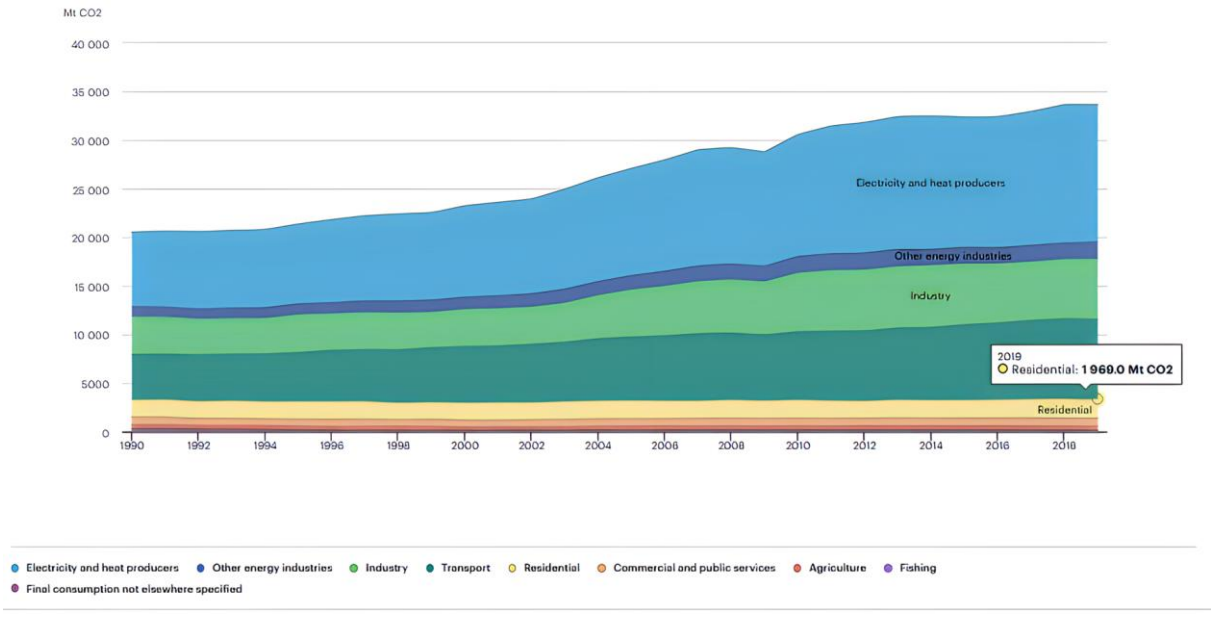

Figure I.5:CO2 emissions by sector, World 1990-2019 IEA

After flattening between 2013 and 2016, energy-related CO2 emissions from buildings have risen in recent years. In 2019, direct and indirect emissions from electricity and commercial heat used in buildings reached a record high of 10 GtCO2.. Due to the continuous use of fossil fuel-based assets, a lack of effective energy-efficiency policies, and insufficient investment in sustainable buildings, enormous emissions reduction potential remains untapped [19][21].

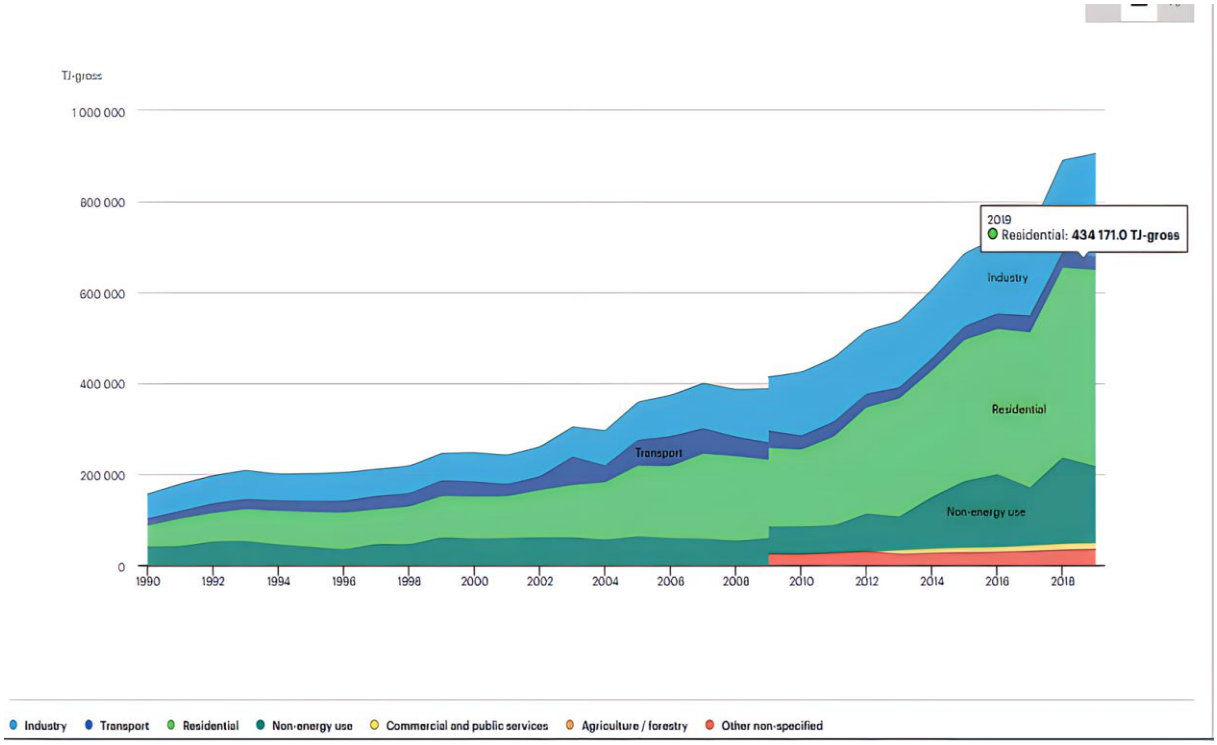

Figure I.6: Natural gas total final consumption by sector Algeria IEA

Between 1990 and 2019, overall final energy consumption climbed by 77.2%, with the residential sector accounting for the majority of the increase. Final consumption of electricity in residentential sector has been increasing over the years It becomes the first sector consume energy before Industry, Commercial and public services, Transport and Agriculture respectively [20].

The rise of economic activities and population growth can both be attributed to the high demand for energy. Despite the fact that the Algerian government has established several development plans to boost economic growth by developing and modernizing the industry sector, which has resulted in increased electricity consumption, Algerian residential electricity consumption has grown faster than industry in recent years.

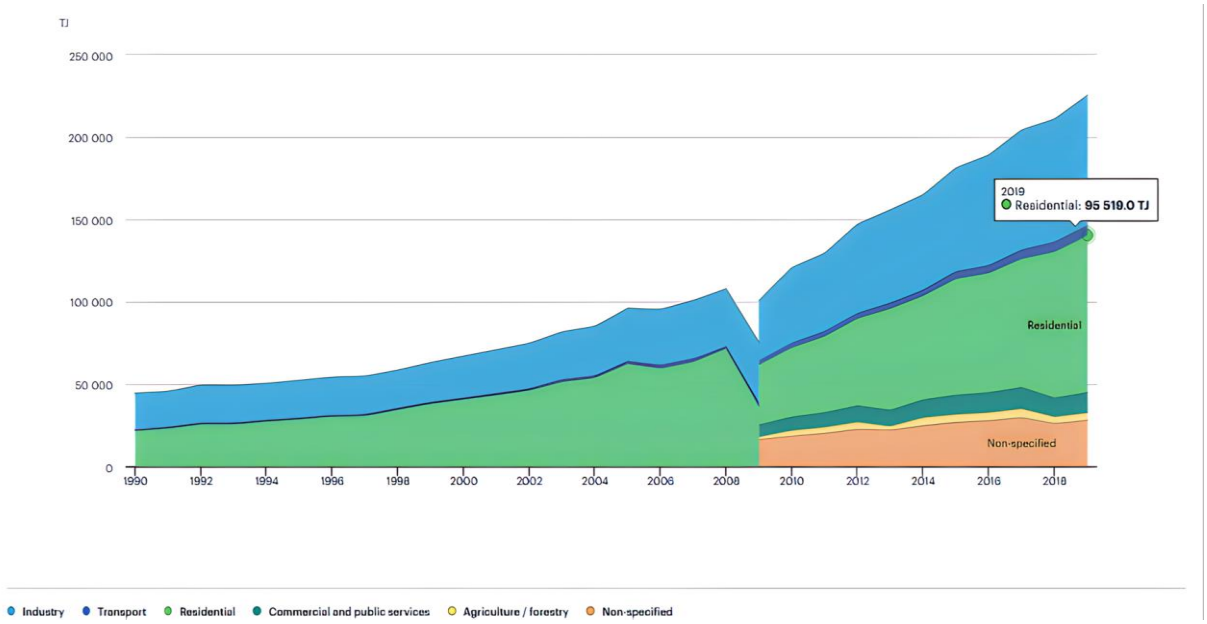

Figure I.7: Electricity consumption by sector, Algeria 1990-2019 IEA

In 1990, the industry sector consumed 48.5 percent of total power consumption, while the residential sector consumed 49.15 percent; in 2014, the industry sector consumed only 48.5 percent of total electricity consumption Electricity consumption in the industrial sector was just 35% in 2014, while residential use was over 63%. Several causes, such as changes in lifestyles, could account for the increased domestic electricity consumption [21].

Shares/years	**1990**	**2019**
Transport share in TFC	42%	35.20%
Residential share in TFC	24.70%	30.40%
Industry share in TFC	19.30%	17.10%
Share/years	**2009**	**2019**
Commercial and public services share in TFC	0.70%	1.40%

Table I.1: Share of electricity final consumption by sector in Algeria APRUE

The table illustrates some interesting facts about Algeria's share of final electricity consumption by sector. It allows to compare the percentage of electricity consumed by each share sector between 1990 and 2019 for Transport share, Residential share, and Industry share, between 2009 and 2019 for Commercial and public services share

As we notice All portions decrease over time in different percentage except for Residential share and Commercial and public services share which are far apart due to reasons mentioned before

I.4 CO2 emissions by sector

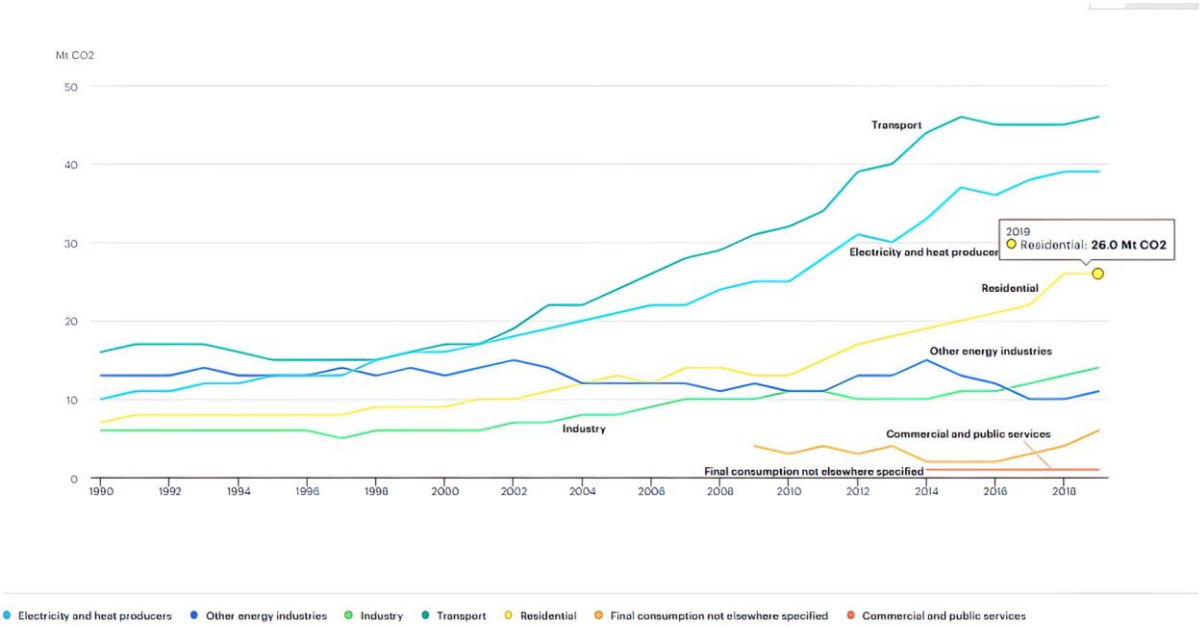

Figure I.8: CO2 emissions by sector, 1990-2019 in Algeria IEA

Over one-third of global final energy consumption and almost 40% of total direct and indirect CO2 emissions are attributed to the building and buildings sector. Building and buildings construction energy demand is continuing to rise, owing to increasing energy availability in developing nations, increased ownership and use of energy-consuming gadgets, and significant development in global building floor area.

Algeria is the African country with the third highest CO2 emissions [7] [22].

I.5 Thermal comfort

Knowledge of physiological principles is essential for any HVAC engineer addressing air treatment problems for the comfort and health needs of occupants of ventilated, heated or air-conditioned premises.

Physiological factors include:

• Purity of the ambient air, its composition, outdoor, etc.;

•Air temperature;

•Relative humidity %;

•Speed (movement) of air;

•Fresh air flow (number of air changes);

•Nature of the occupants' activity and clothing;

•Noise level.

The human body exchanges heat with the surrounding environment through conduction, convection, radiation, water vaporization (evaporation and transpiration) and respiration. This exchange is done in such a way as to maintain the average skin temperature at 98.6°F or 36.9°C.

It is therefore necessary to create an atmosphere that allows to establish the thermal balance between our body, which plays the role of "a source of metabolic heat", and the atmosphere while taking into account the activity and clothing of the occupants

The graph (Fig I.1) shows the heat loss of an individual dressed, at rest and in calm air. It can be noted that the total heat loss from 18°C stabilizes at about 119 W, while evaporative losses from 10°C increase steadily.

Evaporation always has two distinct aspects: physical (evaporation) and physiological (sweating). In the first case, evaporation is due to the heat ceded by the skin and its boundary layer, which causes the temperature of the skin to drop. In the second case, when the ambient temperature reaches 29 ° C, sweating occurs (there must be water production for evaporation). A body exposed to heat can lose 0.5 to 12 liters of water per day.

it should also be noted that from 34 ° C there is only one mode of heat exchange, that is to say evaporation.

Generally the most important parameters for defining a given indoor environment are:

• the dry air temperature;

•the average radiant temperature;

•air humidity;

•air speed

•occupant clothing

•the nature of the occupants' activity.

With the exception of activity level, these factors can be modified to minimize energy consumption.

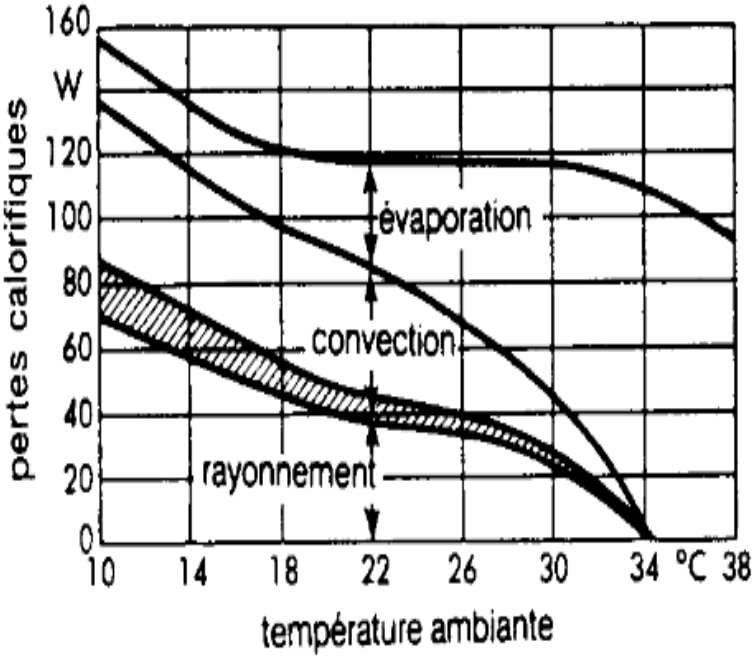

FigureI.9: Heat loss of a normally dressed individual at rest and in calm air ASHRAE

In principle, there is no valid precise physiological observation to make an informed assessment of thermal comfort. A thermal neutrality zone will vary depending on clothing, season, activity and many other factors controlling heat production.

To describe the thermal sensation the following expressions are used: very hot, hot, slightly warm, neutral, slightly cool, cool, cold. This sensation is strongly influenced by the clothing which plays the role of thermal insulation (the thermal resistance unit of the garment is 1 clo = 0.155 (m^2°C/W) = 0.88 (pi2 hre°F/ BTU); a two-piece suit has a value of 1 clo, while short pants have 0.05 clo.

Since each individual has a different feeling of heat or cold, the ASHRAE standard determines the thermal conditions that are acceptable to at least 80% of the occupants. This is the standard "Standard 55-1992 Thermal Environmental Conditions for Human Occupancy"[23].

These conditions are presented on a comfort zone chart plotted on the psychrometric diagram (Figure I.10). There is a part of this area that is common for winter and summer (thermal sensation in this area can be described as slightly cool in summer and slightly warm in winter).

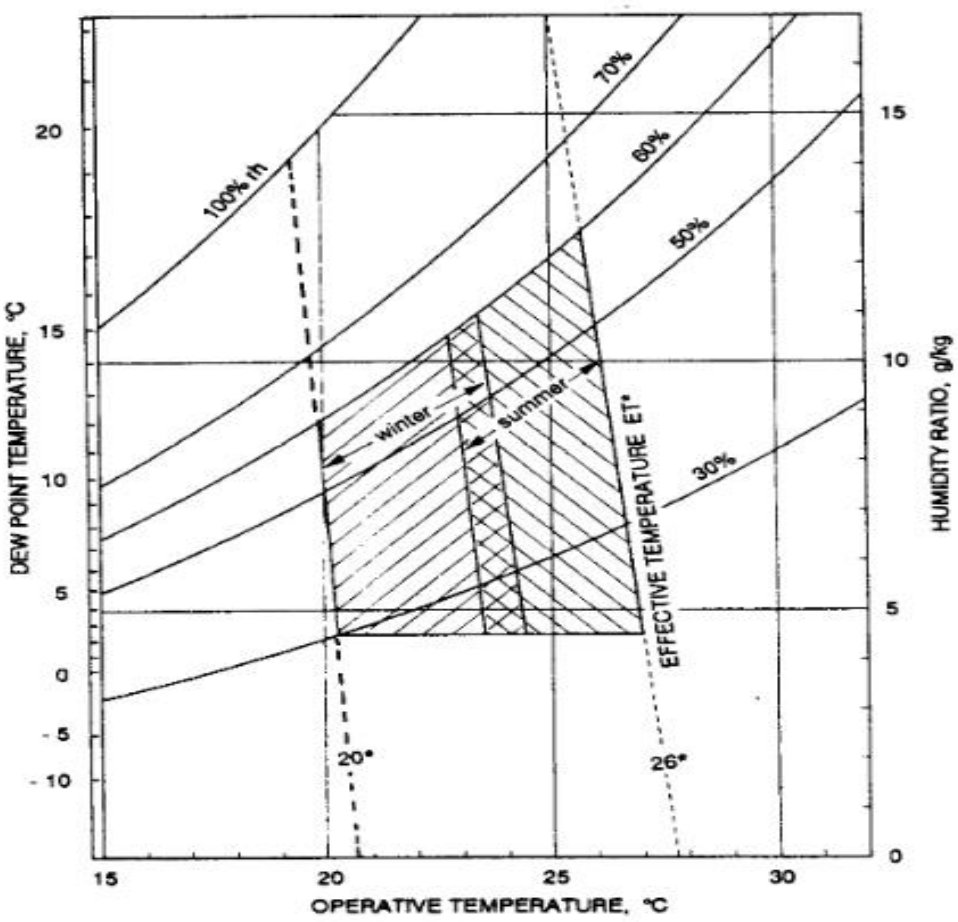

Figure I.10: The thermal comfort zone ASHRAE.

The winter and summer areas are designed for an air velocity of less than 0.15 m/s (30 ppm) and less than 0.25 m/s (50 ppm) respectively and for clothing, respectively 0.9 and 0.5 clo.

The comfort zone is, in addition, designed for the activity considered sedentary and for the radiant average temperature (MTR) equal to the ambient temperature. It is envisaged to change the limit temperature of this zone, by -1°F (-0.6°C), for each 0.1 clo more than 0.9 and 0.5 clo and by increments of 1°F (0.6°C), for each 0.152 m/s (30 ppm) more than the speed values mentioned above.

I.5.1 Air temperature and humidity

On the other hand, the ASHRAE standard 90.1-1989 (Energy Conservation in New Building Design) recommends 78 oF in summer and 72 oF in winter.

The temperature of 78 ^{o}F is certainly recommended for energy saving but it can cause some thermal disturbance especially in the case of a long occupation of the premises. The relative air humidity of 30-60% is quite acceptable for thermal comfort conditions provided that dry temperatures are respected[24].

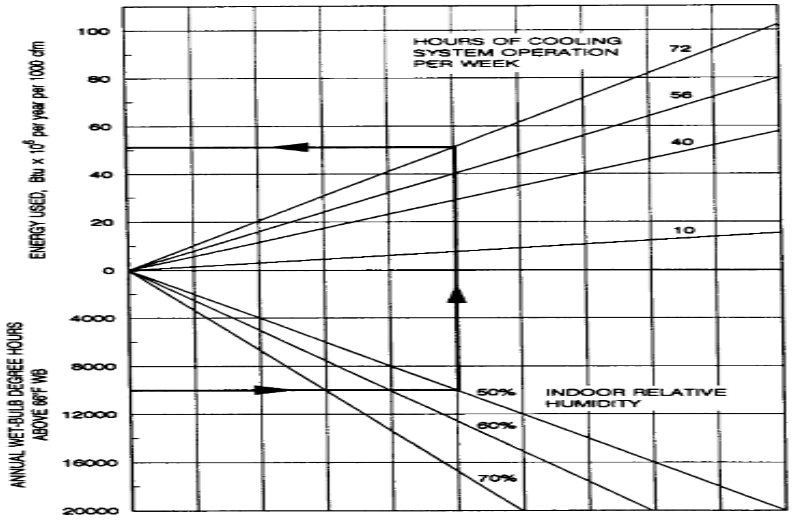

Figure I.11: Energy required for dehumidification ASHRAE

humidity between 30 and 60% in winter is not so reasonable for the following reasons:

increased energy consumption for humidification,

(2) danger of condensation of water vapour on cold surfaces

(3) increased maintenance of humidification equipment.

As a result, the minimum humidity of 30% is considered in winter to be quite acceptable.

In summer, the higher the acceptable relative humidity, the greater the energy saving. Figure I.11 illustrates this phenomenon and allows to determine the approximate amount of energy consumed for dehumidification when the indoor temperature is 78 oF

Each thermal zone must be equipped with control instruments (at least one thermostat) to maintain the thermal comfort conditions mentioned above. A thermal zone is a space (a

part of a room or an entire room) or several spaces having the charge of air conditioning and heating and the variation of this load at least similar.

I.5.2 Minimum fresh air flow

The minimum air flow is recommended by ASHRAE Standard 62-1989 (1989b). The basic value in most cases is 15 pcm per person. If the control system includes a CO2 probe this flow rate may be higher depending on the request of the probe [24].

I.6 The Sun

The sun is a sphere of intensely hot gaseous matter. It is the central star of our solar system. It consists mainly of hydrogen and helium. Some basic facts are summarised in table I.1 and its structure is sketched in Figure I.12. The mass of the Sun is so large that it contributes to 99.68% of the total mass of the solar system. In the centre of the Sun the pressure-temperature conditions are such that nuclear fusion can take place. In the major nuclear reaction [25],

Mean distance from the Earth:	149 600 000 km (the astronomic unit, AU)
Diameter:	1 392 000 km (109 * that of the Earth)
Volume :	1 300 000 * that of the Earth
Mass :	1.993 * 1027 kg (332 000 times that of the Earth)
Density (at its center):	>105 kg m 3 (over 100 times that of water)
Pressure (at its center):	Over 1 billion atmospheres
Temperature (at its center):	About 15 000 000 K
Temperature (at the surface):	6 000 K
Energy radiation:	3.8 * 1026 W
The Earth receives:	1.7 * 1018 W

Table I.2. Some basic facts [25]

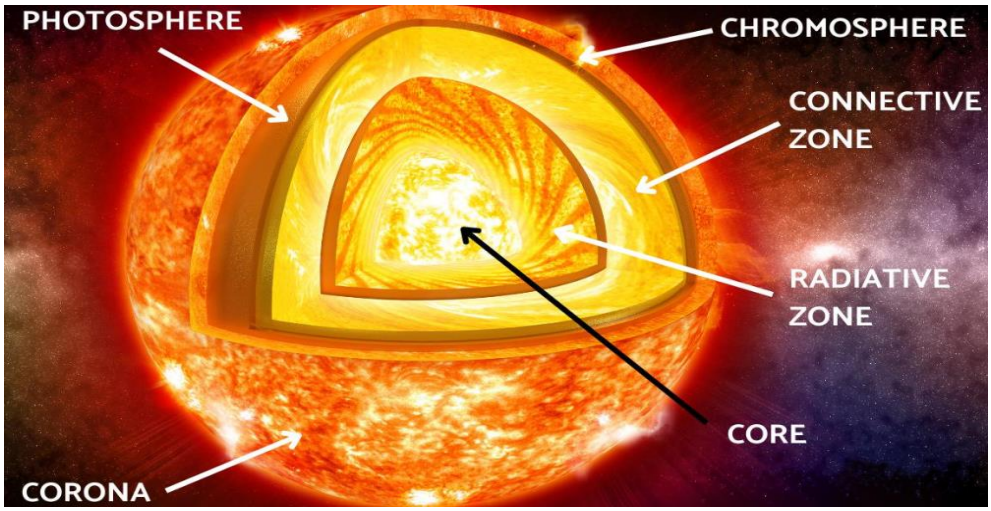

Figure I.12: The Sun with its layer structure [25]

I.6.1 Solar constant

Figure I.13 shows schematically the geometry of the sun-earth relationships. The eccentricity of the earth's orbit is such that the distance between the sun and the earth varies by 1.7%.

The sun's radiation and its spatial relationship to the planet result in a practically constant intensity of solar radiation outside the earth's atmosphere. The solar constant Gsc is the amount of energy received from the sun per unit time on a unit area of surface perpendicular to the direction of radiation propagation at the mean earth-sun distance outside the atmosphere. [25].

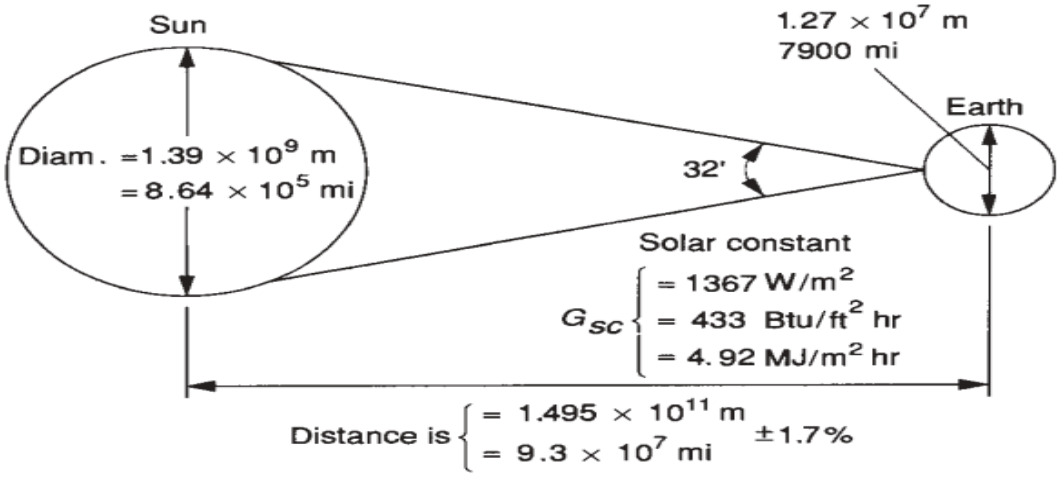

Figure I.13: Sun , Earth relationship[25]

I.6.2 Geometric aspects of solar radiation

With the subsequent aim of calculating the flux received by an inclined plane placed on the surface of the earth and oriented in a fixed direction, our interest will focus in what follows on the geometric aspects of solar radiation intercepted by Earth. Knowledge of this flow is the basis for sizing any solar system.

I.6.2.1 Earth movements

The path of the earth around the sun is an ellipse of which the sun is one of the focal points. The plane of this ellipse is called the ecliptic [11]. The eccentricity of this ellipse is small, which means that the Earth / Sun distance varies only by ± 1.7% compared to the average distance which is about 149 600 000 km. The earth also rotates on itself around an axis called the pole axis and passing through the center of the earth called the equator. The

axis of the poles is not perpendicular to the ecliptic in fact the equator and the ecliptic form between them an angle called inclination of the order of 23 ° 27.

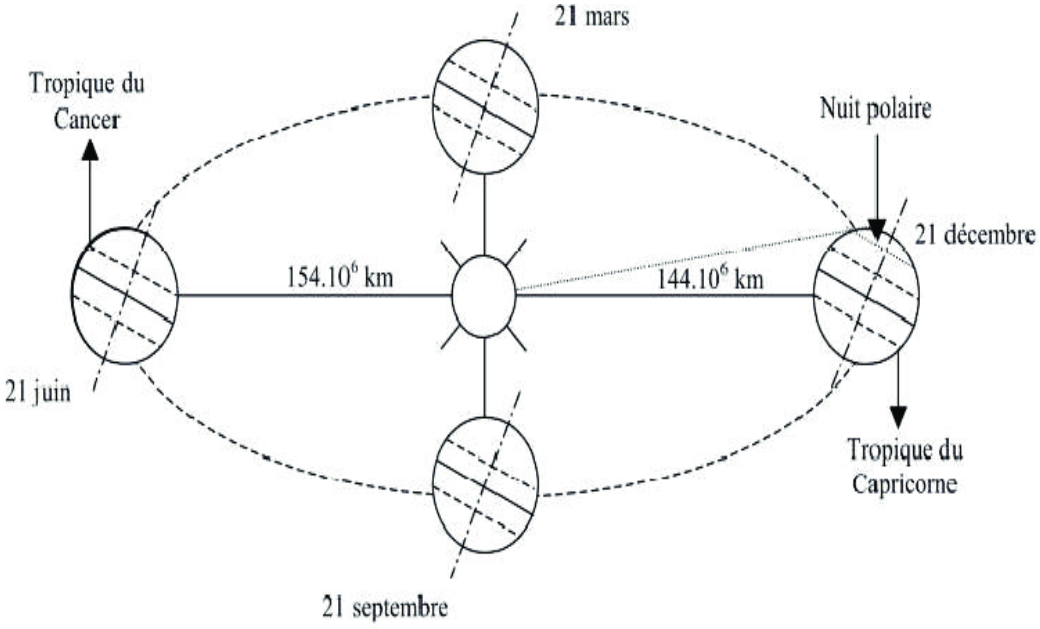

Figure I.14: The movement of the earth around the sun[25]

The earth is in rotation on itself then it turns around the sun in a period Tt = 365 days 5h 48mn 40s ≈ 365.25 days. It describes an elliptical orbit in which the sun occupies one of the focal points. This orbit is located in a plane called the plane of the ecliptic where the sun is almost in the centre, as shown in Figure I.3.It corresponds to a circle with an average radius of 150 million kilometers [6]. The earth revolves around the sun with an average speed Vt ≈ 29.77 km / s [maximum speed], in winter 30.27 km / s and minimum in summer 29.77 km / s. This movement takes place in the direct trigonometric direction and causes the seasons to cycle. The pole axis is not perpendicular to the ecliptic; the equator and the ecliptic form between them an angle called declination which is 23.45 ° as shown in figure I.3. It varies during the year between -23.45 ° and + 23.45 °, it is zero at the equinoxes (March 21 and September 21) and maximum at the summer solstice (June 21) and minimum at the solstice of winter (December 21). The value of the declination (in °) can be calculated by the following formula: $\delta=23.45*\sin[0.980(d+284)]$ ……(I.1)

I.6.3 Energetic aspects of solar radiation:

Solar radiation undergoes a number of random alterations and attenuations while passing through the atmosphere; reflection on atmospheric layers, molecular absorption,

molecular diffusion and by aerosols (dust, droplets ...). At ground level, due to scattering, part of the radiation is diffuse (i.e. isotropic). The other so-called direct part is anisotropic

I.6.3.1 Solar radiation:

The energy received at ground level is lower than 1354 w / m2 (the solar constant) because the atmosphere absorbs some of the solar radiation (about 15%) and re-emits it in all directions as diffuse radiation. The atmosphere reflects another part of the solar radiation back to space (about 6%). The global radiation at ground level is therefore defined as the sum of the direct radiation and the diffuse radiation figure (I.15) The energy received by a surface also depends on the season, the latitude, the meteorological conditions, pollution, orientation of the surface considered (wall and roof of the building).

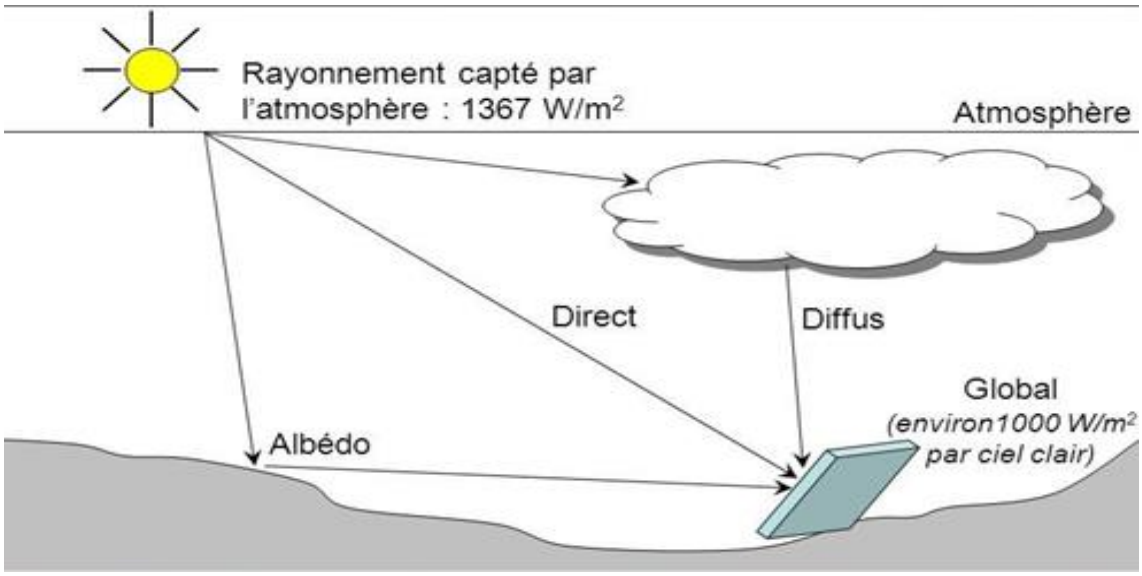

Figure I.15 : The components of solar radiation

- **Direct radiation:** is radiation from the sun that has not been dispersed by the atmosphere. (Beam radiation is also known as direct solar radiation; however, to avoid confusion between the subscripts for direct and diffuse, we use the phrase beam radiation.)
- **Diffuse radiation**: is radiation emitted by obstacles (clouds, ground, and buildings) and comes from all directions. The share of diffuse radiation is not negligible and can reach 50% of the overall radiation (depending on the geographical location of the place). The global radiation on earth and its share of diffuse radiation varies throughout the year.

- **Total Solar Radiation** This is the total of direct and diffuse solar energy on the surface (The most frequent solar radiation measurements are total radiation on a horizontal surface, also known as global radiation on the surface.)

I.6.4 Direction of direct radiation

Several angles can be used to represent the geometric relationships between a plane of any orientation respect to the earth at any time (whether that plane is fixed or moving relative to the globe) and the incoming direct solar radiation, that is, the location of the sun relative to that plane. Figure I.16 depicts some of the angles. The following are the angles and a set of consistent sign conventions:

- **Φ**: Latitude, the angular location north or south of the equator, north positive; $-90° \leq \varphi \leq 90°$.
- **δ**: Declination, the angular position of the sun at solar noon (i.e., when the sun is on the local meridian) with respect to the plane of the equator, north positive; $-23.45° \leq \delta \leq 23.45°$.
- **β**: Slope, the angle between the plane of the surface in question and the horizontal; $0° \leq \beta \leq 180°$

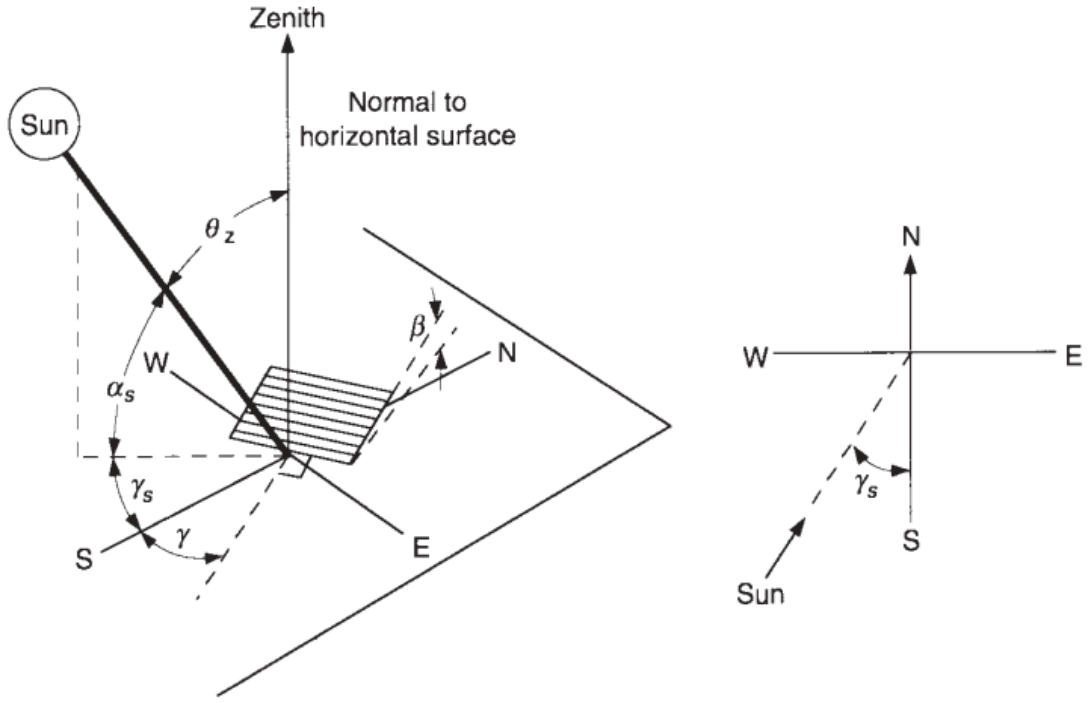

Figure I.16: Different direct radiation angles[9]

- **γ**: Surface azimuth angle, the deviation of the projection on a horizontal plane of the normal to the surface from the local meridian, with zero due south, east negative, and west positive; $-180^\circ \leq \gamma \leq 180^\circ$
- **ω**: Hour angle, the angular displacement of the sun east or west of the local meridian due to rotation of the earth on its axis at 15◦ per hour; morning negative, afternoon positive.
- **θ**: Angle of incidence, the angle between the beam radiation on a surface and the normal to that surface.

The angles that describe the position of the sun in the sky:

- **θz** Zenith angle, the angle between the vertical and the line to the sun, that is, the angle of incidence of beam radiation on a horizontal surface.

$$\cos\theta_z = \cos\Phi\ \cos\delta + \sin\Phi\ \sin\delta \quad \text{.....(I.2)}$$

- **αs** Solar altitude angle, the angle between the horizontal and the line to the sun, that is, the complement of the zenith angle.

$$\sin\alpha_s = \sin(90 - \theta_z) \quad \text{.....(I.3)}$$

- **γs** Solar azimuth angle, the angular displacement from south of the projection of direct radiation on the horizontal plane, shown in Figure I.16 (On the right side). Displacements east of south are negative and west of south are positive.

$$\gamma_s = sign\ (\omega)\left|\cos^{-1}\left(\frac{\cos\theta_z\ \sin\Phi - \sin\delta}{\sin\theta_z\ \cos\Phi}\right)\right| \quad \text{.....(I.4)}$$

I .6.5 The use of solar energy

I.6.5.1 Solar thermal:

This technology converts solar energy into heat. The atoms making up the material of solar collectors are excited by photons. As they regain some of their energy, atoms change their energetic state, creating thermal agitation. The atoms will then release the excess energy in the form of thermal energy, manifesting itself in the form of heat. This will be transported

by a heat transfer fluid (water, gas, etc.): when heated, it will be able to gradually distribute its heat (underfloor heating for example), or be stored (hot water tank for example) for use ulterior.

I.6.5.2 Thermodynamic solar:

The principle is to convert solar energy into heat, then into electricity at a later stage. As with solar thermal, sensors excited by photons will produce heat. By concentrating the sun's rays by a system of mirrors (reflectors), the temperatures reached are higher (from 250 ° C to 1000 ° C). A heat transfer fluid transports this heat, and it is then transmitted to a thermodynamic fluid. Under the effect of changes in temperature (and therefore pressure), the thermodynamic fluid will produce thrust forces (mechanical energy), activating a turbine connected to an alternator, thereby converting this energy into electricity.

I .6.5.3 Photovoltaic solar:

This technology directly converts solar energy into electricity. The material of the sensors, often based on silicon (Si), is a semiconductor: it can be either insulating or conductive, depending on the conditions in which it is placed. The photons will excite electrons in this material, transferring part of their energy to them and making them mobile. These electrons set in motion will thus produce a direct current, which can supply an electrical network. An inverter converts this direct current into alternating current, which can be used by electrical devices (household appliances, etc.)[17].

I.6.6 Sun-Path Diagram

The projection of the sun’s path on the horizontal plane is called a sun-path diagram. Such diagrams are very useful in determining shading phenomena associated with solar collectors, windows, and shading. The solar angles depend upon the hour angle, declination, and latitude. Since only two of these variables can be plotted on a two- dimensional graph, the usual method is to prepare a different sun-path diagram for each latitude with variations of hour angle and declination shown for a full year. A typical sun-path diagram is shown in

Figure I.17 for Msila location. Sun-path diagrams for a given latitude are used by entering them with appropriate values of declination **δ** and hour angle **ω**. The point at the intersection of the corresponding **δ** and **ω** lines represents the instantaneous location of the sun. The solar altitude can then be read from the concentric circles in the diagram

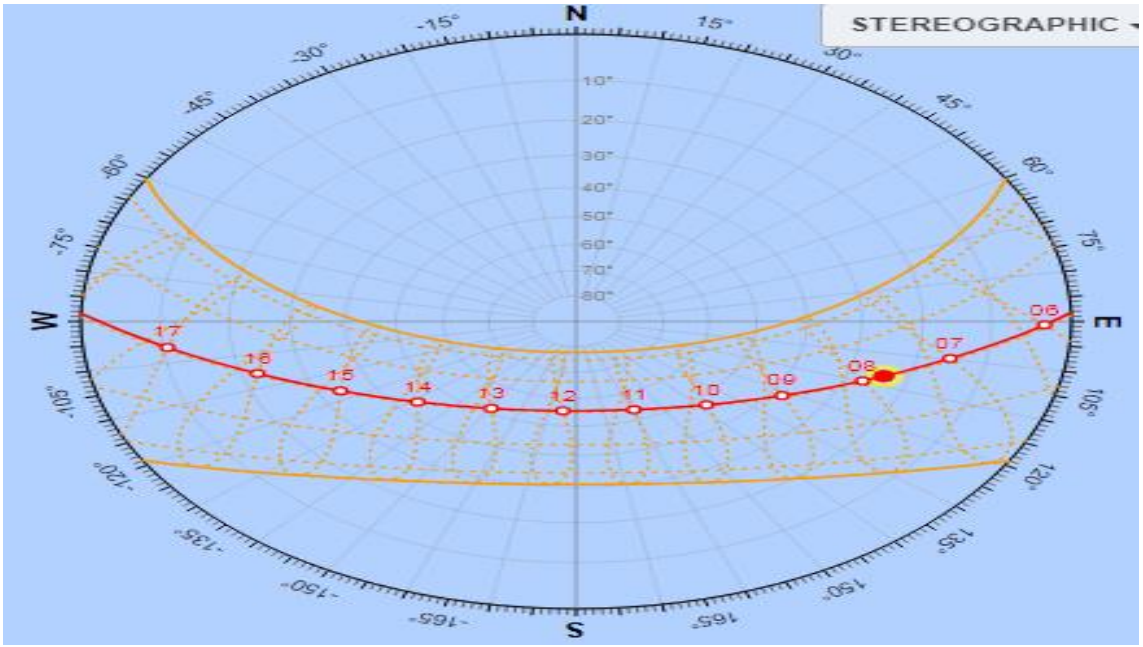

Figure I.17: Sun-path diagram for M'sila (16/09/2021) [26]

I.6.7 The integration of solar energy in the building

The passive and active techniques shown in Figures (I.18) and (I.19) are used to reduce energy consumption inside a building . The figures illustrate solar passive and active technologies that, when combined, can result in low-energy buildings [27].

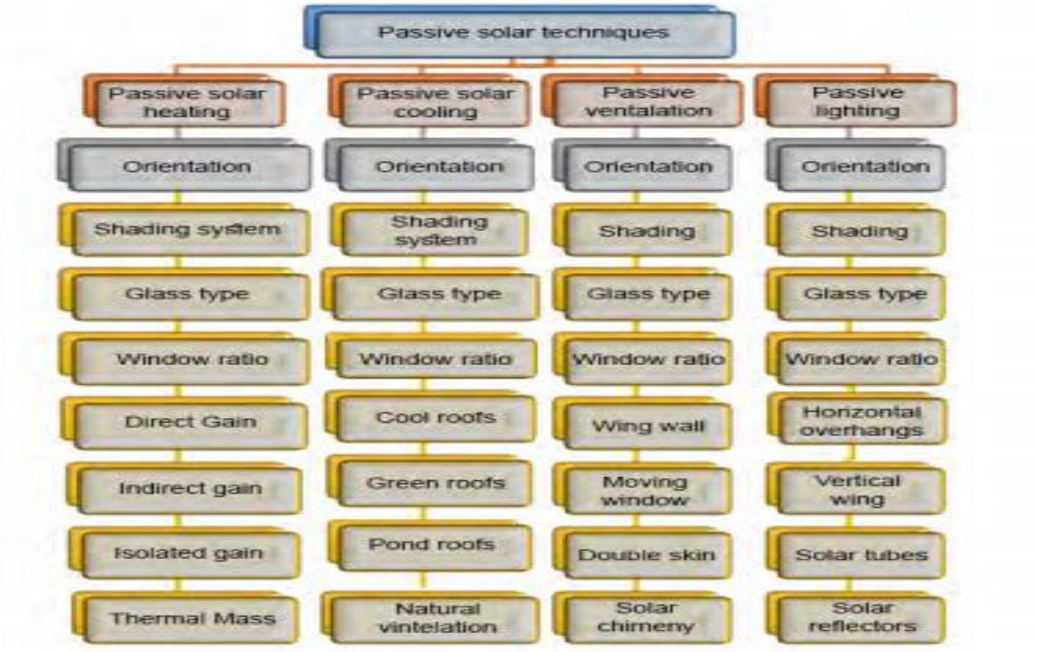

FigureI.18: Strategies for using passive solar to reduce energy consumption inside buildings [27]

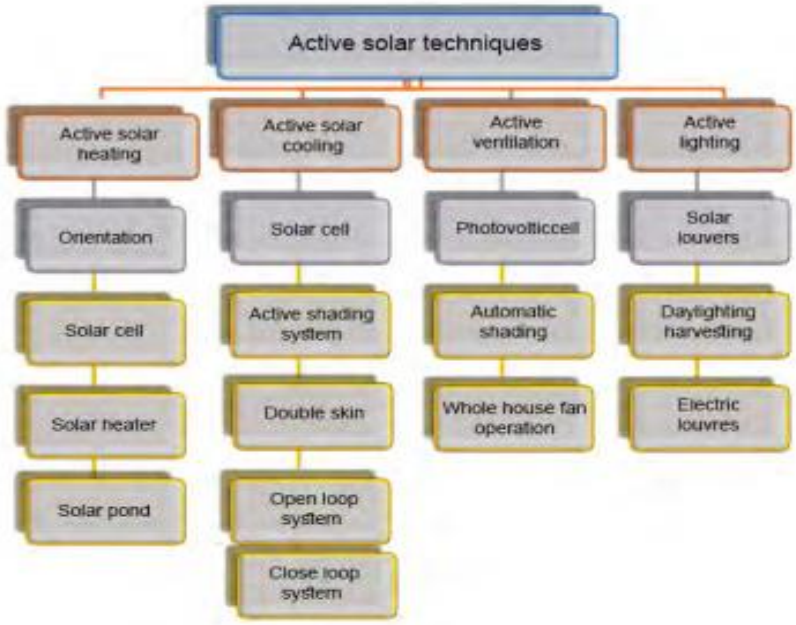

Figure I.19:3Strategies for using active solar to reduce energy consumption inside buildings [27]

I.6.7.1 Active solar energy

Nowadays active solar energy use in buildings contributes essentially to assembly power requirements by photovoltaics and to warm water through warm collectors exposed to solar radiation

If the potential of conventional insulation has been completely exhausted, or if special requirements, such as protecting monuments or preserving facades, do not allow the use of external insulation, a solar system is a good choice to meet your space heating needs. Heating support by collector, A small contribution of about 10-30% is always possible without significant loss of specific surface area. Preheating the outdoor air with a collector can also contribute significantly to reducing ventilation heat loss.

Thermal cooling processes such as open and closed adsorption processes in the air-conditioning buildings can be powered by active solar components. Given the potential contribution of solar energy to a building's various energy needs (heating, cooling, electricity), the solar radiation, the conversion efficiency of the solar technology considered and the usable surface potential of the building, as well as the economically viable potential.

Sofiane Bahria and all concluded that the application of the SHC system in the Algerian regions is promising because of its high solar potential. In fact, the system works all year round. Thier results show the ratio between the monthly solar fraction and the collector surface. they found that the optimal collection surface is 24 m2 in Algiers and Djelfa (32% of

the habitable surface) and about 28 m2 in Tamanrasset (38% of the habitable surface). For Algiers, Djelfa, and Tamanrasset, loads were reduced by 12%, 44%, and 22%, respectively. On the other hand, they showed the adaptation of the SHC system to the Algerian climate (adopted in the National Plan for Renewable Energy and Energy Efficiency Program 2011-2030), [28-29]

The building-integrated photovoltaic/thermal BIPVT Systems Integrated into Building Converts Available Solar Energy to Electric and Converts Heat for Various Purposes in Residential and Non-Residential Buildings To do. The BIPVT system is a predictable solution for ensuring energy security and reducing greenhouse gas emissions. Many installations of BIPVT systems have been initialized due to regulatory compliance around the world to reduce carbon dioxide emissions into the atmosphere. Maghrabie,and all in their review, Benefits, Limitations, Applications, Electric and Thermal Efficiency, various BIPVT systems achieved over last many years fig(1) were talked about and summed up with accentuation on the advantages, restrictions, applications, electrical and warm efficiencies, the degree for boundaries, difficulties, and future possibilities. The future turns of events and manageable viewpoints of the BIPVT frameworks rely upon the various boundaries examined, and it is declared assorted answers for improving the BIPVT frameworks in various applications[30].

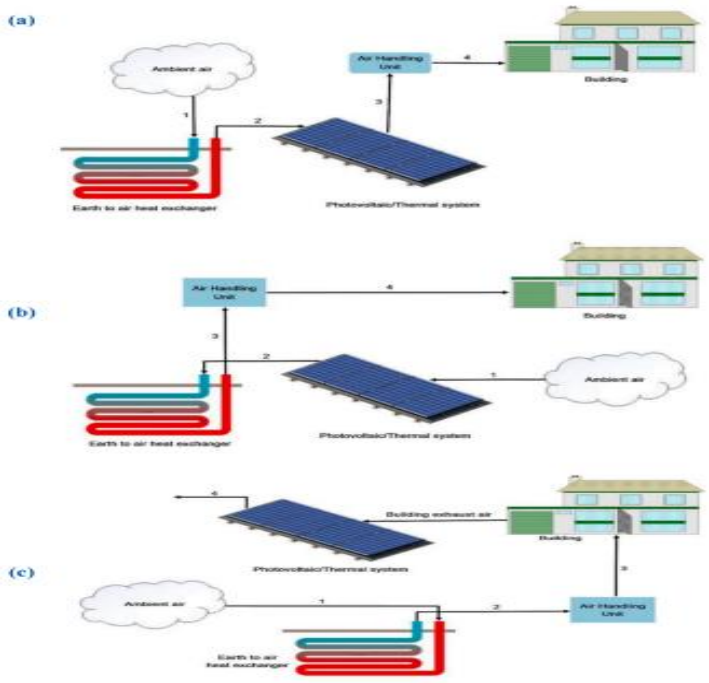

Figure I.20: The working principles with different configurations (a) heating mode (system A) (b) heating mode (system B) (c) cooling mode (3) [30].

I.6.7.2 Passive solar energy

The smart building design allows us to set or reduce the energy requirements for heating or cooling a building without a support system. Take additional steps to passively reduce energy requirements.

- Rational orientation of the building
- Maximum volume to surface ratio
- Orientation of windows to the sun
- Use of heat-generating materials inside
- High level of insulation in the building envelope

If possible, these steps should be taken prior to considering additional systems such as active heat or solar to build. A constructive criterion for this heat is that no matter how well or poorly the solar collector is working or not, it is always lost or purchased through the building envelope, so it is important to minimize these losses and get as many gains as possible. Threat, minimal need for heat will also be a way to increase solar share

The concept of passive solar houses has recently received a lot of attention due to the very low energy housing i.e Germany and Sweden (although there is some confusion as well as the term building integration) , mainly the largest. Definition of heating demand Figure This should be less than 15 Kwh/m^2 This should not be achieved at the cost of increased energy use for other purposes such as electricity. Do not exceed 120 Kwh/m^2. Currently, the problem is the use of radiation to cover as much energy supply as possible or to set more stringent requirements. The common denominator is that buildings should be designed with high ambitious demands to reduce auxiliary energy demand

Knowledge of the solar capacity of heating exists from the beginning of life, and cave settlements have been discovered in several civilizations with designs obtained by the sun (historically Greek mathematician and inventor Archimeda created the first disgn of Passive Solar House facing south. Design Passive Solar House Vents and heat mass a term used in the American solar house design movement in the 1970s. In response to the oil crisis. It has a large heat capacity, so heat can be stored in the material to prevent overheating in the sun and use the heat when the material cools down at night to prevent overheating during. Summer This strategy requires a reasonable shade[31].

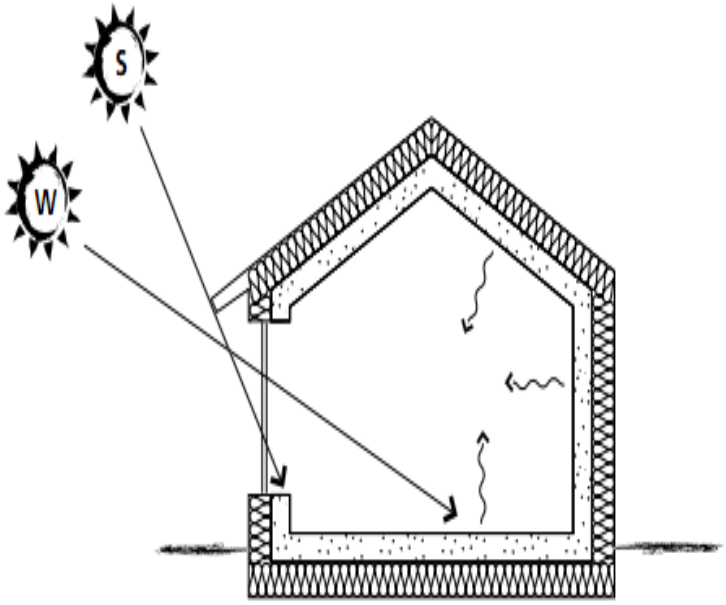

Figure I.21: The principle of a passive solar house design

I.7 Factors influencing the thermal performance of buildings

A building's thermal performance is determined by a variety of factors. These parameters were characterized by Nayak and Prajapati [32] as design variables, physical attributes, weather data, and building usage data.

- **The variables of the design:** Many aspects must be considered throughout the structure's design:

  • The shape of the building; this defines the size and direction of the outer envelope exposed to the outside environment. A smart design and orientation decision can cut energy use by 40%. [33] The exposed surface and the surface / volume ratio influence both the solar energy received and the heat losses. It is a critical element in determining heat loss and gain. The greater the density of a building, the easier it is to meet an energy-efficiency standard. The surface-area-to-volume ratio (S/V ratio) has a significant impact on a building's energy requirements [34].

  • The rate of direct solar radiation and its influence are controlled by the building's direction and the effect of winds on the building. The choice must respond to the expected impact of the shading and the solar course according to the latitude and the periods of the year .

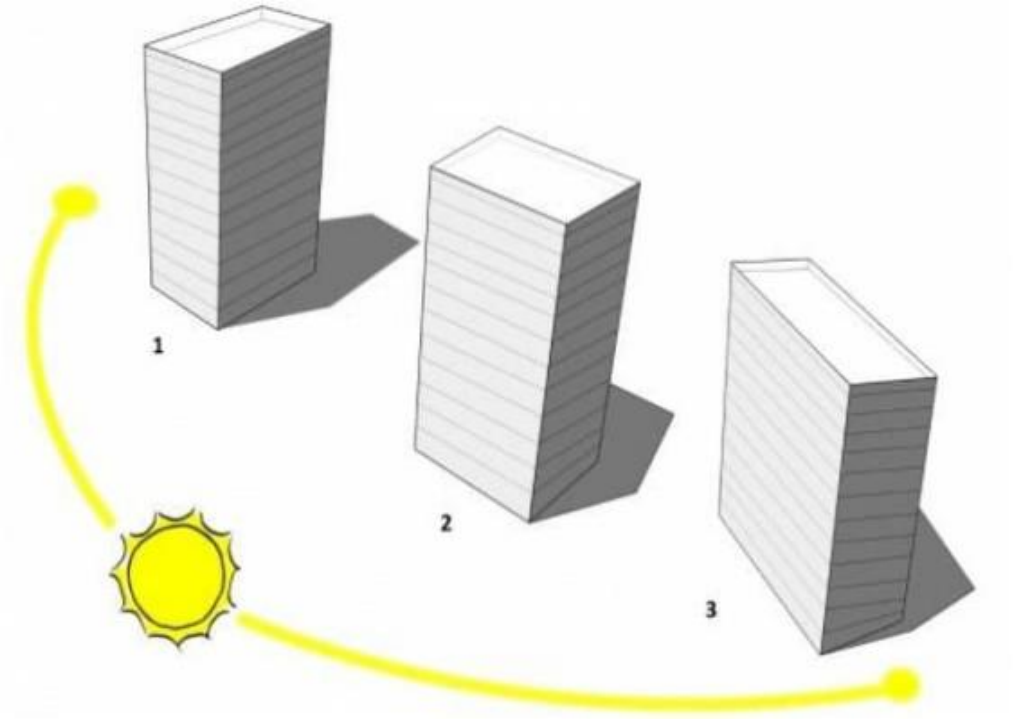

Figure I.22: Building Orientation Based on the Sun Exposure.

- **The building envelope;** because the level of conductivity / thermal resistance of the materials composing the building envelope and thermal bridges affects heat gain / loss and steam penetration, it is critical to select the right envelope based on the environment [35].

- **Shading devices;** they are beneficial in Mediterranean and semi-arid regions. Shade can be affected by the time of year, the color of the materials, and their relative transparency. [36].

- **The properties of materials:** The most important thermal properties of building components that determine thermal efficiency, according to Rosenlund [37] are:

  • Thermal conductivity λ

  • The thermal resistance of a material R

  • Thermal transmittance U

  • Density, porosity

- **The occupation and building operation:** Buildings generate heat, steam, and light (internal gains). The overall heat gain is affected by the density of occupancy and the sorts of activities. According to Utzinger and Wasley [38], building equipment and

lighting emit heat equal to the amount of electricity consumed. "Buildings that are mechanically cooled or heated can likewise overheat if the ventilation system is small or improperly regulated," write Lykartsis et al [39]. Overheating is thus a function of not only temperature but also humidity, air speed, and the occupants' clothing and activity."

I.8 Orientation of the Building

The relationship between a building's elevations and its original geographical direction is represented by its orientation. It is critical to consider the actual quantity of solar radiation on a building's façade as a whole during the design phase, since it impacts the thermal load of the building and determines the thermal behaviour and level of thermal comfort of the space (Morrissey, Moore, & Horne, 2011) [40]. Furthermore, it impacts the amount of ventilation crossing inside the building, which affects the amount of energy required in it to meet the thermal and life requirements.

I.8.1 The Window Wall Ratio

Windows are openings that signify weak points in the structure's outer envelope, where the building is susceptible to the most intense radiation through the opening, allowing solar radiation to enter within regions. As a result, window management plays an important role in decreasing heat loads inside the building. The ratio of windows on facades changes depending on orientation. The thermal load on the building's facades fluctuates from one direction to another depending on the movement of the sun in summer and winter, necessitating the reduction of windows in certain areas of the facades and the rise of windows in others (Goia, 2016). [41]

I.8.2 The Glass Thickness

Glass is a key factor of entrances because it allows light rays to enter the interior spaces. When solar radiation strikes the surface of the glass, a portion of it enters the space and is absorbed, another portion is absorbed by the glass substance, and the remainder is reflected outside the space. The reflected part is determined by the angle of incidence of the solar radiation; the absorbed part is transferred via the materials' convection and conduction characteristics [42].

N .Ihaddadene and all prove that double-glazing has a negative impact on the work of the sun powered collector (productivity corruption)[43].

The separate between the double glazing considered altogether decreases the proficiency of the collector; significantly increases the irradiance; and does not influence the temperature of the absorber plate

I.8.3 Shading System

A shade system is a method of addressing various openings in order to drastically reduce heat acquisition entering the building through them. Furthermore, depending on the quantity and placement of windows, it improves the quality of natural illumination in the spaces. It also adds to the visual and thermal comfort of users by minimizing glare and heat acquisition, as well as managing natural ventilation (David, Donn, Garde, & Lenoir, 2011) [44].

I.8.4 Thermal Insulation

Thermal insulation reduces heat movement from the exterior to the interior and vice versa. According to studies, the heat transported through walls and ceilings in the summer accounts for 60-70% of the heat removed by air conditioning. The remainder is provided by windows and air vents, which demands an electrical energy usage of up to 66% of total energy consumption. As a result, heat-insulating materials must be used to decrease the entrance and flow of heat through the various structural elements, assisting in the reduction of power consumed in summer cooling and winter heating (Eben Saleh, 1990) [45].

I.9 Thermal inertia of materials

The resistive capacity of a wall is an essential component in the design of an energy efficient building, other intrinsic properties of materials characterize the dynamic behavior of an envelope. In addition to slowing down the flow of heat, materials have a thermal capacity that allows them to store heat to a greater or lesser extent. It is therefore interesting to know how the heat is stored and at what speed:

We speak then of the effusivity of a material. Another physical property, the diffusivity indicates the speed of diffusion of heat within the material. These notions, more commonly known as thermal inertia, give buildings dynamic thermal properties that must be mastered in the renovation of existing buildings or in the design of tomorrow's buildings. This

is the first step towards bioclimatic. Capturing and controlling solar gain are essential elements of bioclimatic design [46-47].

Inside inertia refers to the ability of a wall's internal face to absorb energy.store and restitute calories, and of transmission inertia for the total thickness that dampens and shifts the temperature variations between the interior and the exterior. The damping of the temperature variations corresponds to the reduction of amplitude. The sun's rays that hit the walls or enter the building reach a surface that reflects them. Depending on the color and nature of the materials, the non-reflected part of the rays is more or less absorbed as heat. A highly reflective material such as polished aluminum hardly heats up at all. Materials that can absorb a significant amount of the heat received are those with a high thermal capacity. Figure 1.5 shows a classification of common building materials according to their ability to store and release heat [46-47].

The classification is as follows [47]:

Family A: materials not suitable for creating inertial mass ;

Family B: materials that can be used but only make a partial contribution to inertia;

Family C: materials suitable for the creation of daily or sequential inertia.

The thermal inertia of transmission concerns mainly the walls receiving the most solar calories, depending on the season. In our latitudes, it is generally the wall exposed to the south in winter and the roof in summer. The thermal inertia of transmission is mainly characterized by the time of phase shift, expressed in hour, between the moment when the calories arrive at the contact of the outside of the building and that when they penetrate in the building. In general, a day/night phase shift is sought, so that the solar rays of the day are transmitted in the form of heat from the beginning of the evening, which corresponds to phase shift values of 8 to 10 hours. For the summer, this same phase shift time allows the heat to enter when the outside temperature has begun to decrease, which limits the risk of overheating by ventilating.

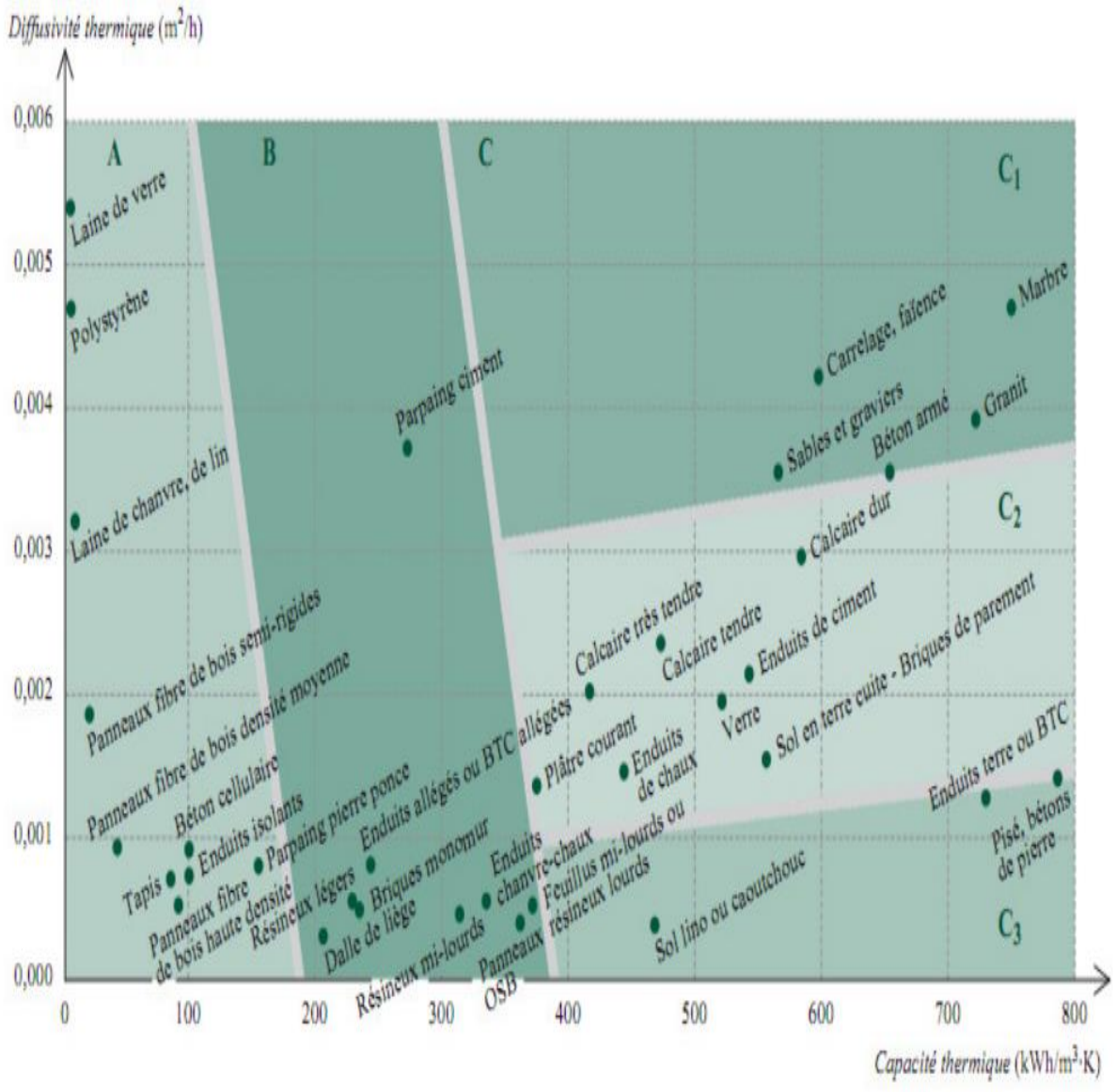

Figure I.23: Heat capacity and diffusivity of various materials [47]

I.9.1 Thermal capacity

The heat capacity of a material represents its propensity to store heat as a function of its volume. It is expressed in kJ/m^{3}C°. The higher the thermal capacity of a material, the more heat it will be able to store and release in winter, or cool in summer. The main benefit of a high thermal capacity is to smooth out the temperature variations of a building. However, if the thermal capacity can be the ally of the comfort and the energy sobriety of a building, it can be penalizing in certain cases. In a building with high inertia and intermittent use, such as a second home or a public building, long periods of comfort temperature setting will be observed since the walls will have to capture a large number of calories before reaching an ideal temperature [46-47].

I.9.2 Effusivity

The effusivity of a material, commonly called subjective heat, is the rate at which the surface temperature of a material varies. Noted Ef, this parameter has for unit the J/m2 S °C. If the effusivity is not taken into account in a heat balance, it remains however a significant parameter of thermal comfort: a material with a high effusivity absorbs a large amount of energy quickly without heating up noticeably; if its effusivity is low, the material heats up at the surface in a short time. It is the effusivity that gives the sensation of a cold wall in winter, synonymous with thermal discomfort.

If you put your hand against a wall made of earthenware (Ef = 1100 J/m2 S °C), it feels cold because this material with high effusivity quickly absorbs the heat from the skin. In the design of a wall, this parameter makes it possible to choose the quality of the covering according to the climate and the future use of the room. For example, in a cold climate, a parquet floor with high subjective heat will be used in bedrooms; conversely, in a warm climate, a tile floor will make the room feel cooler. Effusivity can help mitigate the disadvantages of a high inertia building by making it more comfortable early in the heating season[47].

I.9.3 Diffusivity

The thermal diffusivity of a material characterizes the speed of heat diffusion in its core. Named D or α , it is expressed in m2/s. The higher the diffusivity, the faster the material heats and cools. Diffusivity is directly related to the thermal conductivity, heat capacity, and density of a material. It increases with the thermal conductivity of a material and decreases with its heat capacity and density. Applied to a building, the diffusivity of a wall material allows to manage the time of heat restitution. For example, it can be used to size the thickness of an accumulator wall that captures heat during the day and releases it a few hours later to a living room at night. The phase shift thus created is an essential parameter in the optimization of the summer comfort of a house. A strong phase shift makes it possible to shift in time a temperature peak. A strong heat of a summer day reaches the interior of the building 12 hours after having impacted the external faces. It is thus possible to evacuate this surplus of calories by over ventilating the building and thus to limit the thermal discomfort in the rooms[47].

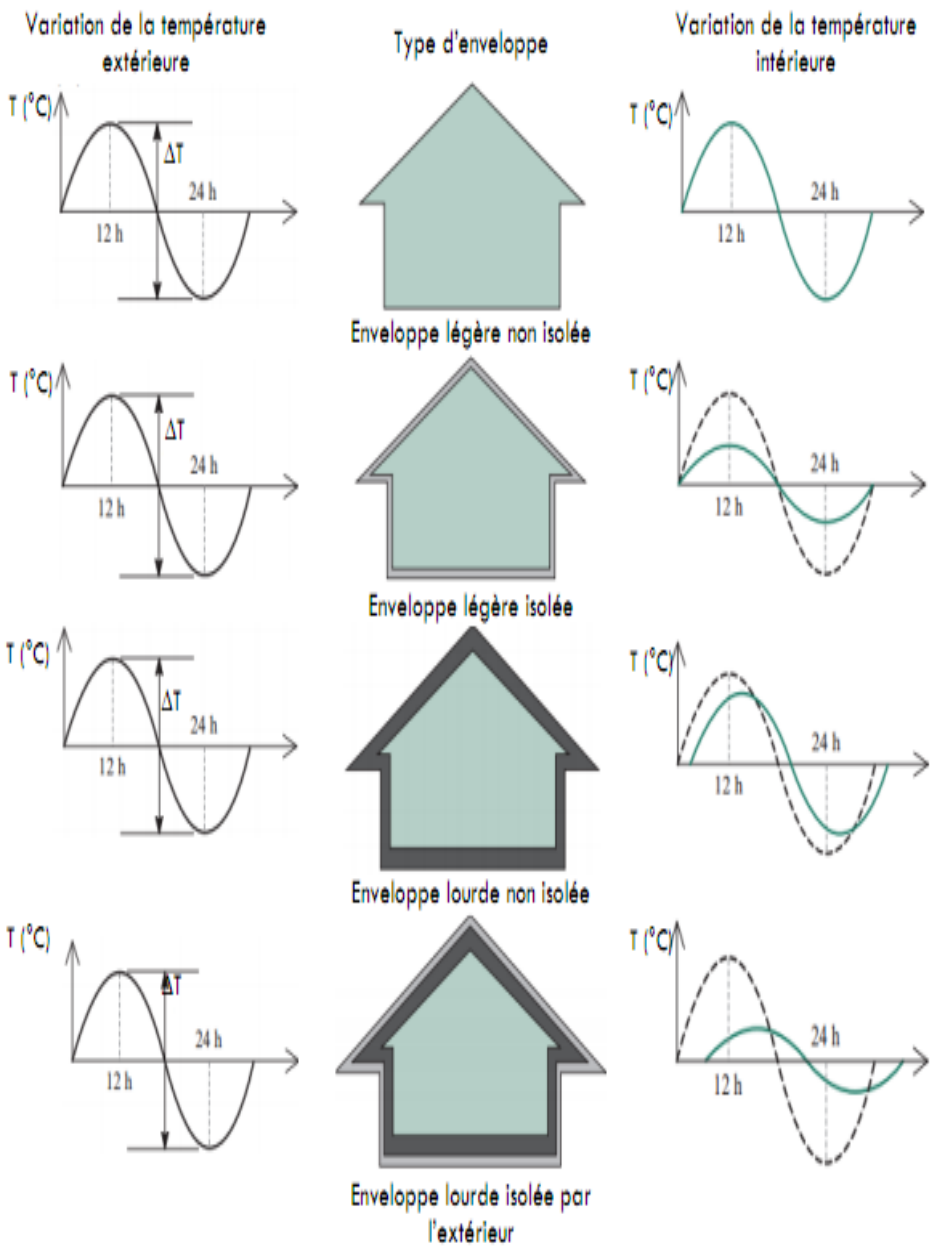

Figure I.24: Thermal behaviour of an envelope according to its constitution[47]

Chapter II

Materials and Methods

.

Introduction

In this chapter, we will present a comprehensive overview of our research methodology and the materials utilized throughout our study.In the first section, we will describe the device responsible for collecting solar radiation and temperature data present at the meteorological station. This device is essential for understanding the environmental conditions that influence our research. Following this, we will outline the method employed for data treatment, ensuring accurate analysis and interpretation of the collected data.In the second section, we will delve into the materials used to identify the type of soil studied, which is crucial for examining its thermal behavior. To achieve this, we employed a statistical test known as ANOVA (Analysis of Variance), which allows us to determine if there are statistically significant differences between the thermal properties of different soil types.Finally, in the last section, we will detail the materials used to conduct our experiments in three distinct chambers. These experiments aim to study the thermal behavior of the materials used in Algeria under real conditions. An electronic acquisition system was utilized to ensure precise data collection throughout the experimental process.

II.1 The M'Sila weather station

The M'Sila weather station (see Figure II.1) is located 7 km southwest of the town of M'Sila.It was put into operation on March 23, 1976. The latter is spread over an area of 1600 m2.

Figure II.1: M’sila weather station

Weather stations are equipped with equipment to monitor the Earth's atmosphere and thus provide information on the weather and therefore on the climate over the course of several years. Measurements taken at weather stations include temperature, atmospheric pressure, humidity, wind speed and direction, and precipitation.

A network of large-scale meteorological stations monitors meteorological conditions by periodically and regularly transmitting readings via the means of communication.

II.2. Manual and automatic station

The weather station was equipped with two types of stations.

- Manual station

A manual station is one where the measurement is done by a meteorological technician on a regular schedule, while an automatic weather station is a station whose sensors report a series of meteorological data at intervals without human intervention. The instruments are often the same in both cases, but some observations are more reliable when they come from a real observer. For example, cloud cover and the type of precipitation are more easily observed by a human being than deduced by an electronic instrument.

- Automatic station

Automatic stations (see Figure II.2) were developed for use in hard-to-reach places (weather buoys at sea or remote areas) but they are increasingly replacing manned stations because of their lower cost . Developed for meteorological services, they are now also used in meteorological research, for various specialized uses like agricultural meteorology and road conditions monitoring, even amateur meteorologists use this kind of station. They are most often grouped into networks to cover a given territory, their density varying from a few kilometers between stations (mesonets) to several hundred kilometers depending on the needs and accessibility of the sites.

The M’Sila weather station has benefited from an automatic mini-station since October 2015 (see Figure II.2), which allows more accurate readings of meteorological parameters every minute. Automatic station display placed outside the station inside M’Sila Mini Automatic Station .

Figure II.2: Mini station

II.2.1 Components of the weather station

There are several models of meteorological station, we describe in the following the model that is made available to us: The wired Vantage Pro 2 station developed by Davis Instrument (equipped in addition with UV and direct solar radiation sensors). In this weather station we find the following components:

- **Main unit**

The main unit is a console for receiving and displaying information from the station. Its large backlit touch screen is used to configure the options and choose the values to be displayed (figure II.3). The connection between the sensors and the unit is made by cable of several tens of meters. This console can be connected to a PC via a serial link. An additional data logger allows the information provided to be stored during PC shutdown[48]

Figure II.3: Console

- **Sensors**

For the wired Ventage Pro 2 station, the distance between the console and the sensor assembly is 30 m, which can be extended to 300 m. The sensors can be joined in a single block or in two blocks, allowing the separate installation of the vane anemometer. The sensors used are as follows:

a) Indoor Thermo-Hygro-barometer

It is a sensor integrated into the console that measures the temperature, humidity (hygrometry) and atmospheric pressure inside.

b) External Thermo-Hygro-barometer

This sensor is used to measure outdoor temperature and humidity values. It is integrated into the main station. And placed in the shade so as not to obtain false values. It is watertight which allows it to be placed in difficult conditions.

c) Wind vane and anemometer

It is a device capable of measuring both wind speed and direction. For optimal measurements, the sensor must be placed on a mast so as not to be disturbed by the environment close to the sensor. The anemometer provides instantaneous and average speed

measurements and records the strongest gust and its direction. Each speed can be consulted in several units (m/s); kph; knots).

d) Rain gauge

This sensor makes it possible to measure rainfall and its intensity. The sensor of the Vantage Pro weather station is integrated into the main station (Figure II.3), its resolution is 0.2 mm for rainfall [48].

II.2.2 Operation of the weather station

The set of integrated sensors collects outdoor and indoor metrological data, transmits them to the Vantage Pro2 console, the console displays this data, produces graphs, offers alarm functions and keeps the history of measurements for several years, however for finer storage, it is advisable to add a "Datalogger" data logger and to transfer the data regularly to the station PC. The autonomy of the Datalogger is variable according to the recording step which is configured by the user of the station.

The computer is the essential complement of the weather station, it is provided by the Weather Link software provided by the manufacturer of the station.

II.3 Meteorological data useful to process

The data to be processed in our thesis are the samples concerning the characteristic parameters of the atmosphere are the temperature and solar radiation using exel

First, we classified data according to the month then we create sheet for each day inside it ; we made table which help us automatically do calculation based on the function programmed inside see Figure II.4

Récapitulatif du 06/2017				
Tmoy (°C)	32,17	durée d'insolation	04:28	19:01
Global Rad (W/m2)	419821,00	14:33		
Mean Rad (W/m2)	480,34	Temp C max	40,30	
Global Energy (kJ/m2)	25183,08	Temp C min	23,40	
Mean Energy (kJ/m2)	28,81	Heure TAMX	15:11	
Max Rad (W/m2)	1118,00	Heure Tmin	05:04	
MinRad (W/m2)	0,00	EN max	66,94	
80% Rad Max	894,4			
Duré 80%	03:51	Heure En MAX	13:53	

Figure II.4: Table summarizing parameters studie

We also generate automatically graph inside the same sheet (with the table) to figure out the manner of the parameter's change see Figure II.5

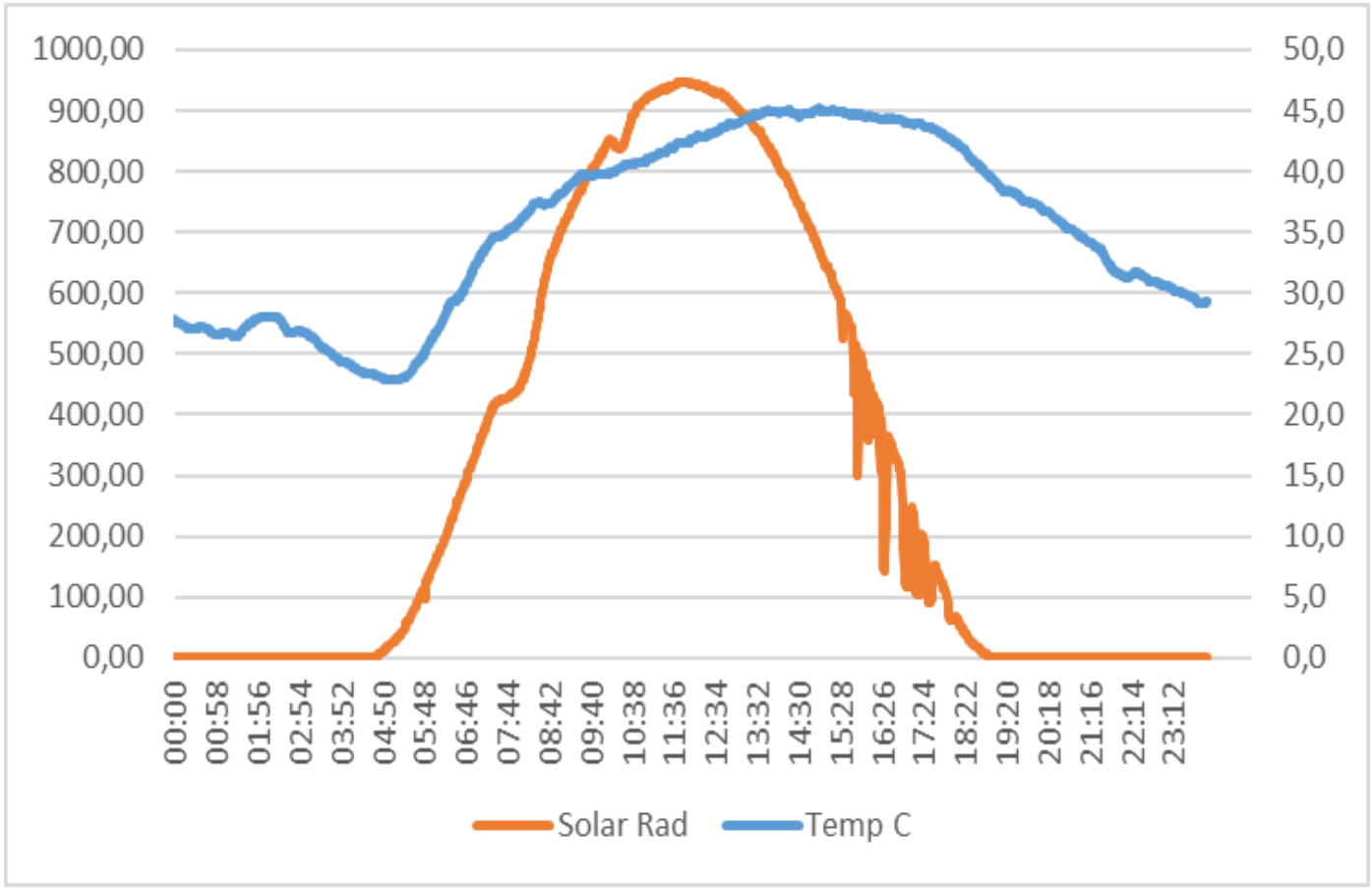

Figure II.5: Evolution of solar radiation and the temperature during one day

In the next step we create table which help us automatically to summarize the parameters calculated for each day in one table see Figure II.6

Mois	Date	Tmoy (°C)	Global Rad (W/m2)	Mean Rad (W/m2)	Global Energy (kJ/m2)	Mean Energy (kJ/m2)	Heure TAMX	Heure en Max	Ecart	Duree 80%	STAR	END	T min	Tmax	T min
Juin	01/06/17	27,57	441134,00	512,95	26467,15	30,78	14:31	10:34	3:57	03:21	09:54	13:15	4:38	34,80	17,9
	02/06/17	29,70	438430,00	509,21	26301,46	30,55	15:14	11:15	3:59	05:04	09:12	14:16	5:18	37,10	22,1
	03/06/17	28,96	419663,00	497,23	25180,57	29,83	13:54	11:48	2:06	06:15	08:56	15:11	23:51	37,90	21,9
	04/06/17	23,79	296146,00	380,16	17773,21	22,82	13:36	12:13	1:23	04:22	10:21	14:43	23:58	32,70	18,4
	05/06/17	20,17	292524,00	351,16	17553,97	21,10	16:15	10:57	5:18	03:44	10:21	14:05	23:35	26,10	15,9
	06/06/17	23,13	477476,00	553,27	28640,74	33,23	15:46	11:31	4:15	05:17	09:09	14:26	5:08	31,70	14,8
	07/06/17	27,60	478442,00	553,11	28423,59	33,22	14:11	11:29	2:42	05:16	09:08	14:24	3:38	33,20	14,8
	08/06/17	25,10	473817,00	547,13	28703,50	32,82	15:13	11:28	3:45	05:17	09:06	14:23	4:22	35,80	17,4
	09/06/17	31,20	414386,00	484,66	24855,47	29,07	15:19	12:29	2:50	04:43	09:41	14:24	3:11	38,20	24,9
	10/06/17	31,14	434919,00	499,91	26085,98	29,98	14:43	10:56	3:47	04:47	09:20	14:07	4:07	38,40	22,6
	11/06/17	31,05	462917,00	534,55	27771,30	32,07	14:37	11:35	3:02	05:15	09:10	14:25	4:20	37,40	24,6
	12/06/17	30,61	466241,00	534,68	27976,73	32,12	16:14	11:22	4:52	05:09	09:14	14:23	3:40	39,10	20,80
	13/06/17	28,76	476707,00	546,06	28594,71	32,75	15:07	11:42	3:25	05:09	09:13	14:22	4:27	35,10	22,5
	14/06/17	30,33	476382,00	548,20	28577,98	32,89	15:17	11:33	3:44	05:15	09:09	14:24	4:47	38,00	22,30
	15/06/17	32,92	431084,00	496,64	25866,32	29,87	14:09	12:17	1:52	04:59	09:39	14:38	4:51	41,20	22,90
	16/06/17	32,17	419821,00	480,34	25183,08	28,81	15:11	13:53	1:18	03:51	10:11	14:02	5:04	40,30	23,40
	17/06/17	30,86	455309,00	522,74	27310,64	31,36	14:30	11:31	2:59	05:14	09:18	14:32	3:49	40,50	21,80
	18/06/17	31,48	477487,00	546,95	28649,52	32,82	14:12	11:54	2:18	05:16	09:14	14:30	4:50	39,10	22,90
	19/06/17	29,68	464949,00	535,04	27894,73	32,10	14:40	12:09	2:31	04:56	09:23	14:19	4:55	35,60	21
	20/06/17	28,20	413903,00	540,34	24826,18	32,41	14:48	11:43	3:05	04:33	09:41	14:14	23:44	36,20	21,6
	21/06/17	29,76	436853,00	503,29	26211,09	30,20	14:46	11:45	3:01	05:17	09:13	14:30	3:20	37,70	20,1
	22/06/17	31,51	464932,00	534,40	27900,17	32,07	15:11	11:37	3:34	05:34	09:13	14:47	3:41	37,80	25,2
	23/06/17	30,61	474191,00	544,42	28443,67	32,69	15:25	11:49	3:36	05:06	09:18	14:24	4:52	37,60	21,7
	24/06/17	31,20	476807,00	548,05	28606,01	32,88	15:06	11:48	3:18	05:11	09:14	14:25	0:52	38,70	24,90
	25/06/17	33,16	472103,00	543,27	28318,99	32,59	14:37	12:14	2:23	04:18	09:47	14:05	3:14	41,00	23,6
	26/06/17	35,51	427764,00	508,64	25662,98	30,55	16:00	13:59	2:01	03:57	10:17	14:14	4:28	43,50	27,6
	27/06/17	35,45	348539,00	417,41	20908,28	25,07	12:57	11:51	1:06	04:25	10:00	14:25	4:32	42,80	25,7
	28/06/17	32,57	431582,00	497,79	25887,24	29,86	14:51	11:37	3:14	05:06	09:17	14:23	23:49	37,80	25,6
	29/06/17	28,82	431582,00	524,28	27268,38	31,45	14:48	11:55	2:53	05:04	09:15	14:19	4:04	36,80	20,2
	30/06/17	25,91	256341,00	297,38	15382,48	17,85	15:08	10:31	4:37	02:39	10:30	13:09	4:09	31,30	21,7

Figure II.6: Table summarizing parameters studied for each month

The final step is exporting all data from tables that present each month in one table This table summarize all data recorded by M'Sila weather station during 365 days in intervals of 5 minutes (big data). about 348378 line in 365 line

II.4 Identification and classification tests

All the tests of identification the type of the soil was done at Public Works and Buildings laboratory "DERARDJA FARIDE" Sidi Aissa MSILA

II.4.1 Grain size analysis

Two methods are used to do the analysis. Sieve Grain Size Analysis can determine particle sizes in the range of 0.08 mm to 125 mm. Visual categorization will be used for grains greater than 100mm, while the Hydrometer Method can be used to disperse particles smaller than 0.08 mm.

II.4.1.1 Sieve Grain Size Analysis

The standard P 94-560 used to define the procedure for determining the granularity of aggregates [49], the dimensions of which are between 0.008- and 12.5-mm figure II.6 shows different steps.

Figure II.7: Steps follow to determine grain size sieve

The test is conducted out using a set of sieves with varying mesh sizes. Every sieve contains a specific number of squared-shaped apertures. The sieve filters between larger and smaller particles, resulting in two volumes of soil sample. The sieve retains grains with diameters greater than the apertures, while smaller grain diameters pass through The test is performed by stacking a series of sieves with decreasing mesh sizes on top of one another and running a soil sample through the "tower" of sieves. The soil particles are dispersed as a result of the different sieves keeping them. The particles that pass through the final filter are gathered in a pan to trap them.

II.4.1.2 Experimental procedure

First, we take 1kg from weigh a dry soil sample each experiment .The weight of the sieves and the pan that will be used during the analysis is then recorded. Before the test, each sieve should be completely cleaned.

Assemble the sieves in ascending sequence, with the larger openings at the top. Therefore, Place the soil sample in the top sieve and cover it with a cap.Shake the stack for 10 minutes in a mechanical shaker.

Finally, we remove the sieve stack from the shaker and measure the weight of the soil retained using the pan after putting it in the oven to make sure that the soil become dry see figure II.7.

The soil retained on each sieve is estimated by subtracting the weight of the empty pan from the weight of the pan after the test.

The percentage retained on each sieve is calculated by dividing the total weight of the soil sample by the initial weight of the soil sample. The total percentage passing through each sieve is then computed by subtracting the cumulative percentage kept in that sieve and those above it from totality [49].

Figure II.8: Using pans to do sieve analyses

II.4.2 Hydrometer Grain Size Analysis

The standard NF P 94-570 used to define the procedure for determining hydrometer analysis As it is knowing hydrometer analysis is used for particle sizes finer than 80 μm These particles pass through the last sieve[50] .

A hydrometer is a device used to measure the relative density of a liquid, which is the ratio of the substance's real density to the density of water.

When soil particles sink, hydrometer particle size analysis takes advantage of the change in the relative density of the soil-water mixture. The test is based on the fact that when dirt is thrown into a liquid, the relative density of the soil-water mixture rises. As the dirt particles sink, their density reduces until it reaches the initial density of the liquid. The heaviest particles (those with the largest diameter) sink first.

II.4.2.1 Experimental procedure:

Take note of the soil's dry weight (typically, 80 gr), After collecting enough soil and passing it through the last screen, we insert 500 ml of distilled water in a steel mixing cup.

The dirt is then added to the mixture along with 5gr of sodium hexametaphosphate solution and mixed for 5-6 minutes with a high-speed mixer.

Fill a 1-liter cylindrical container halfway with distilled water with the mixture.

Place the container on top of a table and begin measuring time immediately after shaking.

Insert the hydrometer slowly into the container and take readings every 10, 20, 40, 80, 240, 1140 minutes. The height of the produced meniscus should be measured. Use of thermometer to measure the temperature [50].

Figure II.9: First Step to determine hydrometer grain size sieve

Figure II.10: Steps follow to determine hydrometer grain size sieve

II.4.2.2 Hydrometer Grain Size Analysis Calculations

For each series of measurements, the percentage by weight of the element contained in the suspension that is less than or equal to D and the equivalent diameter D of the largest non-sedimented particles are determined using the the equation mentioned below[51].

- **Percentage of element**

Percentage of element less than or equal to D contained in the suspension at time t is calculated by the following equation

$$p = \frac{V_s}{m} \times \frac{\rho_s}{\rho_s \times \rho_w} \times \rho_w \times \left[\frac{\rho_t}{\rho_w} - 1\right] \quad \text{(II.1)}$$

- **The density of solid particles**

The density of solid particles was calculated using the standard P 18-054 it well explained in the following pages

- **Density of the suspension**

The density of the suspension at time t is obtained from the following equation:

$$\rho_t = R_c \times \rho_w = (R + C_t + C_m + C_d) \times \rho_w \quad \text{.....(II.2)}$$

- **Equivalent diameter**

The equivalent diameter D of the largest non-sedimented particles are determined using the the equation

$$D = \left[\frac{1}{g} \times \frac{18 \times \eta}{\rho_s - \rho_w} \times \frac{H_t}{t}\right] \quad \text{.....(II.3)}$$

- **Dynamic viscosity of the solution**

To calculate the equivalent diameter D ,dynamic viscosity is determine by the following formula

$$\eta = \frac{0.00197}{1 + (\alpha \times \theta) + (\beta \times \theta^2)} \quad \text{.....(II.4)}$$

- **Effective depth of push center**

To calculate the equivalent diameter D. The effective depth of the densimeter's center is derived from the following relation

$$H_t = H - 100 \times H_1 \times (R + C_m - 1) - H_c \quad \text{.....(II.5)}$$

- **Displacement height of the solution due to the densimeter**

To determine Effective depth of push center we need to determine the height of displacement of solution due to density meter

$$H_c = 0.5 \times \frac{V_d}{A} \quad \text{.....(II.6)}$$

Finally, the particle size distribution presented in graphical form; the particle size in millimeters plotted on the abscissa (logarithmic scale) and their weight percentage on the ordinate with increasing scale see appendix A

II.4.2.3 Determination of the water content:

The water content is the most important parameter, the variation of which modifies all the physical properties of the soil. The oven-drying method for determination of water which is reliable with appropriate terms .

The water content is a physical quantity defined theoretically as being the ratio between the weight of water and the weight of the dry matter, the following equation is used to calculate it :

$$W = \frac{m_d}{M_w} \times 100 \qquad \text{.....(II.7)}$$

We did two test to take the average. to start the test , we take a clean, dry and tared container(pan), we place a sample of wet soil with a predetermined weight Then we put them in the oven after 15 hours, we take the weight. In principle between the two weighing's, the difference is less than 0.1%[52].

II.4.2.4 Specific weight

The volume of the sample will be:

$$V_s = \frac{(m_2 - m_3)}{\rho_w} - \frac{(m_2 - m_1)}{\rho_{wax}} \qquad \text{.....(II.8)}$$

The specific gravity of the wet soil will be :

$$\gamma_w = \frac{V_w}{m_1} \qquad \text{.....(II.9)}$$

The dry apparent specific gravity, It is given by the formula

$$\gamma_d = \frac{\gamma_w}{1 + \frac{W}{100}} \qquad \text{.....(II..10)}$$

Figure II.11: Steps follow to determine specific weight

II.4.2.5 Limits of Atterberg

Given their structures, clays have the property to absorb very large quantities of water or to dry out depending on the humidity conditions to which they are subjected.

Whatever the nature and the type of clay, this one mixed with more and more important quantities of water, ends up transforming itself into mud. The clay is in a liquid behavior, in an opposite situation where the clay is sufficiently dried the grains are very tightened and the bonds become intense, the clay is in a solid behavior. Between these two extreme states, the clay is malleable, it has a plastic behavior.

The Atterberg limits are intended to define the moisture states corresponding to the limits between these three states, the moisture state of the soil being expressed by its water content.

II.4.2.5.1 Experimental procedure:

The standard P 94-051 used to define the procedure for determining hydrometer analysis[52] The test is carried out on a portion of the material sieved with a 0.40 mm sieve. The water content of a soil is the ratio between the weight of water contained in a

certain volume of soil and the weight of solid grains contained in the same volume. It is expressed in [%] and has the symbol W (water)

- The liquid limit WL: reflects the transition between the liquid and plastic state.
  WL =W (N/25)0.121
- The plasticity limit WP: corresponds to the transition between the plastic and solid state. water content is WP
- The plasticity index IP: The plasticity of a soil (i.e. its capacity to become very deformable by absorbing water) is assessed by the couple (WL, IP) which depend on the nature of the clay minerals contained in the soil and their quantity.

This is how Casagrande defined a diagram known as the "Casagrande Plasticity Abacus", which allows fine soils to be classified.

IP = WL – WP …….……..(II.11)

Figure II.12: Steps follow to determine Atterberg limits

We place the soil in the small container, taking care not to enclose any air bubbles. Place the container under the penetrometer. Using the screw, lower the cone + frame assembly until it touches the ground Act on the circle to set it to 0 Carry out a release Measure the penetration by gently acting on the needle (central wheel).

❖ **Liquid Limit (WL)**

The soil is mixed with a quantity of water. The resulting paste is placed in a dish with a diameter of about 100 mm. A standardised groove is drawn on the smoothed paste with a special tool.

A series of shocks is applied to the cup with a cam. At the end of the experiment, the contact of the two lips of the groove is observed. The liquidity limit is the water content in (%) which corresponds to a closure in 25 shocks.

❖ **Plasticity limit (WP)**

Measured with the roller method represents the water content of the transition from the plastic to the solid state. The sample is mixed with varying amounts of water and the dough is used to form a roll with a diameter of 6 mm and a length of about 100 mm. After 5 to 10 revolutions maximum, the diameter of 3 mm is reached by rolling it (often with the fingers).

The plasticity limit is the % water content of the roll that cracks and breaks when it reaches a diameter of 3 mm.

The accuracy of the test is in the order of half a point of water content for the determination of the liquid limit and of one water content point for the determination of the plastic limit. plasticity

II.5 Thermal conductivity determination

II.5.1 Sample preparation technique

The samples utilized in this study were created using the conventional method for making construction bricks used in the province of M'Sila. M'Sila is a northern Algerian interior province. Its climate has now shifted from semi-arid to arid (climate change). [53] Raw material preparation, forming, and drying are the three basic phases in the production of clay bricks (samples in our case)[54-57]. These stages are shared by all traditional techniques throughout the world. In this study, two types of soil were used: soil from an agricultural area near M'Sila town (in the province of M'Sila) and soil collected from a type of desert terrain (Hamada). Both soils were used to construct structures. Sand, silt, and clay are three elements found in all soils in varying quantities.

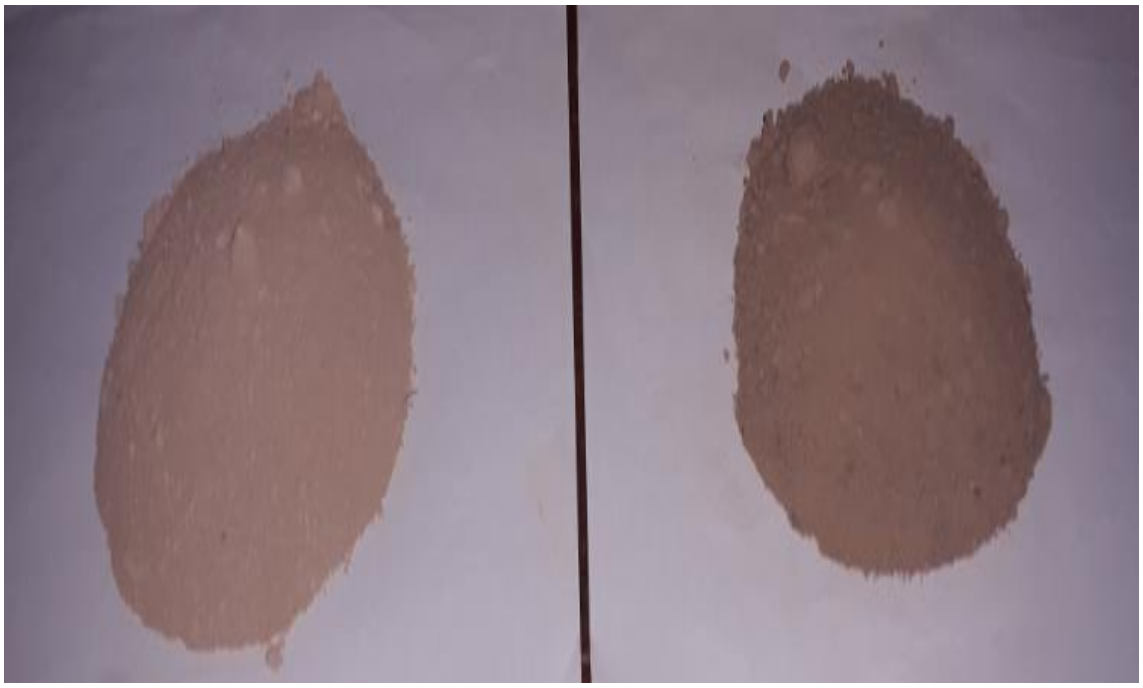

FigureII.13:Two kinds of soil tested

Wheat straw is a widespread and low-cost byproduct of wheat grain harvesting (figure II.14). These wheat stalks were sun-dried and chopped into small bands without any of the conventional treatments (alkaline treatment, acetylation, hydrothermal treatment, and water repellent coating).

Figure II.14: Straw added

Each soil type was sieved to homogenize and eliminate undesirable elements before being blended in various amounts with the short strip wheat dry straw. The criterion used in this study to assess the influence of straw addition on the thermal conductivity of earthen bricks is the ratio of soil mass to straw mass R (R= Soil mass/Straw mass). Thus, for each

soil, five samples were prepared and analyzed, namely R=20, R=40, R=50, and R=60, in addition to the reference sample without straw (see figure II.12). Add water to the soil and straw combination and kneaded by hand until malleable dough was obtained. Parallelepiped wooden molds were used to make samples of 10 10 1 cm3 from the malleable mixture that was poured and pressed into them (see figure II.15). After drying, the produced samples shrink slightly. As a result, the dimensions of the molds utilized were somewhat larger than those of the samples. The samples in the molds were sun-dried for several days before being removed and allowed to dry naturally again.

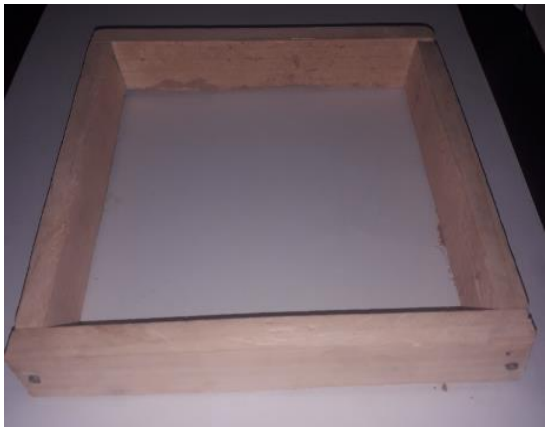

Figure II.15: Mold used

Figure II.16: Prepared samples reference one without straw R=20, R=40, R=50, and R=60

The finalized samples were wiped up to smooth their surfaces and, if necessary, reduce their size. Figure II.16 shows an example of one of the samples produced..

The experimental technique utilized in this study demands that the sample be split into two equal halves in order to determine thermal conductivity.

II.5.2 Experimental Setup

The hot wire method [58-61], first proposed by Carslaw and Jaeger [62], is one of the most widely used methods for determining the thermal conductivity of a medium (solid, liquid, or gas) in a transient regime. The temperature rise in a defined distance from a linear heat source (hot wire) immersed in the sample test material is measured using this approach. It has been effectively applied to poor heat conductivity materials and soils. It just takes a short time to implement and achieve the intended effects, which is why it is classified as a quick and simple technique.

The hot-wire measurement setup used for this study is made up of the following components (see Figure II.17): a heated wire (embedded in the investigated sample), a thermocouple placed in the middle of the wire, an HP power supply (current source and voltage meter), and a digital display connected to the thermocouple that displays the measured temperatures. As shown in Figure II.B.9, the heated wire is connected to the HPE3632A power supply (two white wires).

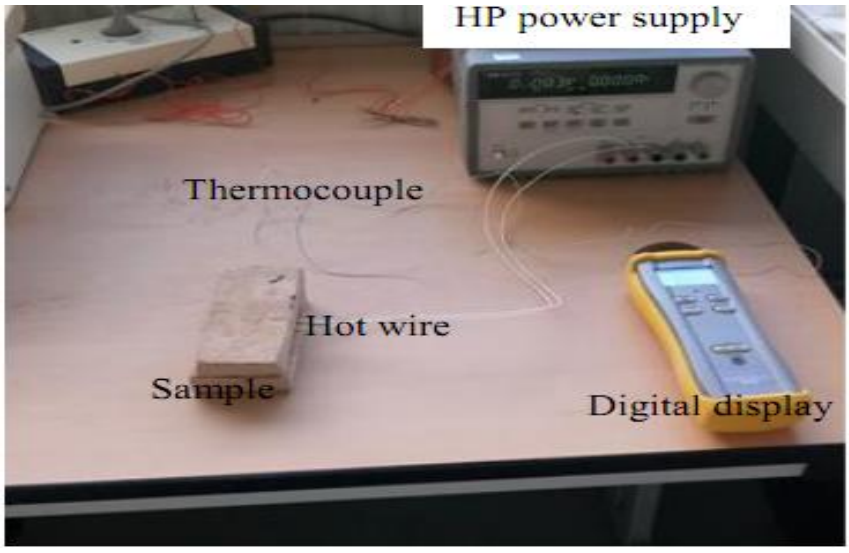

Figure II.17: Hot wire experimental device

The hot wire is a long and thin wire that is heated by running a steady electrical current across it, which is supplied by the HP power source. A thermocouple (heat sensor) is wrapped around the hot wire to electrically insulate it and the thermocouple from the test

material. Over a known time interval, the observed temperature varies linearly as a function of ln t. The following equation, with a decent estimate, gives it:

$$T(t) = \frac{\phi}{4\pi L\alpha} ln(t) + Cte \qquad \text{.....(II.12)}$$

The thermal conductivity of the material tested can be calculated from the slope of the line depicting the progression of temperature as a function of the natural logarithm of the measurement time Ln t as follows:

$$\lambda = \frac{\phi}{4\pi L\alpha} \qquad \text{.....(II.13)}$$

II.5.3 Experimental procedure

The samples were divided into two equal portions. The heating wire was integrated between two equal pieces of the same sample, put one on top of the other, for each experiment (Figure II.18).

Good thermal contact between the hot wire and the sample was achieved by filling the existing space with fine particles produced by polishing the sample surface, as well as placing a heavy object on the upper part of the sample to slightly compress the two sections in touch. Each experiment lasted for 180 seconds (short period). Thermal conductivity, which defines the ease or difficulty of distributing heat through a material, was measured in both longitudinal and transverse directions, depending on the position of the heating wire in relation to the sample dimensions.

The heating wire is heated by a steady electric current produced by the HPE3632A power generator. The temperature in the core of the hot wire was manually recorded every 20 seconds for a total of 180 seconds from the commencement of heating.

Each test was done three times to ensure that the experimental approach was reliable.

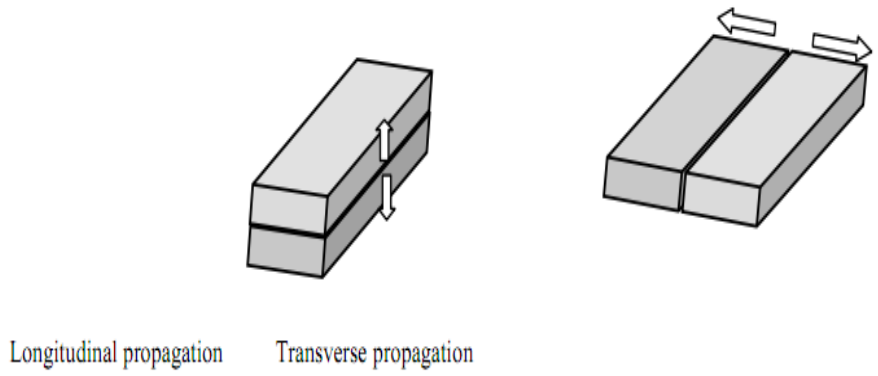

Figure II.18: Heat propagation directions

II.6 Analysis of variance

The analysis of variance (term often abbreviated by the term ANOVA: Analysis Of Variance) is a way of verifying that several samples come from the same population. [63]

This test applies when measuring one or more categorical explanatory variables (then called variability factors, their different modalities sometimes being called “levels”) that have an influence on the distribution of a continuous variable to be explained. One speaks of one-factor analysis, when the analysis relates to a model described by a factor of variability, of two-factor analysis or of multifactorial analysis. [63-64]

In ANOVA the fluctuation is conceptualised as entireties of squared deviations from the mean, which is as a rule abbreviated to wholes of squares and signified by SS. So we have three sums of squares to calculate:

- Total sum of squares, called SS total
- Between-groups sum of squares. Usually the change that represents the contrast between the bunches, and typically calle SS between. Now and then it alludes to the between bunches whole of squares for one indicator, in which case it’s called SS predictor. In our case, the indicator is the thermal conductivity, so we would call it SS thermal conductivity. The between-groups change is the fluctuation that we are really curious about. We are inquiring whether the distinction between the bunches (or the impact of the indicator) is enormous sufficient that we seem say it isn't due to chance.
- Error sum of squares, too called within-groups sum of squares. It’s inside the groups, because distinctive individuals, who have had the same thermal conductivity, have diverse values. And they have different value because of error. So, this is called either SS_{within}, or SS_{error}[4]

II.6.1 Fundamental assumptions

The general form of the analysis of variance is based on the Fisher test and therefore on the normality of the distributions and the independence of the samples. [63-64]

II.6.1.1 Hypotheses to be tested:

The null hypothesis compares to the case where the distributions follow the same normal law. The alternative hypothesis is that there is at least one distribution whose mean deviates from the other means .In our study case for :

- **One way ANOVA** which use to prove the reliability of our experience the null hypothesis is :

The thermal conductivity measurement repeated 3 times it means

$$\mu 1 = \mu 2 = \mu 3 \quad \text{(II.14)}$$

In other word e can say there is no significant effect in the repeated experience (the measurement of the thermal conductivity)

- **Two way ANOVA** the null hypothesis are:

- Measurement by direction has no significant effect on the thermal conductivity.
- Portion of soil /staw has no significant effect on the thermal conductivity.
- The direction of the measurement and the portion interaction has no significant effect on the thermal conductivity.

II.6.2 Calculating of sum of squares

We have to be calculate the three sorts of wholes of squares

- **Total sum of squares**

SS total is the sum of the squared differences between the mean and each score. The formula is:

$$SS_{\text{total}} = \sum (x - \bar{x})^2 \quad \text{(II.15)}$$

where x is each value, and x – is the mean of all values.

- **Within sum of squares**

The next step is to calculate SSwithin. The procedure is very similar, but this time we are seeking for the sum of squares within each group. Instead of using the total mean, we use the mean for each group. The formula is:

$$SS_{\text{within}} = \sum (x - \bar{x}_g)^2 \quad \text{(II.16)}$$

where x is each value, and x – is the mean of all values in each group

- **Between-groups sum of squares**

SSbetween can be calculated by two way the easiest is by using this formula

$$SS_{\text{total}} = SS_{\text{within}} + SS_{\text{between}} \quad \text{(II.17)}$$

II.6.3 Calculating statistical significance

To calculate the statistical significance of the impact of thermal conductivity we utilize the sums of squares once more. the statistical significance is dependent on the test measure[63-64],

To calculate the statistical significance, we first need to calculate the mean squares, often written as MS. And we have MS within for mean squares within groups, and MS between for mean squares between groups. We don't have MS total though .to calculate them we need three sets of degrees of freedom, called df_{total} ,$df_{between}$ and df_{within} (or df_{error})as step 01 all this factor are related by this formula

$$df_{total} = df_{between} + df_{within} \quad \text{.....(II.18)}$$

To calculate df_{total} we use

$$df_{total} = N - 1 \quad \text{.....(II.19)}$$

Where N present the number the sample size,

To calculate dfbetween, we use the number of groups

$$df_{between} = g - 1 \quad \text{.....(II.20)}$$

The most effortless way of calculating dfwithin is to utilize:

$$df_{within} = df_{total} - df_{between} \quad \text{.....(II.21)}$$

Step 2: Calculate the mean squares.

We do this by dividing the sums of squares by the degrees of freedom. For MSbetween:

$$MS_{between} = \frac{SS_{between}}{df_{between}} \quad \text{.....(II.22)}$$

For MSwithin:

$$MS_{within} = \frac{SS_{within}}{df_{within}} \quad \text{.....(II.23)}$$

Step 3: Calculate F.

At last we calculate the relative measure of the two values, by dividing MSbetween by MSwithin. This gives us the test statistic for ANOVA, which is called F, or in some cases the

F-ratio. Similar to the other test statistics, F doesn't mean anything, we just utilize it to calculate the probability.

$$F = \frac{MS_{\text{between}}}{MS_{\text{within}}} \qquad \text{……..……..…….(II.24)}$$

Step 4: Calculate the p-value.

To find the probability associated with F we need to have two sets of degrees of freedom, the between and the within.

$$\text{P-value} = \text{fdist}(df_{\text{between}}; df_{\text{within}}) \text{ ……..……(II.25)}$$

Knowing the p-value let us decide if we can reject the null hypothesis or not base on the value if it is greater than 0.05, so we cannot reject else we can .

II.7 Building material soil and straw

It is worthy to note that all the preparation was done at home with our means. Figure II.17 shows the different steps followed during the construction of compound walls earth and straw.

Figure II.19: Steps followed during the construction of the old brick walls.

In fact, we mixed a quantity of sifted earth (impurities) with dry straw in well-defined proportions according to the technique used in the region of M'sila [65] . water is then added to this mixture in order to obtain a manageable paste which has been poured into molds of very precise dimensions, and left to air dry naturally The walls thus obtained are used in the construction of the old brick chamber

II.8 Digital acquisition system

This system is used to record the evolution of the temperature inside the designed rooms and on the faces of the walls of different materials for 24 hours at one-minute intervals. It is mainly composed of:

- Arduino board,

- Temperature sensors, in addition to connector cables.

II.8.1 Arduino board

The essential component of an Arduino UNO is the ATmega328p microcontroller from Atmel (now MicrochipTM), which is the big chip with 28 legs in Figure 4.1. It's an 8-bit register controller with a 16MHz clock frequency. It has 32 kB of RAM memory and 1 kB of non-volatile EEPROM memory, both of which can be used to hold durable data that must withstand tuning adjustments and supply voltage fluctuations. On the board, there are three timers, which are essentially counters that count clock cycles and can be programmed to do a specific action once the number reaches a certain value.

The UNO communicates with its surroundings via 13 digital input/output (IO) pins, the majority of which may be configured as input or output and has software-configurable pull-up resistors. Several pins can be set up to handle I2C, SPI, or RS-232 communication. There are also six analog input pins. They can measure voltages up to 5 volts, which is the supply voltage. A 1.1V reference is provided by an internal reference voltage source. In Figure II.18, all digital and analog pins are routed to pin headers on both sides of the Arduino printed circuit board (PCB). Furthermore, an RS-232-to-USB converter is linked to the built-in hardware RS-232 connector, allowing connection and programming from a host computer. There is no support for WiFi, Bluetooth, or Ethernet on this device. [66] [67].

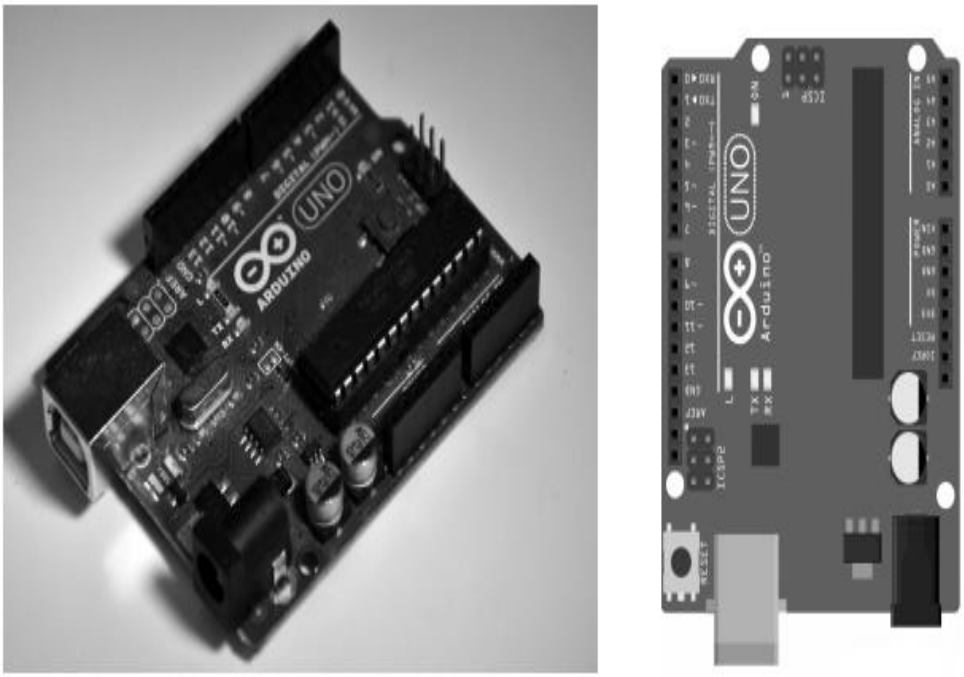

Figure II.20: An Arduino UNO

II.8.2 LM35 temperature sensor

The output voltage Vs of the LM35 is proportional to the temperature T, with Vs = T=100: The temperature is recorded in degrees Celsius, and Vs is measured in volts, so a temperature of 23 ^{o}C results in a voltage of 0.23V. The LM35 has three pins: one connected to ground, one to the supply voltage, and the third carrying the temperature-proportional voltage Vs. Figure II.21 shows the polarity for attaching the LM35. The smooth surface on the left-hand side is pointing at the wires[67].

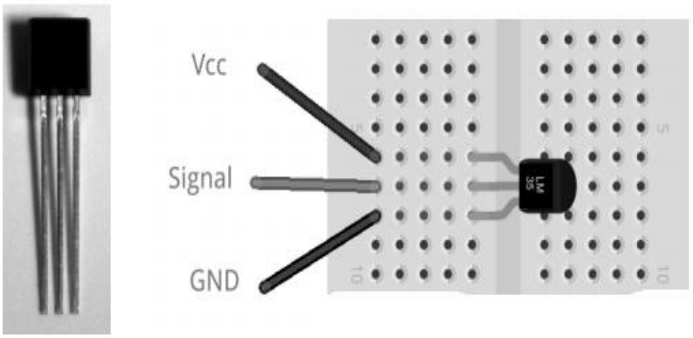

Figure II.21: LM35 temperature sensor

II.8.3 Connector cables

Figure II.22 shows the different cables used to connect the electronic assembly described above.

Figure II.22: Wiring of the electronic assembly used

II.9 Experimental procedure

To analyze the progression of the temperature inside three similar chambers of 20*20*20 cm3 made of sheep wool, adobe brick, and ordinary brick, as shown in Figure II.23,

Figure II.23: Three identical chambers

The tent is made of sheep wool fabric that wraps around a timber frame that is the same size as the other two rooms. It's worth noting that the three chambers have the same interior volume. The brick rooms' walls (adobe and ordinary bricks) are of similar thickness (5 cm). As a result, the outer volume of these two chambers is the same.

The tent, on the other hand, has the smallest external volume due to the 0.5 cm thickness of the wool cloth. The average brick room's walls are well cemented.

Three temperature sensors were set in the center of three chambers that were 10 cm apart and aligned . Using digital capture technology, the temperature within the chambers made of various materials was recorded for 24 hours at one-minute intervals.

Chapter III

Results and discussion

Introduction

In this chapter, we will address the data concerning temperature and solar radiation incident on a horizontal surface, recorded by the meteorological station of M'Sila over a span of 365 days at 5-minute intervals. This extensive dataset, often-referred to as big data, is critical for estimating the solar energy potential in the region. Furthermore, we will provide a detailed description of the graphical interface of the 'Calculateur Solaire' that we have developed. This interface enables users to calculate various solar angles pertinent to all Wilaya of Algeria, enhancing the accessibility and application of solar energy data. Moving on, we will present the results obtained from our experiments aimed at identifying the properties of the soils studied. These findings will be contextualized with explanations drawn from the existing literature, offering insights into the characteristics and behaviour of different soil types under various conditions. This section serves to bridge our experimental observations with theoretical frameworks, ensuring a comprehensive understanding of soil properties. Lastly, we will discuss the results from our experiments investigating the thermal behaviour of three distinct building materials commonly used in Algeria. These experiments were conducted.

III.1 Duration of the day in M'Sila

The day is the time interval between sunrise and sunset. The day is preceded by dawn in the morning and gives way to twilight in the evening. Its beginning and duration depend on the time of year and the latitude; thus, the day can last 6 months at the Earth's poles. Figure III.1 shows the daily evolution of the duration of the day in M'Sila during one year of study.

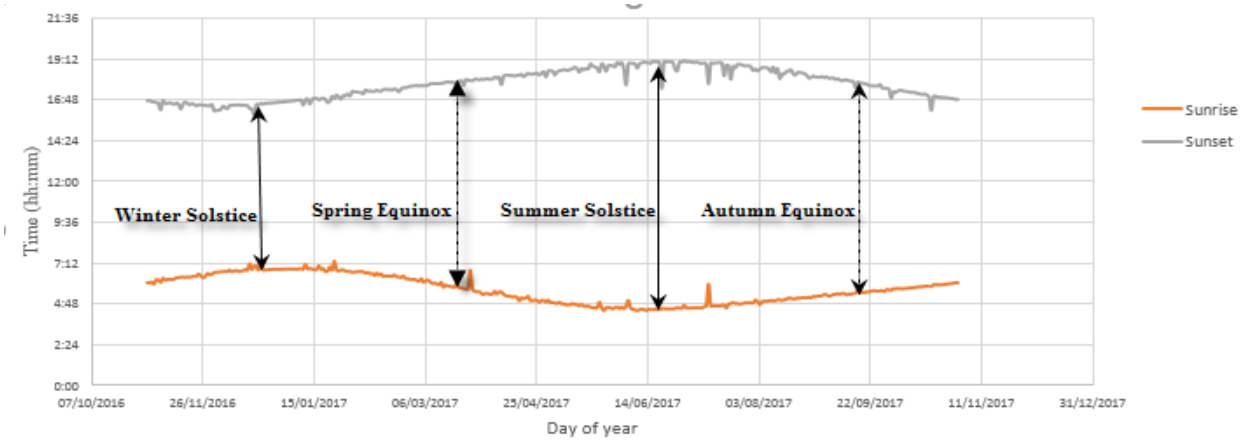

Figure III.1: Daily evolution of day length in M'Sila during one year of study.

Figure III.1 shows that the longest day (summer solstice) occurs on June 18 and lasts 14h 19min and 48s, while the shortest day (winter solstice) recorded on December 19 lasts 8h 30min and 36s.

Indeed, the winter solstice is the day of the year when the course of the Sun in the sky is the shortest and the lowest above the horizon. Compared to all other days of the year, the Sun rises farthest from the east, rises lowest at the noon or meridian (this is the declination) and sets farthest from the west. The summer solstice is the day of the year when the Sun's course in the sky is longest and highest above the horizon (see Figure III.2).

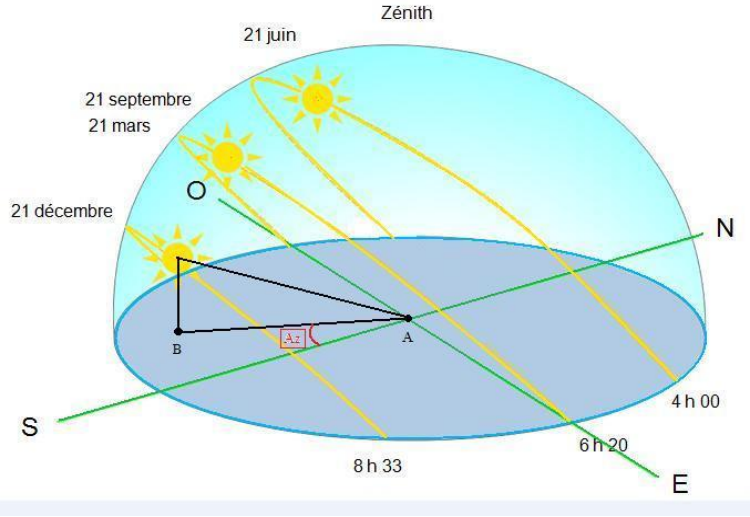

Figure III.2: Path of the sun in the sky during the beginning of the seasons.

An equinox is a time of the year when the Sun crosses the Earth's equatorial plane; changing celestial hemisphere. It designates the moment when the duration of the day is equal to that of the night (12h). On that day, at noon, the Sun is exactly at the zenith on the Earth's equator. The spring equinox occurs in M'Sila on March 18, and the fall equinox on September 22.

Figure III.2 shows that from the fall equinox occurring on September 22 (early fall and late summer), the days continue to decrease until December 19, the winter solstice (early winter and late fall), then increase until June 18, the summer solstice (early summer and late spring) through the spring equinox on March 18 (early spring and late winter).

Taking into consideration the length of the day, we can say that M'Sila is sunny for 4388 hours during one year. On average, the sun is present in M'Sila's sky for 12h 1min and 18s per day, or 365h and 40min per month.

July is the sunniest month with a day length of 434h 18min and 18s. We also note that December is the least sunny month with 298h 7min and 48s.

The average day length for the six (06) months of April, May, June, July, August and September exceeds the annual average estimated duration of 12h 1min and 18s per day.

After this analysis, it is noted that the duration of the day in M'Sila exceeds 8h 30min and 36s per day and does not reach 14h 30min per day.

III.2 Evolution of the air temperature in M'Sila

Modern meteorological stations instantaneously record air temperatures, under cover at 1.5 meters above the ground, to define the daily temperature evolution curve at a given location. The average monthly temperature is also determined in order to draw the annual temperature evolution curve at a location.

III.2.1 Daily evolution of the air temperature in M'Sila

Figure III.3 shows the evolution of the instantaneous air temperature during the day, the summer and winter solstices and the spring and autumn equinoxes.

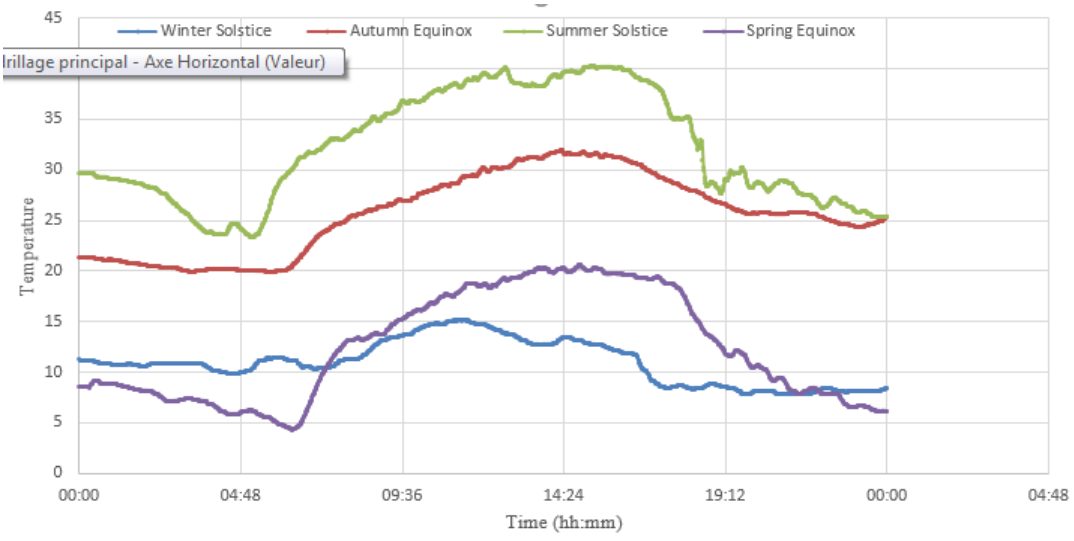

Figure III.3: Daily temperature evolution at M'Sila at the beginning of the four seasons.

The curves describing the daily evolution of the air temperature in M'Sila show the same pattern, they admit two extremes (limit values), a peak (Tmax) which occurs during the day on average around 14h 21min, and a minimum (Tmin) occurring at night on average at 5h 11min.

It can be seen in Figure III.3 that the air warms during the day, resulting in an increase in temperature, due to incident solar radiation, and cools at night by infrared radiation towards the celestial vault. According to Figure III.3, the air temperature is influenced by the position Earth - Sun (Day/Night, time of the year).

During the day and under clear skies, the difference between the two extremes (Tmax and Tmin) is important, it can reach up to 22.3°C (See Figure III.4), due to the heat exchanges between the terrestrial globe and the extraterrestrial. This difference, on the other hand, is less pronounced under cloudy skies, it is of the order of 1.9°C (See Figure III.4b), due to the cloud mask that slows down the heat exchanges.

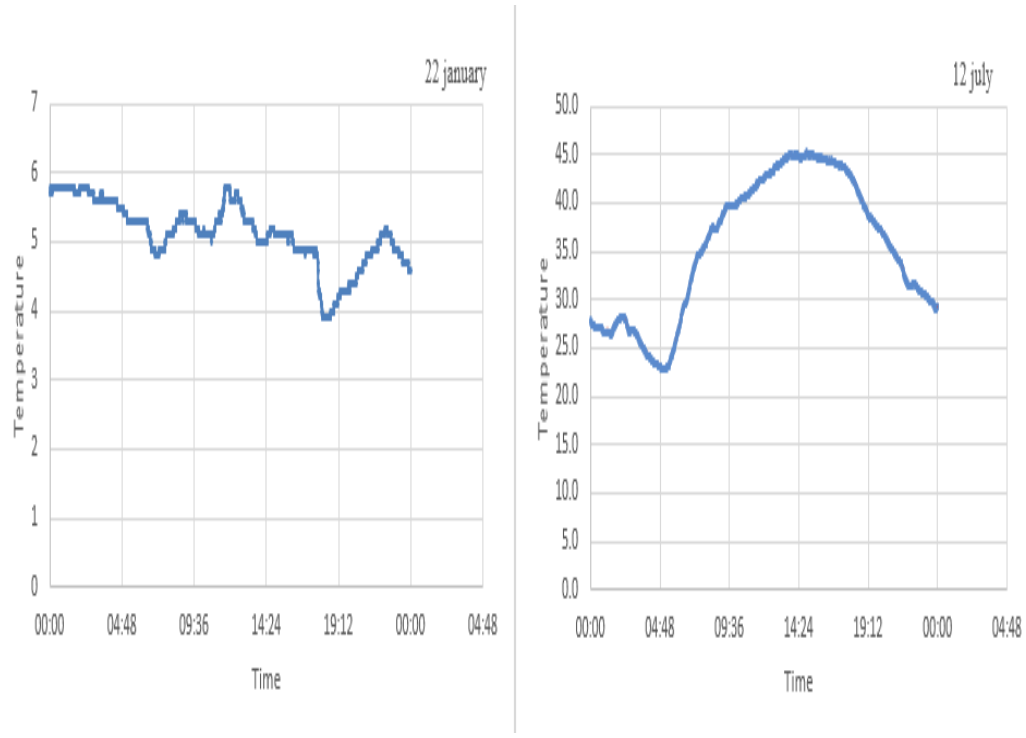

Figure III.4: Effect of the nature of the sky on the daily temperature evolution at M'Sila (a. clear sky; curve with two distinct peaks (12July) b. cloudy sky; flatten curve 22 January

III.2.2 Monthly evolution of the air temperature in M'Sila

Figure III.5 shows the evolution of the mean daily air temperature during the months of March, September, June and December.

It can be seen that the monthly evolution of the air temperature is not uniform, as was the case previously seen for the daily evolution. Indeed, the average daily temperatures tend to rise in the months of March and June and to fall in the months of September and December.

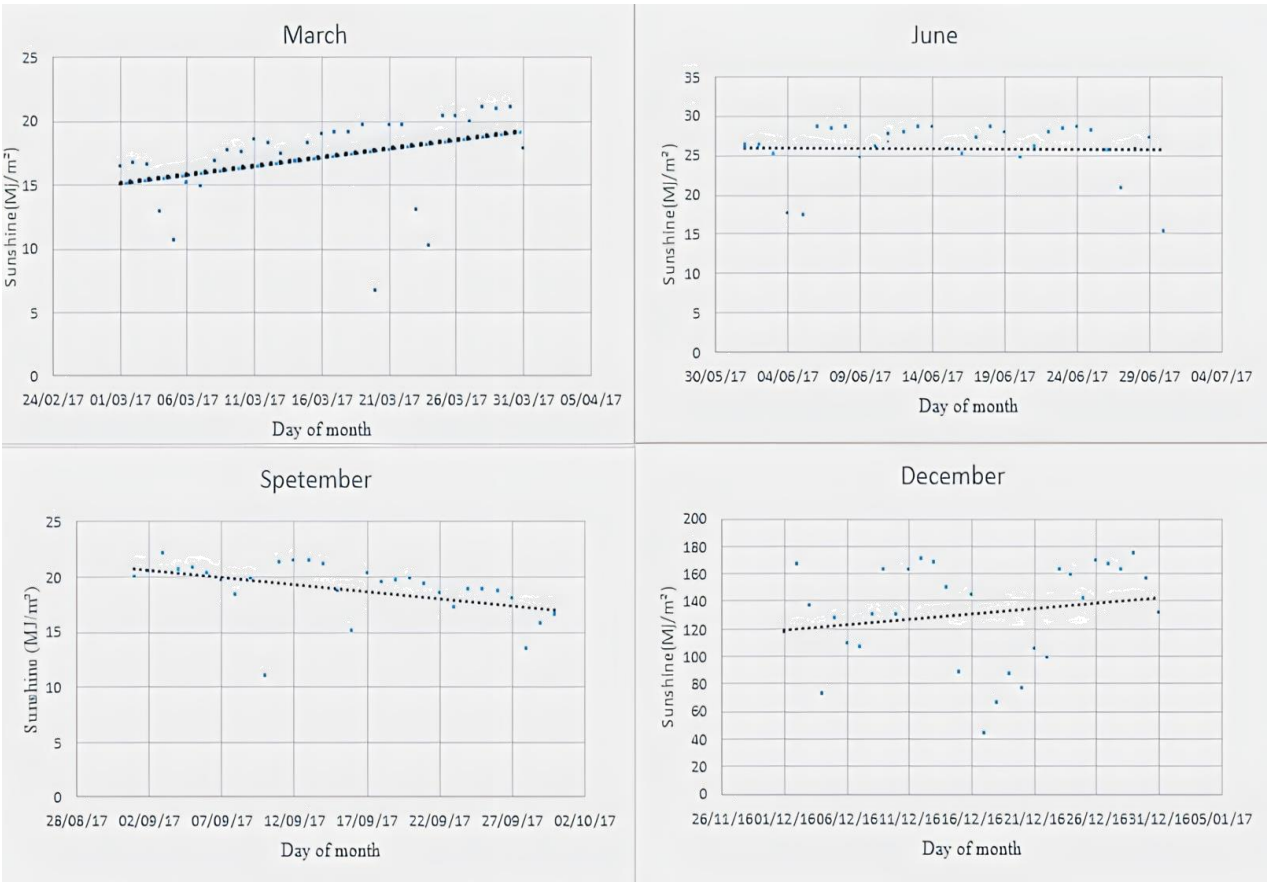

Figure III.5: Monthly evolution of air temperature in M'Sila for the months of March, September, June and December.

III.2.3 Annual evolution of the air temperature in M'Sila

Figures III.6 show the evolution of the monthly and daily mean air temperature during the study year respectively. It can be seen that the two curves have the same appearance except that the one giving the evolution of the monthly mean temperature is finer (more refined), showing fewer fluctuations.

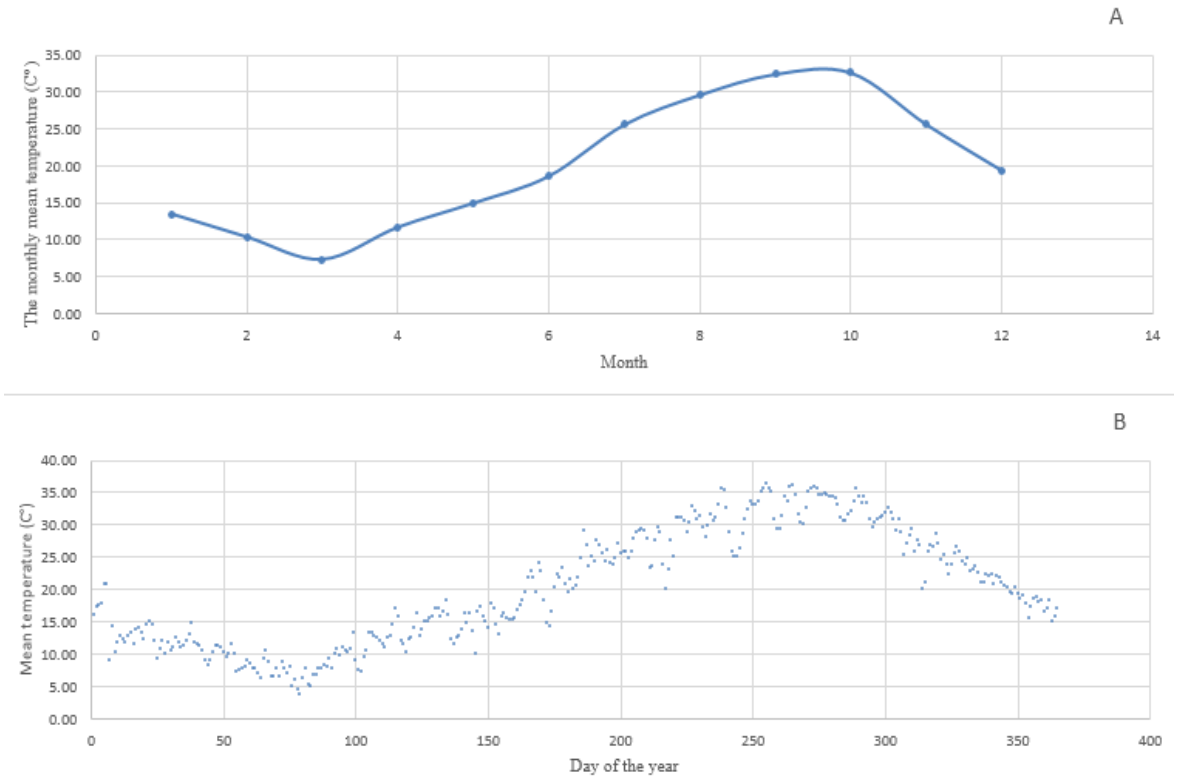

Figure III.6: Evolution of air temperature at M'Sila during one year of study.

We also notice that these two curves have the same appearance as the one giving the daily evolution of the temperature. Indeed, they admit two extreme values (one max and one min). The maximum monthly average temperature recorded during the study year occurs in the month of August with a value of 32.63°C. Figure II.6b shows that on July 13, the temperature recorded is maximum and is of the order of 36.42°C.

The mean minimum temperatures recorded are 7.26°C and 3.83°C recorded for the month of January and 18 January respectively.

For the five (05) months of May, June, July, August and September, the average monthly temperature is above the estimated annual average temperature of 20.12°C at M'Sila.

For the three (03) months of June, July and August, the average monthly temperature is greater than or equal to 80% of the maximum monthly average temperature at M'Sila.

Figure III.7 shows the evolution of the mean diurnal (daily) temperature and the duration of the day as a function of the days of the study year.

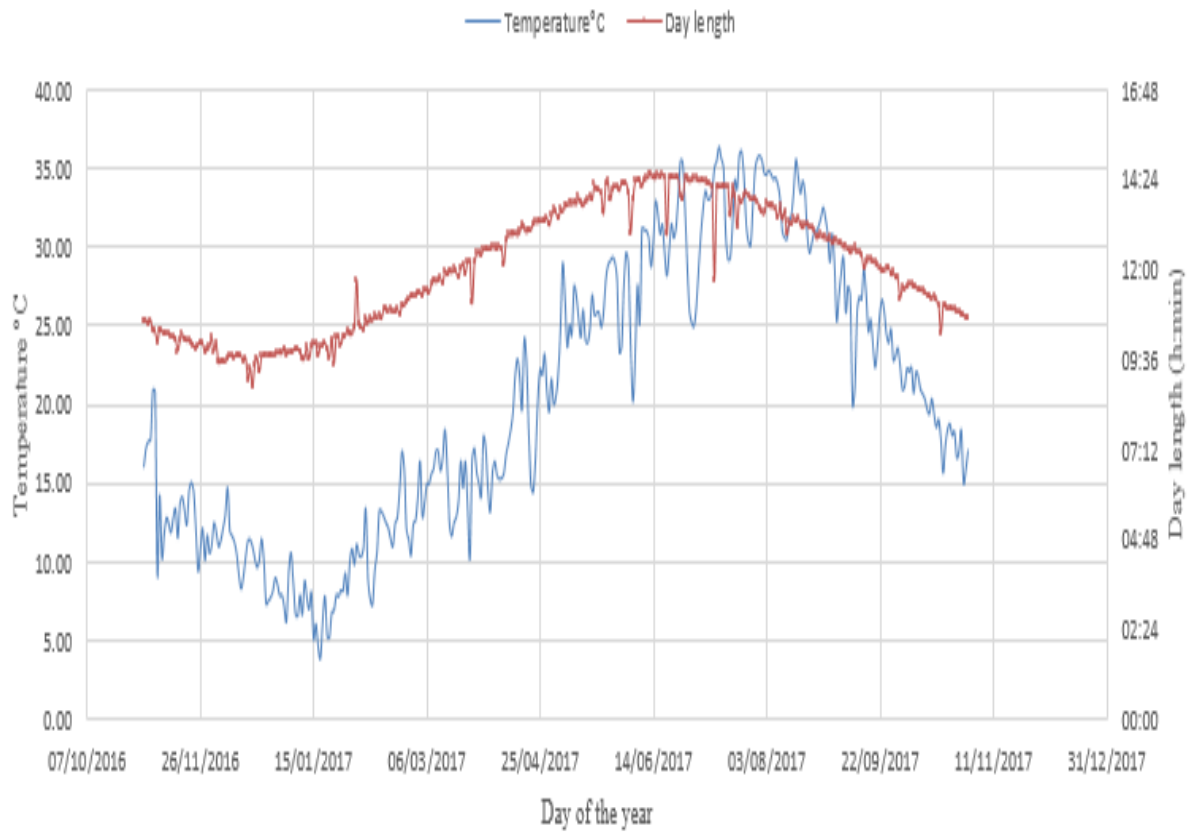

Figure III.7: Evolution of the mean diurnal temperature and day length during the study year.

It can be seen that there is a difference of three (03) weeks and three (03) days between the longest day (June 18) and the day with the highest temperature (July 13) which is due to the thermal capacity of the air.

III.3 Evolution of sunshine / irradiance at M'Sila

Sunshine, also called insolation, is a measure of the solar radiation that a surface receives over a given period of time, expressed in megajoules per square metre, MJ/m2 (as recommended by the World Meteorological Organization) or watt-hours per square metre, Wh/m2. This measurement divided by the recording time provides a measure of power density, called irradiance/irradiance, expressed in watts per square meter (W/m2).

III.3.1 Daily evolution of sunshine / irradiance at M'Sila

Figure III.8 shows the daily evolution of the energy received over a horizontal surface of 1m2 at M'Sila during the summer and winter solstices and the spring and autumn equinoxes. The curves thus obtained have the same shape (the shape of a bell). They start at sunrise, go through a maximum and end at sunset.

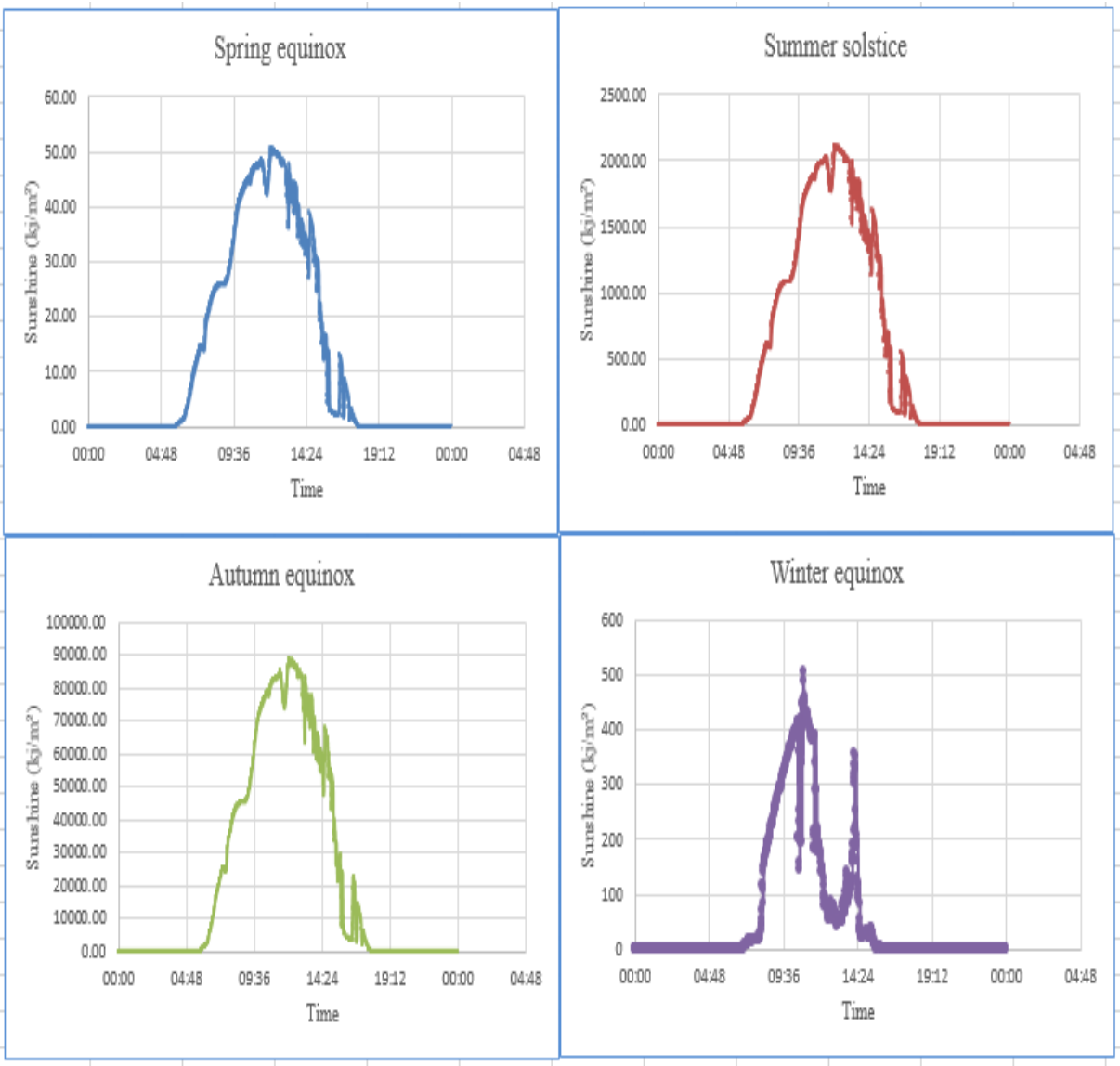

Figure III.8: Daily evolution of sunshine in M'Sila at the beginning of the four seasons.

In fact, during the 365 days of the study, no day was free of clouds. This is confirmed by the fluctuations recorded on the curves giving the evolution of sunshine during the day in M'Sila. In other words, if the sky is clear in the morning, it will not be clear in the middle or at the end of the day.

The time of the beginning and the end of the curve giving the daily evolution of the sunshine in M'Sila depends on the time of sunrise and sunset which vary from day to day.

On average, the daily sunshine reaches its peak in M'Sila around 11:40 am. During the year of study the peak of the daily sunshine in M'Sila occurs between 9:14 am and 1:59 pm.

The maximum sunshine received at M'Sila during the day does not occur at the same time as the peak air temperature. An example is given in Figure II.9. In fact, the air heats up due to the radiation from the sun and reaches its maximum temperature after receiving maximum energy. The difference between the moment when the sunlight is at its maximum and the moment when the temperature is at its peak is explained by the thermal inertia of the air. This phase shift is estimated on average at 2h 36min during the year of study, it varies according to the day of the year and the nature of the sky.

Sunshine and irradiance follow the same evolution whether it is daily, monthly or yearly. For this reason, we will limit ourselves to studying sunshine in more detail.

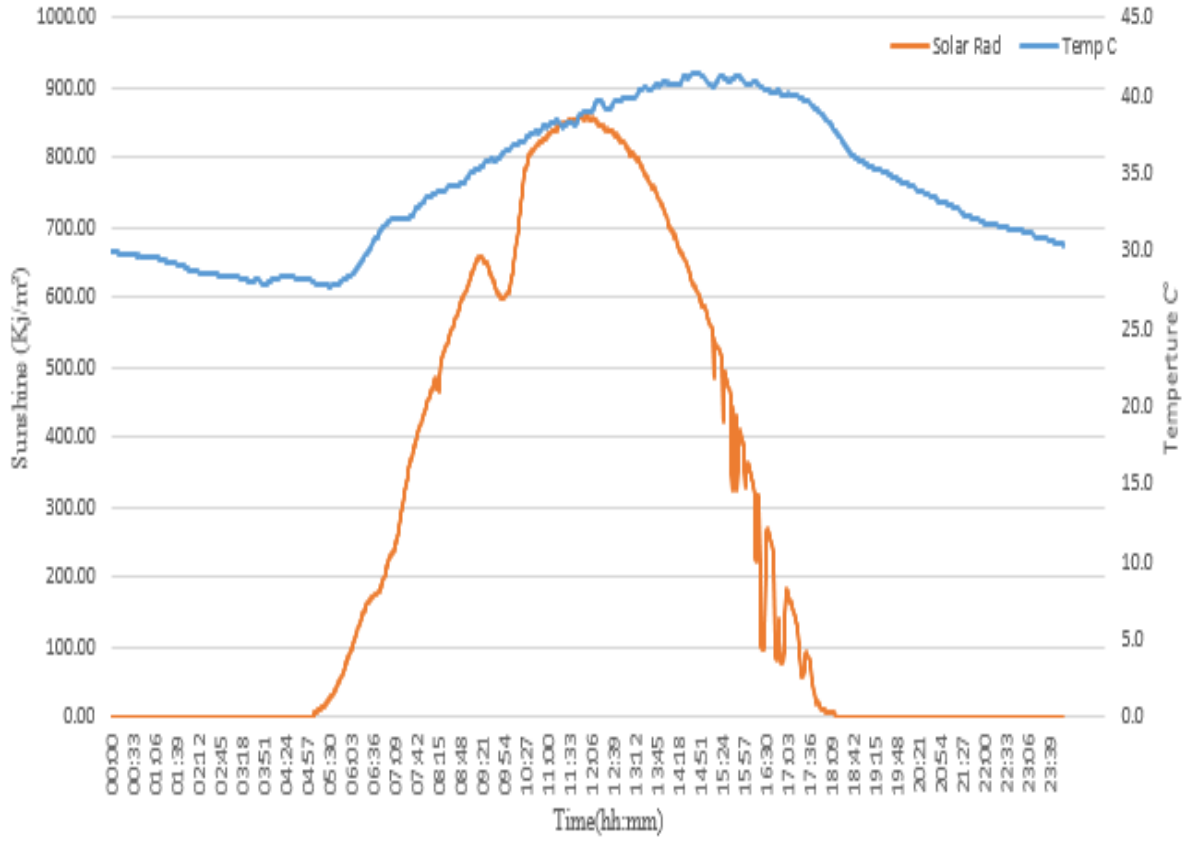

Figure III.9: Daily evolution of sunshine and temperature at M'Sila on August 19.

III.3.2 Monthly evolution of sunshine at M'Sila

Figure III.10 shows the evolution of the average daily sunshine received during the months of March, September, June and December

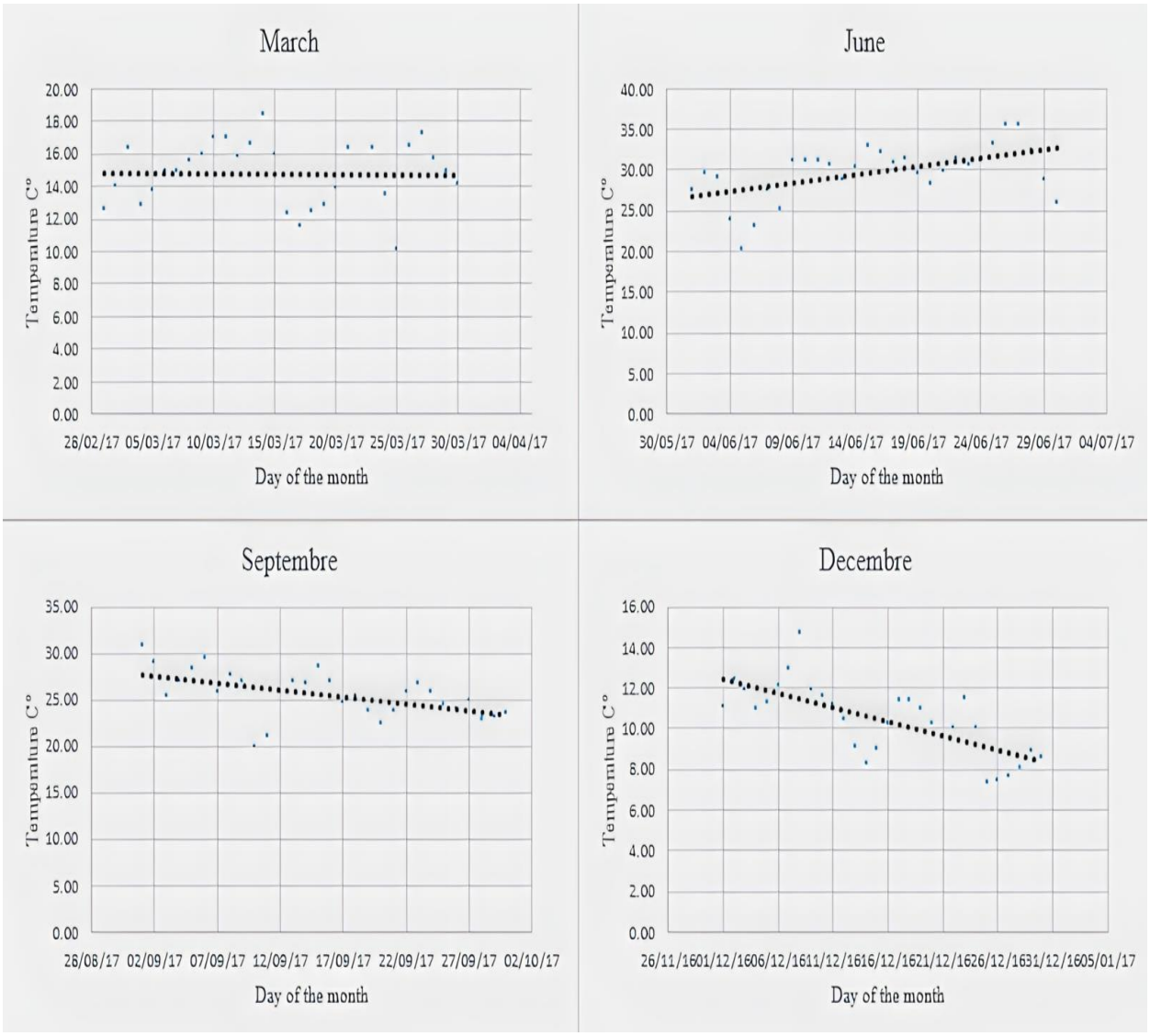

Figure III.10: Monthly evolution of the sunshine received at M'Sila during the months of March, September, June and December.

We notice that the monthly evolution of the sunshine received at M'Sila is not uniform as the case seen previously concerning the daily evolution. In fact, the average daily insolation tends to rise in March and December and to fall in September and June.

III.3.3 Annual evolution of sunlight/irradiance in M'Sila

Figure III.11 shows the evolution of the average daily sunshine and illuminance received during the study year.

It can be seen that the irradiance and sunshine have the same evolution as mentioned above. The analysis of the sunshine data gave the following results:

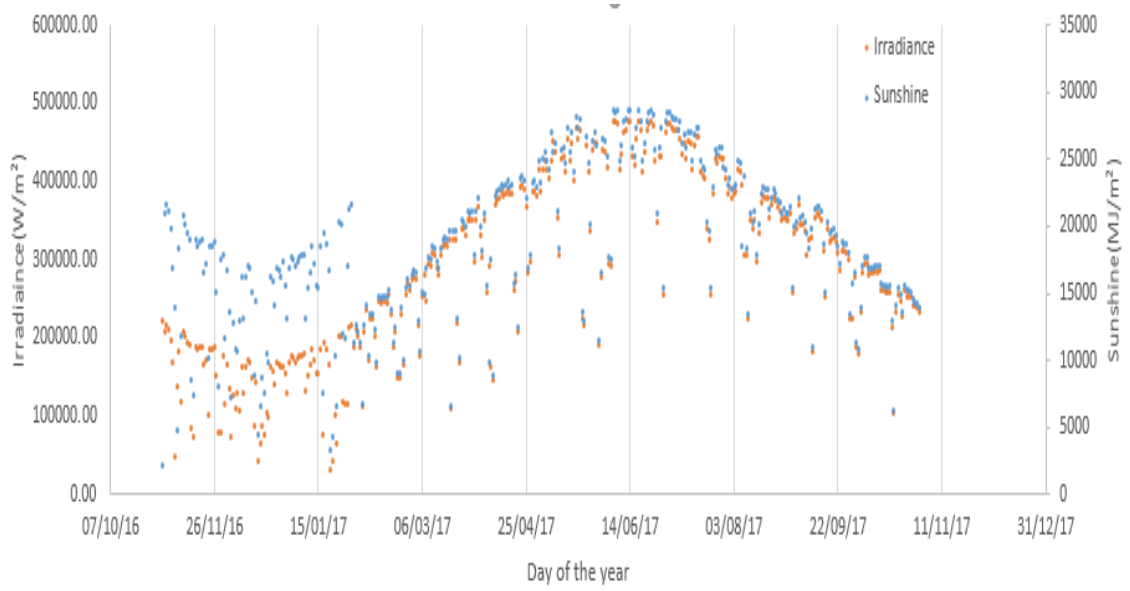

Figure III.11: Annual evolution of sunshine and illumination received at M'Sila.

July is the sunniest month with a total insolation of 790.14 MJ/m2 and an average insolation of 25.49 MJ/m2.

a) December is the least sunny month with a total insolation of 242.52 MJ/m2 and an average insolation of 7.82 MJ/m2.

b) The insolation of the months of March, April, May, June, July, August and September exceeds the annual average insolation.

c)

III.4 General presentation of the interface “Calculateur Solaire”

The ‘Calculateur Solaire’ interface works under Windows, it is written in C language under visual basic which is found in excel and ensures the automation of calculation tasks according to the solar different angel equation mentioned on the litterateur It is based during its calculations on the basis given to coordinate geographically of each Wilaya, Also the date and the time injected (See the Figure II.12).

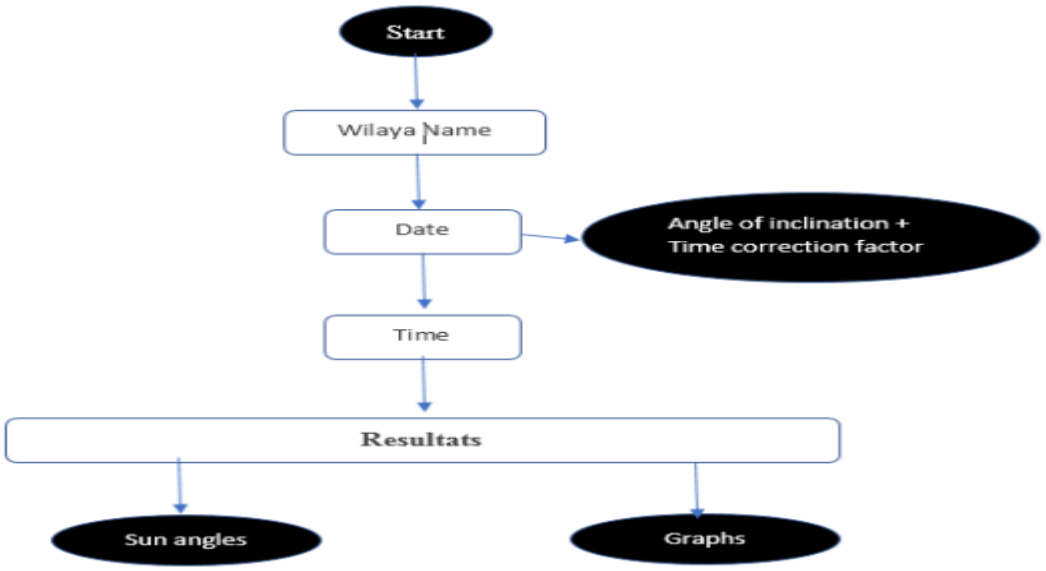

Figure III.12: General flowchart of the interface calculation process

III.4.1 Main Menu

The first page 'Home page' of our ‘Calculateur Solaire’ interface is shown in Figure III.13, it includes title which indicate its purpose and its designers. On this page, the user can access the following functions:

The Start icon: allows access to the calculation page

The close icon: close the interface

Figure III.13: Start window of the Calculateur Solaire’ interface.

III.4.2 Calculation page

Once clicked on the start icon, the following window (Figure III.14) appears. It has three panels described as follows:

- The first groups together all the information concerning the calculation, namely; the name of the wilaya, the latitude, the longitude altitude. On the panel: data, it is enough just to introduce the name wilaya, so that all the other information appears since they are integrated in the interface library.
- The second is related to the date that are needed to determine the angle of inclination and the time correction factors.
- The third is related to the temp which we need to calculate from different solar angles. note that the time variation per second gives the corresponding instantaneous angles

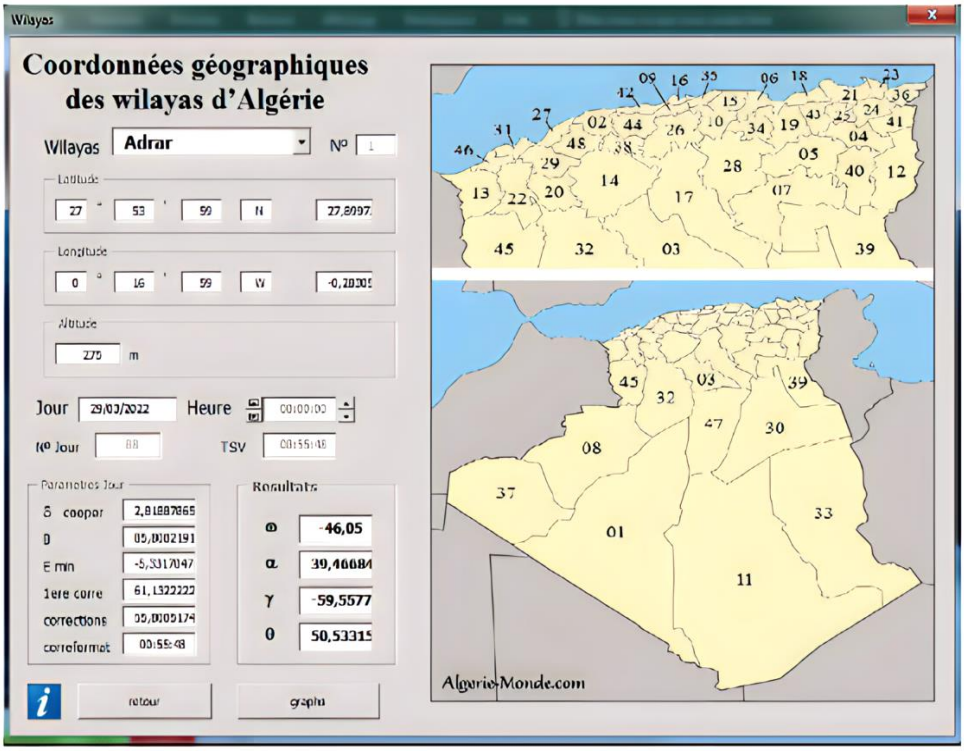

Figure III.14: Capture of the interface relating to the calculation page

The user can access also the following functions

: This icon represents the help it gives information about the meaning and the equation

governing each angel see figure III.15

graphs icon: Once clicked on it, the following window (Figure III.15) appears; graphs for each angle

retour icon: Once clicked on it ; it will take back the first page

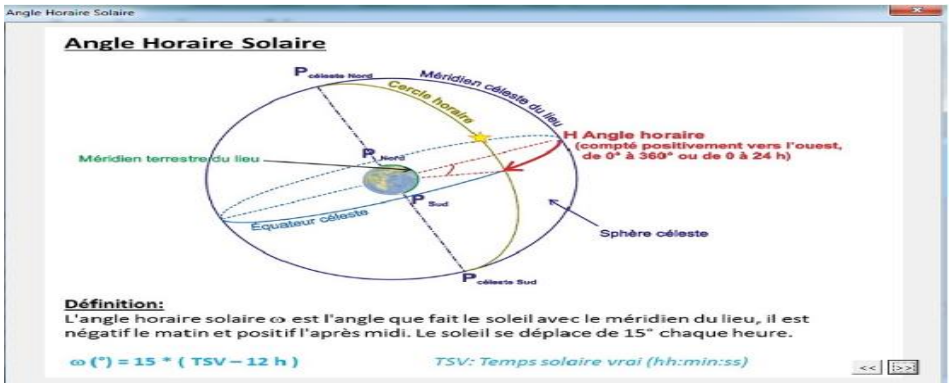

Figure III.15: The definition and identification of calculated equations (help).

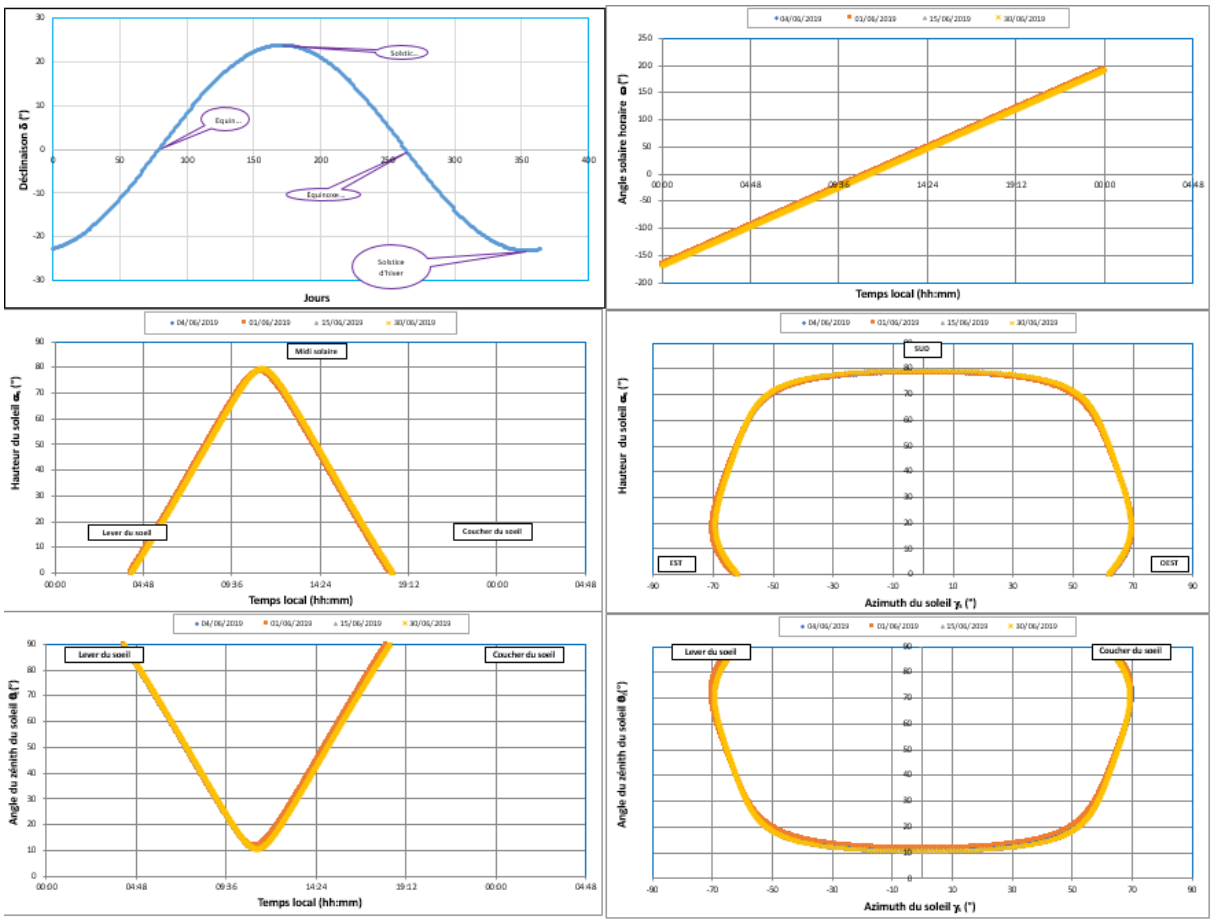

Figure III.16: Generated graphs after calculation

III.5 Soil identification tests

Laboratory tests were carried out on samples of Hamada and agricultural soil according to the following program:

- Identification tests:
  - Granulometric and sedimentometric analysis.
  - Atterberg Limits.
- Physical tests:
  - Natural water content.
  - Dry density.

The results of the laboratory tests are presented in a summary tables given below

	Soil type	
	Agricultural soil	Hamada soil
Composition	-14% Silt (0.002 mm ≤ d < 0.05 mm) -15% Clay (d < 0.002 mm) -71% Sand (0.05 ≤d< 2.00 mm)	-20% Silt (0.002 mm ≤d< 0.05 mm) -10% Clay (d < 0.002 mm) -70% Sand (0.05 ≤d< 2.00 mm)

Table III.2 :Main composition of two samples

The particles that establish soil are categorized into three groups by size – sand, silt, and clay. Sand particles are the largest (0.05 ≤d< 2.00 mm) and clay particles the smallest (d < 0.002 mm). Most soils are a combination of the three. The relative percentages of sand, silt, and clay are what give soil its texture.

Based on the percentage found in the table and the using of the soil texture triangle we conclude that the type of the two soils are **sandy loam** which knowing by : its aggregates weak forms, the mixture of the sand (high percentage) and enough silt makes it somewhat coherent. Individual sand grains can be seen and felt. Squeezed when dry it will form a cast

that will readily fall apart, but when moist it will form a cast that will bear careful handling without breaking. When placed in water it turns the water cloudy.

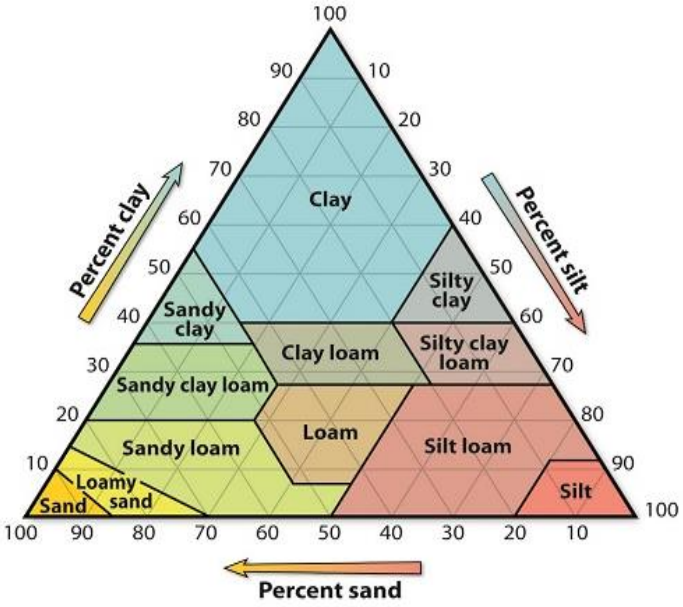

Figure III.17: The soil texture triangle

		Hamada soil	Agricultural soil
Natural water content	W (%)	5.40	6.30
Dry density	γ_D(t/m^3)	1.47	1.7
Grain size pass-through (%)	80 μ	46.06	23.42
Atterberg Limits (%)	Liquidity: WL	21.93	54.78
	Plasticity: IP	6.88	7.88

Table III.2: Result of soil identification

- The water content measurements found between 5.40% to 6.30%, these thresholds present in dry soils. This is normal because the two samples were taken from M'Sila which consider as an arid region, these last years
- The Atterberg limit for the Hamad soil and Agriculture soil gave a plasticity index of 6.88% ,7.88% respectively and have LL=21.93%, 54.78% this value corresponds to a low plastic soil for Hamada soil and high plasticity for Agricultural soil . As we know

the plasticity index measures the extent of the water content range in which he soil is in the plastic state. And Plasticity is a characteristic property of very fine or clayey elements in the soil, in relation to the existence of layers of adsorbed water with or without dissociated electrolytes. It is therefore conceivable that the Atterberg limits and the plasticity index of a soil vary not only with the size of its clay fraction but also with the nature of the clay minerals and the adsorbed cations. which conducted as to say that Hamada soil is poor of mineral and contrary for Agriculture soil

.III.6 Thermal conductivity determination

III.6.1 Reliability of experiments

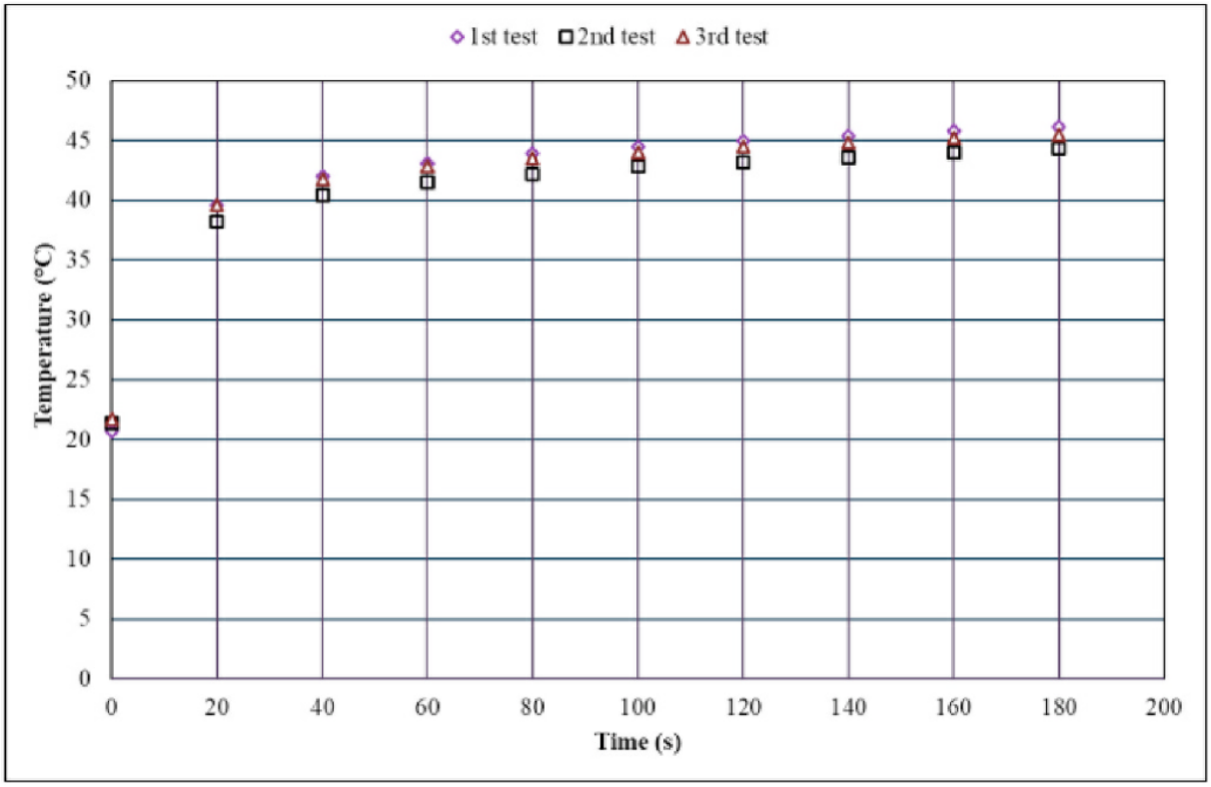

Figure III.18: Temperature evolution at the center of the hot wire for three repeated tests (case of Hamada reference soil, transverse direction)

Figure III.18 depicts the temperature evolution over time for three repeated experiments on Hamada reference soil in the transverse direction. As shown, the temperature in the middle of the heated wire grows over time due to the fixed thermal power created by the Joule's effect when a constant-intensity electric current is passed through the wire. The three reported temperatures differ slightly.

Source of Variation	SS	Df	MS	F	P-value	F crit
Between Groups	71,712	2	35,856	0.486	**0.615**	3.026
Within Groups	21899,44	297	72,735			
Total	21971,15	299				

Table III.3: ANOVA One-way statistical analysis of the temperature measurements taken in longitudinal direction

The table III.3 shows the output of the ANOVA one-way analysis and whether there is a statistically significant difference between our group means. We can see that the significance value is 0.615 (i.e., p = 0.615), which is greater then 0.05. and, therefore, there is no statistically significant difference in the mean of three temperature measurements taken in longitudinal direction.so in the same meaning we can say that the obtained result is reliable and do trust in ours experiments.

Source of Variation	SS	Df	MS	F	P-value	F crit
Between Groups	323,952	2	161,976	2.152	**0.118**	3.026
Within Groups	22353,63	297	75,265			
Total	22677,582	299				

Table III.4: ANOVA One-way statistical analysis of the temperature measurements taken in transverse direction

The table III.4 shows the output of the ANOVA one-way analysis and whether there is a statistically significant difference between our group means. We can see that the significance value is 0.118 (i.e., p = 0.118), which is greater then 0.05. and, therefore, there is no statistically significant difference in the mean of three temperature measurements taken in transverse direction.so in the same meaning we can say that the obtained result is reliable and do trust in ours experiments

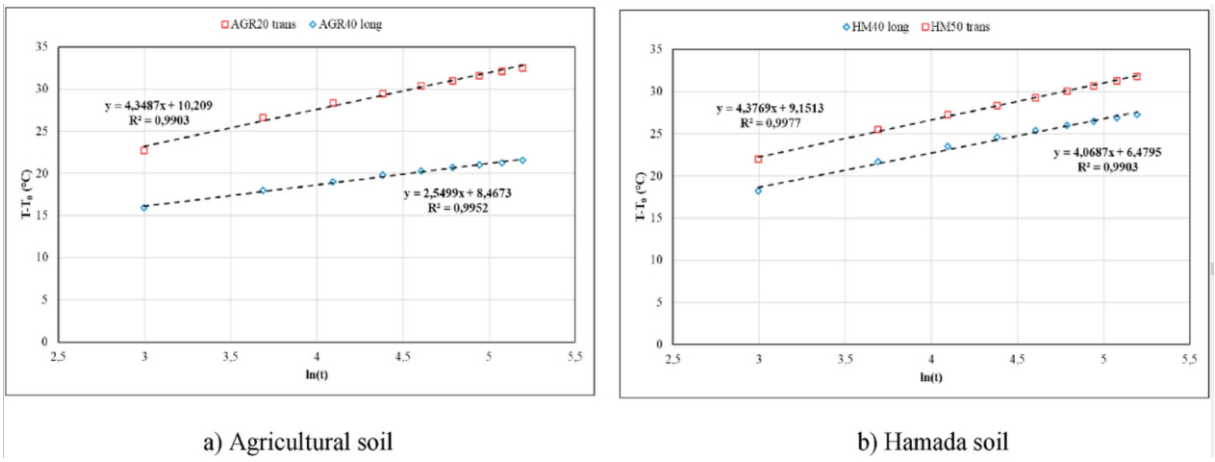

Figure III.19: Temperature difference rise vs. the time natural logarithm for longitudinal and transverse heat

All of the straight lines with varied slopes in the graphs depicting the evolution of the temperature differential (T-T0) as a function of the natural logarithm of the measurement time Ln (t), with T0 the temperature at the center of the hot wire at the beginning instant (t = 0 s). Figure III.19 (a and b) illustrate two typical instances for agricultural and Hamada soils, respectively. The linear relationship discovered between T=T(t)-T0 and Ln (t) demonstrates that the current experiment satisfied the hypothesis of radial heat transmission in a semi-infinite medium. Thus, the thermal conductivity of the samples under consideration can be simply calculated using equation II.20

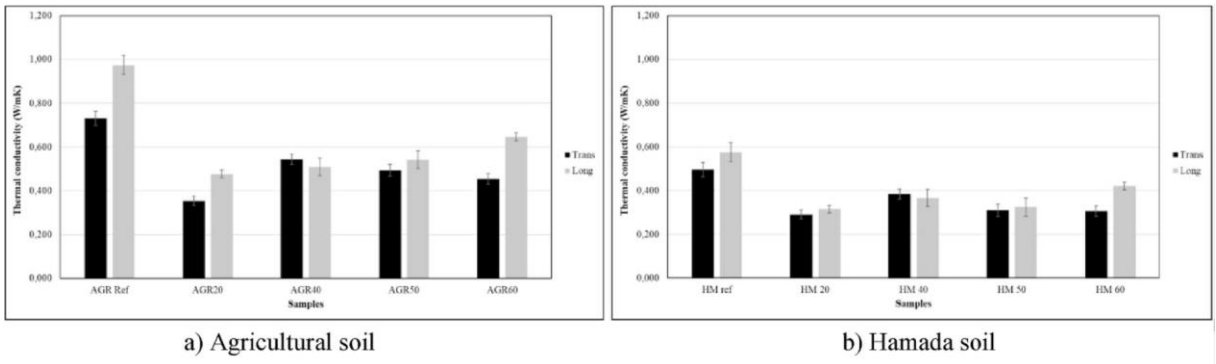

FigureIII.20: Thermal conductivity of the studied earthen materials

This experiment's thermal conductivity is the average of the three thermal conductivities recorded for each tested substance. Figure III.20 depicts the discovered results.

The thermal conductivity of the earthen materials studied is greater than 0.2 W/m K but less than 1 W/m K. These calculated values fall within Franco's [75] usual range of

construction materials, ranging from 0.1 to 2 W/m K. As a result, agricultural and Hamada soils, with and without straw, exceed the thermal requirements of construction materials. Furthermore, as compared to polystyrene, glass fiber, and other insulators with thermal conductivities less than 0.05 W/m K, these materials exhibit a comparatively significant thermal conductivity. Adding straw to any soil reduces heat conductivity and hence increases thermal insulation. This reduction is determined by the kind of soil and the amount of straw used. Indeed, for agricultural soil, it ranges from 26% to 52%, while for Hamada soil, it ranges from 23% to 45%.

As shown in Figure III.15 increasing the content of straw does not result in a steady decrease in thermal conductivity. It allows for an optimal (a minimum for both soils). It was discovered that combining straw mass equivalent to one-twentieth of the mass of soil (5% by mass) provided the best thermal insulation to the Adobe. Furthermore, increasing 5% weight of straw (R=20, more straw) reduces the heat conductivity of agricultural soil by more than 50% (in both directions). In the case of Hamada soil, it is lowered by more than 41%. Even the people of M'Sila employ this ratio (1/20 or 5%) while creating construction bricks (empirical knowledge). This experimental investigation reveals that the inhabitants of M'Sila were correct about the amount of straw needed to build bricks with decreased thermal conductivity. G. Calatan et al. [89] advocate adding 30 to 40% by volume of straw to achieve the best thermal performance of the adobe brick in the same environment. Their result differs from ours (same volume) due to differences in the composition of the soil, production procedure, and test method (what we used).

III.6.2 Effect of straw amount and soil nature

A statistical analysis using two-way ANOVA in order to study the effect of the straw amount (5%,2.5%,2%, 1.67%) and the type of the soil (Hamada and Agriculture soil)

ANOVA						
Source of Variation	SS	Df	MS	F	P-value	F crit
Sample (soil type)	0.547	1	0.547	113.435	**0.000000**	4.034
Columns (Straw amount)	0.752	4	0.188	38.950	**0.000000**	2.557
Interaction	0.085	4	0.021	4.428	**0.00385**	2.557
Within	0.241	50	0.005			
Total	1.626	59				

Table III.5: ANOVA Tow way statistical analysis of the thermal conductivity (effect of straw amount and soil nature)

The table III.5 shows the output of the ANOVA Two-way analysis and whether there is a statistically significant difference between our group means. We observed that the significance value is 0.0000 (p = 0.0000) for soil type, which is less then 0.05. and, therefore, there is statistically significant difference between the thermal conductivity and the type of

the soil tested. In same manner, we observed that the significance value is 0.0000 (p = 0.0000) for Straw amount which is less then 0.05. and, therefore, there is statistically significant difference between the thermal conductivity and the type of the Straw amount added.

Finally, the significance value is 0.00385 (p = 0.00385) for interaction, which is less then 0.05. and, therefore, the soil tested the Straw amount added have statistically significant difference on the thermal conductivity

III.6.3 Effect of measurement directions longitudinal and transverse

A statistical analysis using two-way ANOVA in order to study the effect of the straw amount (5%,2.5%,2%, 1.67%) and the ay of measurement for Agriculture soil

ANOVA						
Source of Variation	SS	df	MS	F	P-value	F crit
Sample (measurement direction)	0,098	1	0,098	105,600	**0,000**	4,351
Columns(Straw amount)	0,653	4	0,163	175,873	0,000	2,866
Interaction	0,075	4	0,019	20,073	0,000	2,866
Within	0,019	20	0,001			
Total	0,844	29				

TableIII.6: ANOVA Two-Factor statistical analysis of the thermal conductivity (Effect of measurement directions; longitudinal and transverse) for argricultural soil

The table III.6 shows the output of the ANOVA Two-way analysis and whether there is a statistically significant difference between our group means. We observed that the significance value is 0.0000 (p = 0.0000) for the measurement direction, which is less then 0.05. and, therefore, there is statistically significant difference between the thermal conductivity and the the measurement direction. In same manner, we observed that the significance value is 0.0000 (p = 0.0000) for Straw amount which is less then 0.05. and, therefore, there is statistically significant difference between the thermal conductivity and the Straw amount added.

Finally, the significance value is 0.0000 (p = 0.0000) for interaction, which is less then 0.05. and, therefore, the the measurement direction and the Straw amount added have statistically significant difference on the thermal conductivity

ANOVA						
Source of Variation	SS	df	MS	F	P-value	F crit
Sample (measurement direction)	0,017	1	0,017	25,864	**0,000**	4,351
Columns(Straw amount)	0,184	4	0,046	72,036	0,000	2,866
Interaction	0,021	4	0,005	8,142	0,000	2,866
Within	0,013	20	0,001			
Total	0,234	29				

Table III.7: ANOVA Two-Factor statistical analysis of the thermal conductivity (Effect of measurement directions; longitudinal and transverse) for Hamada soil

The table III.7 shows the output of the ANOVA Two-way analysis and whether there is a statistically significant difference between our group means. We observed that the significance value is 0.0000 (p = 0.0000) for the measurement direction, which is less then 0.05. and, therefore, there is statistically significant difference between the thermal conductivity and the the measurement direction. In same manner, we observed that the significance value is 0.0000 (p = 0.0000) for Straw amount which is less then 0.05. and, therefore, there is statistically significant difference between the thermal conductivity and the Straw amount added.Finally, the significance value is 0.0000 (p = 0.0000) for interaction, which is less then 0.05. and, therefore, the the measurement direction and the Straw amount added have statistically significant difference on the thermal conductivity

III.7 The impact of adding straw on thermal conductivity

The figure III.24 illustrate the effet of adding straw on thermal conductivity, the point A represents the soils without staw ,the thermal conductivity decrease by adding straw to the soils until reach the optimum point B this could be explained by increasing the porosity and water contain in the straw and The process is known as evaporation-condensation; rising temperature causes water to evaporate, absorbing a latent heat of vaporization of 586 cal/g (at 20'C). As a result, the local vapor pressure rises, and water vapor diffuses via the linked pores to lower vapor pressure locations, with the diffusion coefficient varying with temperature [68-73].

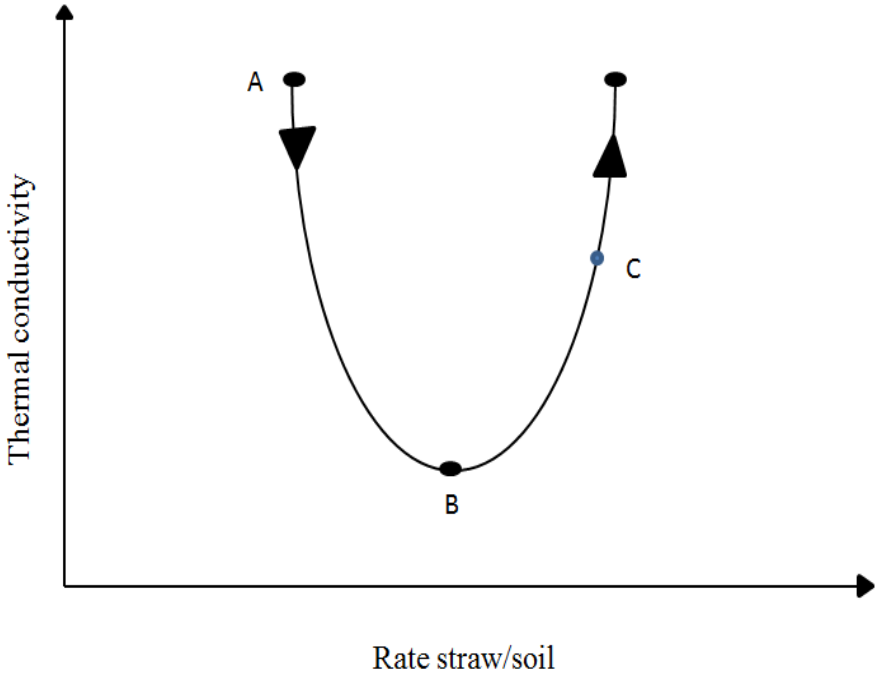

FigureIII.24: Effect of rate straw/soil on the thermal conductivity

III.8 Temperature evolution

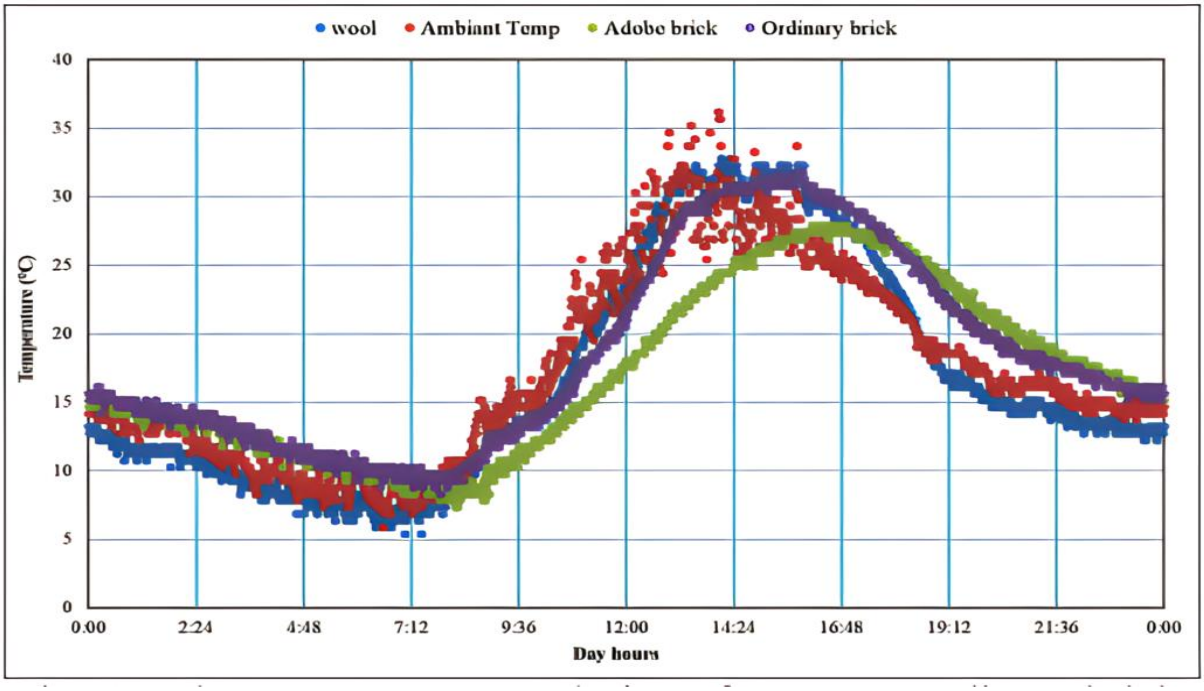

Figure III.21: Indoor temperature evolution of three room for 24 hours

Figure III.21 illustrates the temperature progression in the center of three comparable rooms composed of different materials, specifically sheep wool (tent), ordinary brick, and traditional brick (earth + straw), as contrasted to the ambient temperature on a sunny day in April (24 hours). It is frequently seen that the temperatures in the center of the three chambers (interior temperatures) follow the same rate as the outdoor temperatures. They allow for two extremes: a minimum in the morning and a maximum in the afternoon. As is well known, the temperature of the air (ambient temperature) is determined by the amount of solar radiation received by the earth's surface.

As illustrated on figure the temperature increase from 6:35 AM to 2:03 PM due to solar radiation received by the earth which warms the ambient air during the day

Furthermore, while the sun is high in the sky, the earth receives the most solar energy. The ambient air temperature follows the same trend and reaches its greatest value after solar noon due to the heat capacity of the air. The sun continued to rise in the west and set there. In this course, its intensity diminishes until light reaches 0 W/m2 at sunset. As a result, the air temperature will fall, as indicated in Figure III.16.

Due to heat exchange with the universe, the earth cools during the night (from sunset to sunrise), and the temperature of the air continues to drop until sunrise, when it begins to rise again. The temperature of the air changes every day.

The materials used to construct the chambers have an impact on the indoor temperature, which varies from room to room (see again Figure III.21). During the day, the maximum external ambient temperature is reduced by 3.42 degrees Celsius within the tent, 8.31 degrees Celsius inside the traditional brick chamber, and 4.4 degrees Celsius inside the standard brick chamber.

Furthermore, the highest temperatures inside the three chambers do not coincide with the outside temperature (time lag). As seen in Figure III.21, the graphs depicting the evolution of the three rooms' inside temperatures are shifted to the right of the graph depicting the outdoor temperature.

Also, the time lag for the tent, regular brick room, and conventional brick room is estimated to be 4 minutes, 1 hour 22 minutes, and 2 hours and 6 minutes, respectively. The maximum temperature inside the three rooms occurs after that of the exterior due to the heat capacity of the building materials used.

As a result, because the internal temperatures throughout the day are lower than those in the outside environment, the dwellings serve as shelters from the elements (thermal resistance to heat gains).

During the day, the conventional brick chamber has the largest time lag and the lowest temperature peak. In contrast, the tent has the lowest time lag and the highest temperature peak Heat from the outside can easily pass through the sheep wool fabric but not through conventional brick. This is due to the thermophysical properties (thermal conductivity, heat capacity, and density) of the materials used, as well as the thickness of the chambers' envelopes, as previously indicated (walls and roof)

Regardless of the fact that sheep wool has a low thermal conductivity of 0.04 W/m.K [74] (classified as insulation), its thin thickness (0.5cm) promotes heat exchange between the outside environment and the inside of the tent, resulting in a little variation in temperature between the two (Figure III.22.1and Figure III 23). Asan's numerical conclusions are supported by this experimental result. [75]

The base (ground) of tents used in Saharan conditions is really humidified., which cools the interior environment and provides thermal comfort throughout the summer. This shape, in addition to the fact that the tent is not a closed cube , improves the tent's thermal comfort.

Furthermore, because this study is looking at the influence of different construction materials, we maintained the room's shape and proportions the same while changing the building material.

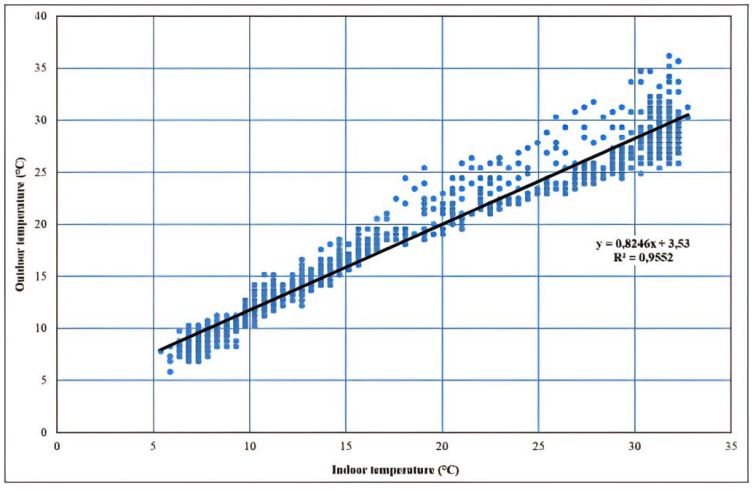

Figure III.22 : Outdoor temperature vs tent indoor temperature

Because of the differing thermal diffusivity of their building material, the two remaining chambers have the same thickness but react differently (see Figures III.22 and III.23).Thermal diffusivity is a property of materials. It describes the rate of temperature dispersion across a material and characterizes unstable heat conduction.

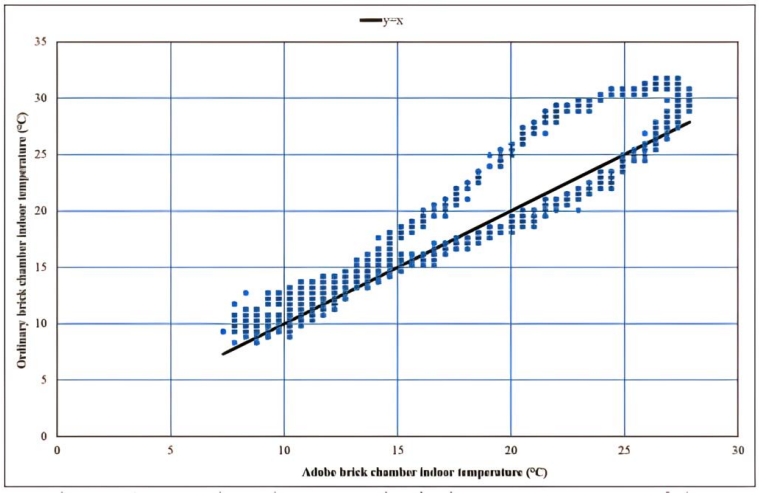

Figure III.23: Indoor temperature of ordinary brick vs indoor of the adobe brick chamber

As a result of this experiment, one can deduce that regular brick has a higher thermal diffusivity than adobe brick. As indicated in Figure 9, the temperature within the adobe brick chamber does not surpass 30 °C, although the temperature inside the regular brick chamber does. This helps to explain why classic brick houses without air conditioning are cold in the summer. Furthermore, it is discovered that the thermal diffusivity of the examined materials is inversely related to the time lag. In fact, the tent with the highest thermal diffusivity has the shortest time lag, whereas the typical brick has the longest.

This experimental result, once again, corresponds with Asan's numerical result. [75]

The minimum external ambient temperature reduces by 0.49 °C within the tent throughout the night, rises by 1.46 °C inside the traditional brick chamber, and rises by 2.44 °C inside the conventional brick chamber (see again Figure III.22). Furthermore, the time lag for the tent, ordinary brick room, and conventional brick room is anticipated to be 29 minutes, 1 hour 17 minutes, and 1 hour 38 minutes, respectively. Because of the heat capacity of the chosen construction materials, the minimum temperature inside the three rooms occurs after the outside temperature (storage energy).

The tent has the least time lag and the lowest overnight minimum temperature (Figure III.23). This is because it has the greatest thermal diffusivity (low thermal

conductivity and low thermal capacitance). In other words, the tent's internal heat is easily transported to the outside environment via the sheep wool fabric. As a result, the temperature inside the tent may be lower than the temperature outside. At night, the tent acts as a cold room. In contrast, traditional and conventional brick rooms are slightly warmer than the surrounding environment.

There is no significant variation in indoor temperature between the adobe brick chamber and the conventional brick chamber (see Figure III.23). The similar outcome was discovered for In truth, the adobe chamber requires heating during the winter months, which corresponds to the night in our experience, but once heated, the heat does not permeate through its exterior (minimum heat loss). The brick chamber, on the other hand, has a lot of heat losses. As a result, thermal insulation is required (money spent).

Traditional brick houses have been objectively proven to be cold during the day and warm at night. The adobe brick retains heat during the day and releases it at night. . It is more suitable for placement than ordinary brick.

Conclusion

This section dedicated to estimating M'Sila's energy potential by processing the data of one year's readings has enabled us to retain the following information:

- The longest day (summer solstice) occurs on June 18 and lasts 14h 19min and 48s,

- The shortest day (winter solstice) recorded on December 19 lasts 8h 30min and 36s.

- The spring equinox occurs on March 18, and the fall equinox on September 22,

- M'Sila is sunny for 4388 hours during one year, that is 12h 1min and 18s per day,

- July is the sunniest month with a day length of 434h 18min and 18s and December is the least sunny month with a day length of 298h 7min and 48s,

- The daily temperature in M'sila reaches its peak around 14h 21min on average, and its minimum at night around 5h 11min on average.

- The average monthly maximum temperature is recorded in August with a value of 32.63°C,

- The average minimum temperature is recorded in January with a value of 7.26°C,

- Five (05) months in M'Sila (May, June, July, August and September) with average monthly temperatures above the annual average temperature,

- There is a difference of three (03) weeks and three (03) days between the longest day and the hottest day due to the thermal inertia of the air.

- During the 365 days of the study, no day was free of clouds at M'Sila,

- The daily sunshine reaches its peak in M'Sila around 11h 40min, which occurs between 9h 14min and 13h 59min,

- The maximum sunshine received at M'Sila during the day does not occur at the same time as the peak air temperature.

- July is the sunniest month with a total insolation of 790.14 MJ/m2 and an average insolation of 25.49 MJ/m2.

- December is the least sunny month with a total insolation of 242.52 MJ/m2 and an average insolation of 7.82 MJ/m2.

- The insolation of the months of March, April, May, June, July, August and September exceeds the annual average insolation.

- M'Sila receives a total sunshine of 6316.42 MJ/m2 during the study year, which is an average sunshine of 526.37 MJ/m2.

This section allowed us to discover the possibility to design a graphical interface under VISUELBASIC which served as a support for us to create the ‘Calculateur Solaire’ interface intended for the calculations of the different angles at any place in Algeria. It also allowed us to better understand the behavior of the values corresponding to the solar angles.

It may then condense in such places, releasing its latent heat. A substantial quantity of heat may be transported by this process, due to the high latent heat of evaporation of water. As an expression for the resulting the effect of the pore air's and water contain in straw on effective .Thermal conductivity In addition to the change in structure . The point C represented new materiel with deferent thermal conductivity from the the first point

- Hamada and agricultural soils meet the thermal requirements of building materials;

- Hamada soil provides better thermal insulation than agricultural soil.

- The addition of straw to hamada or agricultural soils influences the end product's heat conductivity.

- For the best thermal performance, add a straw mass equal to one-twentieth of the mass of both soils (5% by mass) (a minimum thermal conductivity),

- The thermal conductivity of a fibered earthen brick is determined by the type of fiber, its length, the amount of treatment applied, the nature of the soil, the production procedure, and the test method.

- Because of their benefits, it is advised that these free materials be reused in Algeria.

Under real-world conditions, this experimental study investigates the thermal behavior of three different building materials often used in Algeria, namely sheep wool, traditional brick, and conventional brick. The thickness of the building envelope (walls and roof), as well as the thermo-physical qualities (thermal diffusivity) of the building materials, are found to have a significant impact on heat exchange between the internal and outdoor spaces.

Traditional brick houses have been quantitatively proved to be cold during the day (summer) and warm at night (winter). The heat is held in the adobe brick during the day and released at night as the temperature outside drops. It is more suitable for placement than plain brick. The purpose of this study is to promote the reuse of traditional bricks because of their energy-saving and environmental benefits

Conclusion and Perspective

Conclusion

As part of this thesis, we have given a contribution concerning the thermal building.The goal is to reduce energy consumption to achieve the known thermal comfort which appears in the first place in the use of solar energy and integrated by both passive and active ways as an example we have determined the solar energy supplied to M'sila and we have noticed:

M'Sila has a significant solar energy potential. Indeed, the incident solar energy on M'Sila has a magnitude of 17MJ/m2/day. Seven months of the year in M'Sila region received monthly radiation above the annual average. The highest radiation levels were measured between 9:14 and 13:59. It should be noted that M'Sila receives 80% of its maximum solar energy between 9:57 and 13:38 on average.

With result obtained we were able to confirm that we can integrate can be integrated solar radiation on their mode passive and active in the M'sila buildings so minimize energy consumption and reach thermal comfort . We encourage our government officials to integrate the technology (PV or CSP) in this sense .

In the second way in the choice of construction material which plays an important role because the transfer of heat does by it and the property of construction material also as an example we study two different agriculture and Hamada soil that use in old building and with the technique of manufacture and by measurement using ANOVA test we find the following:

- When compared to agricultural soil, hamada soil provides the best thermal insulation;

- Adding straw to hamada or agricultural soils affects the final product's thermal conductivity;

- Hamada and agricultural soils meet the thermal standards for construction materials.

It is recommended to add straw mass equivalent to one twentieth of the mass of both soils for the optimal thermal performance (lowest thermal conductivity) (5 percent by mass). The thermal conductivity of a fibered earthen brick is determined by the type of fibers, their length, the treatment they received, and the amount of fibers, the nature of the soil, the production procedure, and the test method. Given their benefits, Algerians are encouraged to reuse these free resources. To validate this, we conducted an experimental research of the thermal behavior of three different building materials utilized in Algeria, namely sheep wool,

traditional brick, and standard brick, in a real-world setting. Using the aforementioned materials, three identical chambers were built.

Three temperature sensors were installed in the center of three compartments that were 10 cm apart. The Arduino-based digital acquisition system allows us to measure and record temperatures in the midst of three well-closed rooms in one-minute increments for one day (day and night). The ambient air temperature (outside temperature), which served as a reference, was also monitored. It has been discovered that, in addition to the thickness of the building envelope (walls and roof), the thermo-physical properties (thermal diffusivity) of building materials have a considerable effect in the heat exchange between the internal and external environments. This study encourages individuals to reuse conventional bricks because of the benefits they provide in terms of energy savings and environmental preservation.

Perspective

Our work allows a significant contribution to help in the reduction of energy consummation and reach the thermal comfort inside the building, the perspectives of our work revolve around two main axes:

- The first concerns the study of the thermal conductivity of various natural materials with the aim of mixing them and knowing the effect of adding them to the soil to create a material that has certain properties that help create a building with the required specifications; then expanding the study to include all the properties of the material, such as mechanical properties, which also play an important role in the building
- The second is related to the development of interface that has two objectives in order to integrate solar radiation by its method passive and active to the building:

- The first objective is to extract the necessary information when obtaining raw information from various meteorological stations and put it in a unified template in order to effectively contribute to the integration of solar energy in the building this project is under completion and is on its way to register with the competent authorities
- The second objective is to determine the different angles of solar radiation, considering all the states and adding all the necessary equations to calculate the amount of energy and matching it experimentally with the data obtained by meteorological stations in order to find out the equation that governs solar energy for the state itself

References list

References list

[01] Martín, S., Mazarrón, F. R., & Cañas, I. (2010). Study of thermal environment inside rural houses of Navapalos (Spain): The advantages of reuse buildings of high thermal inertia. Construction and Building Materials, 24(5), 666-676. doi: https://doi.org/10.1016/j.conbuildmat.2009.11.002

[02] Vivancos, J.-L., Soto, J., Perez, I., Ros-Lis, J. V., & Martínez-Máñez, R. (2009). A new model based on experimental results for the thermal characterization of bricks. Building and Environment, 44(5), 1047-1052. doi: https://doi.org/10.1016/j.buildenv.2008.07.016

[03] Huo, H., Jing, C., Li, K., & Huo, H. (2015). Synergic relationships between thermophysical properties of wall materials in energy-saving building design. International Journal of Heat and Mass Transfer, 90, 246-253. doi: https://doi.org/10.1016/j.ijheatmasstransfer.2015.06.029

[04] Union, E. C. S. O. o. t. E., Commission, E. U. E., Communities, S. O. o. t. E., & Eurostat, E. U. (2011). Energy, transport and environment indicators: Publications Office of the European Union.

[05] Aditya, L., Mahlia, T. M. I., Rismanchi, B., Ng, H. M., Hasan, M. H., Metselaar, H. S. C., . . . Aditiya, H. B. (2017). A review on insulation materials for energy conservation in buildings. Renewable and Sustainable Energy Reviews, 73, 1352-1365. doi: https://doi.org/10.1016/j.rser.2017.02

[06] Huang, Y., & Niu, J.-l. (2016). Optimal building envelope design based on simulated performance: History, current status and new potentials. Energy and Buildings, 117, 387-398. doi: https://doi.org/10.1016/j.enbuild.2015.09.025

[07] Bulletin trimestriel de l'APRUE « Programme ECO-BAT Signature d'une convention entre

l'APRUE et l'OPGI », N° 15 / Juin 2009

[08] Hong, T. (2009). A close look at the China design standard for energy efficiency of public buildings. Energy and Buildings, 41(4), 426-435.

[09] Acosta, J., Diaz, A. G., Zarazua, G., & Garcia, E. (2010). Adobe as a sustainable material: A thermal performance. Journal of Applied Sciences, 10(19), 2211-2216.

[10] Gunnell, K., Du Plessis, C., & Gibberd, J. (2009). Green building in South Africa: emerging trends.

[11] Ejiga, O., Paul, O., & Cordelia, O. (2012). Sustainability in traditional African architecture: a springboard for sustainable urban cities. June Sustainable futures: architecture and urbanism in global south Kampala, Uganda, 27-30.

[12] Obafemi, A. O., & Kurt, S. (2016). Environmental impacts of adobe as a building material: The north cyprus traditional building case. Case Studies in Construction Materials, 4, 32-41.

[13] Omrany, H., Ghaffarianhoseini, A., Ghaffarianhoseini, A., Raahemifar, K., & Tookey, J. (2016). Application of passive wall systems for improving the energy efficiency in buildings: A comprehensive review. Renewable and Sustainable Energy Reviews, 62, 1252-1269. doi: https://doi.org/10.1016/j.rser.2016.04.010

[14] Pérez-Lombard, L., Ortiz, J., & Pout, C. (2008). A review on buildings energy consumption information. Energy and Buildings, 40(3), 394-398. doi: https://doi.org/10.1016/j.enbuild.2007.03.007

[15] Intergovernmental Panel on Climate Change I, Climate change: synthesis report. http://www.ipcc.ch/S, 2007.

[16] Ireland, D. o. t. E. H., & Local, G. (2010). Energy efficiency in traditional buildings. Dublin: TSO.

[17] Abu-Hamdeh, N. H. J. B. e. (2003). Thermal properties of soils as affected by density and water content. 86(1), 97-102.

[18] Eicker, U. (2010). Solar technologies for buildings.

[19] Mohamed Aziz Hachemi, Exploitation et programmation informatique des documents techniques réglementaires relatifs aux déperditions thermiques de ventilation des bâtiments, thèse de magistère, Université M'hamed Bougara, Boumerdes, 2011-2012.

[20] International Energy Agency, O. f. E. C.-o., & Development. (2004). IEA energy technology RD&D statistics.

[21] Bélaïd, F., & Abderrahmani, F. (2013). Electricity consumption and economic growth in Algeria: A multivariate causality analysis in the presence of structural change. Energy Policy, 55, 286-295. doi: https://doi.org/10.1016/j.enpol.2012.12.004

[22] Residential Electricity Consumption and Economic Growth in Algeria. Energies, 11(7), 1656.

[23] ASHRAE standard 55-1992 Thermal Environmental Conditions for Human Occupancy"

[24] ASHRAE standard 90.1-1989 (Energy Conservation in New Building Design)

[25] Duffie JA Beckman WA. Solar Engineering of Thermal Processes. 4th ed. Hoboken: Wiley; 2013

[26] https://andrewmarsh.com/apps/staging/sunpath3d.html

[27] Ashmawy, R.E., (2015), Establish a sustainable strategy for low energy building. Master thesis, faculty engineering. Tanta University

[28] Bahria, S. A. M. H. A. E. G. M. E. A. S. M. (2016). Parametric study of solar heating and cooling systems in different climates of Algeria - A comparison between conventional and high-energy-performance buildings. Energy., 113, 521-535.

[29] Soufiane, F. A. A. M. M. S. D. (2019). Quantifying the effectiveness of mass proportions and the orientation for buildings on thermal performance in Tebessa, Algeria. IOP Conf. Ser.: Earth Environ. Sci. IOP Conference Series: Earth and Environmental Science, 397, 012008.

[30] Maghrabie, H. M., Elsaid, K., Sayed, E. T., Abdelkareem, M. A., Wilberforce, T., & Olabi, A. G. (2021). Building-integrated photovoltaic/thermal (BIPVT) systems: Applications and challenges. Sustainable Energy Technologies and Assessments, 45, 101151. doi: https://doi.org/10.1016/j.seta.2021.101151

[31] N. Ihaddadene, R. Ihaddadene, A. Betka et al. "Study of the thermal conductivity of clay-based building materials", IAPE'19 (2019), Oxford, United Kingdom.

[32] Nayak, J.K.a. Prajapati, J.A., Handbook on energy conscious buildings. 2006, India: Indian institute of technology, Bombay and Solar energy center Ministry of non-conventional energy sources, Government of India.

[33] Wang, W., H. Rivard, and R. Zmeureanu, Floor shape optimization for green building design. Advanced Engineering Informatics, 2006. 20(4): p. 363-378.

[34] A. Matrosov, Y., M. Chao, and C. Majersik, Increasing Thermal Performance and Energy Efficiency of Buildings in Russia: Problems and Solutions. 2007.

[35] Bahrami, S., Energy efficient buildings in warm climates of the Middle East: Experience in Iran and Israel, in Lund University. 2008, Lund University: Sweden.

[36] Rosenlund, H., Climatic Design of Buildings using Passive Techniques. Building Issues, 2000. 10(1).

[37] Utzinger, M. and J. Wasley, Building Balance Point, in. 1997, Johnson Controls Institute for Environmental Quality in Architecture, and School of Architecture and Urban Planning, University of Wisconsin- Milwaukee.

[38] Lykartsis, Athanasios, B-Jahromi, Ali and Mylona, Anastasia (2017) "Evaluation of thermal comfort and cooling loads for a multistory building," Advances in Energy Research. 5(1), pp. 65–77. doi: 10.12989/ERI.2017.5.1.065.

[39] Mikler, V.B., Albert; Breisnes, Beth and Labrie, Michel Passive Design Toolkit. 2009: City of Vancouver, Canada

[40]. Morrissey, J., Moore, T., & Horne, R. E. (2011). Affordable passive solar design in a temperate climate: An experiment in residential building orientation. Renewable Energy, 36(2), 568-577.

[41] Goia, F. (2016). Search for the optimal window-to-wall ratio in office buildings in different European climates and the implications on total energy saving potential. Solar Energy, 132, 467-492.

[42] Vanhoutteghem, L., Skarning, G. C. J., Hviid, C. A., & Svendsen, S. (2015). Impact of facade window design on energy, daylighting and thermal comfort in nearly zero-energy houses. Energy and Buildings, 102, 149-156.

[43] N. Ihaddadene, R. Ihaddadene, F.hadji et al. "the effect of varing the distance between the double –glazing of a solar thermal collector on its functioning ", renewable energy&power quality journal 2172-03X.

[44] David, M., Donn, M., Garde, F., & Lenoir, A. (2011). Assessment of the thermal and visual efficiency of solar shades. Building and Environment,46(7), 1489-1496.

[45] Eben Saleh, M. A. (1990). Thermal insulation of buildings in a newly built environment of a hot dry climate: the Saudi Arabian experience. International Journal of Ambient Energy, 11(3), 157-168

[46] : C M A HADDAM, Application de quelques notions de la conception bioclimatique pour l'amélioration de la température interne d'un habitat, Thèse de doctorat en physique électronique et modélisation, Université de Tlemcen, 2015.

[47] : T Gallauziaux, D Fedullo, Le Grand livre de l'isolation, Ed. Eyrolles, 2009.

[48] : https://www.davis-europe.nl/product/davis-6152-wireless-vantage-pro2

[49] Association française de, n. (1996). Analyse granulométrique : méthode par tamisage à sec après lavage : NF P 94-056. Association française de normalisation.

[50] Association française de, n. (1996). Analyse granulométrique de sols : méthode sédimentation : NF P 94-057., Association française de normalisation.

[51] Association française de, n. (1996).Détermination de la masse volumique des particules solides des sols – Méthode du pycnomètre à eau NF P 94-054., Association française de normalisation.

[52] Association française de, n. (1996).Détermination des limites d'Atterberg – Limite de liquidité à la coupelle – Limite de plasticité au rouleau NF P 94-051., Association française de normalisation.

[53] N. Ihaddadene, R. Ihaddadene, M. Mostfaoui, Climate change in three different zones in Algeria, J. Earth Sci. Climatic Change 10 (2019).

[54] Mellaikhafi, A., Ouakarrouch, M., Benallel, A., Tilioua, A., Ettakni, M., Babaoui, A., . . . Alaoui Hamdi, M. A. (2021). Characterization and thermal performance assessment of earthen adobes and walls additive with different date palm fibers. Case Studies in Construction Materials, 15, e00693. doi: https://doi.org/10.1016/j.cscm.2021.e00693

[55] Millogo, Y., Morel, J.-C., Aubert, J.-E., & Ghavami, K. (2014). Experimental analysis of Pressed Adobe Blocks reinforced with Hibiscus cannabinus fibers. Construction and Building Materials, 52, 71-78. doi: https://doi.org/10.1016/j.conbuildmat.2013.10.094

[56] Niroumand, H. Z. M. F. M. J. M. (2013). Various Types of Earth Buildings. SBSPRO Procedia - Social and Behavioral Sciences, 89, 226-230.

[57] Picuno, P. (2016). Use of traditional material in farm buildings for a sustainable rural environment. International Journal of Sustainable Built Environment, 5(2), 451-460. doi: https://doi.org/10.1016/j.ijsbe.2016.05.005

[58] Y. Nagazaka, A. Nagashima, Simultaneous measurement of the thermal conductivity and the thermal diffusivity of liquids by the transient hot-wire method, Rev. Sci. Instrum. 52 (1981) 229–232.

[59] R. Coquard, D. Baillis, D. Quenard, Experimental and theoretical study of the hotwire-method applied to low-density thermal insulators, Int. J. Heat Mass Tran. 49 (2006) 4511–4524.

[60] A. Franco, An apparatus for the routine measurement of thermal conductivity of materials for building application based on a transient hot-wire method, Appl. Therm. Eng. 27 (2007) 2495–2504.

[61] Coquard, R., Baillis, D., & Quenard, D. (2006). Experimental and theoretical study of the hot-wire method applied to low-density thermal insulators. International Journal of Heat and Mass Transfer, 49(23), 4511-4524. doi: https://doi.org/10.1016/j.ijheatmasstransfer.2006.05.016

[62] H.S. Carslaw, J.C. Jaeger, Conduction of Heat in Solids, second ed., Clarendon Press, 1959.

[63] Miles, J. B. P. (2014). Understanding and using statistics in psychology : a practical introduction, from https://rbdigital.rbdigital.com

[64] Miles, J. B. P. (2014). "Understanding and using statistics in psychology: a practical introduction."

[65] N. Ihaddadene, R. Ihaddadene, A. Betka et al. "Study of the thermal conductivity of clay-based building materials", IAPE'19 (2019), Oxford, United Kingdom

[66] Huang, B. R. D. (2017). The Arduino inventor's guide : learn electronics by making 10 awesome projects.

[67]Ziemann, V. (2018). A hands-on course in sensors using the Arduino and Raspberry Pi.

[68] Binici, H. A. O. B. M. N. A. E. K. S. (2007). Thermal isolation and mechanical properties of fibre reinforced mud bricks as wall materials. Construction and Building Materials Construction and Building Materials, 21(4), 901-906.

[69] Ebong, S. T., Attai, E. S., & Joshua, E. O. (2016). Measurement of thermal conductivity and specific heat capacity of three major geomorphological units in Akwa Ibom State, Nigeria. British Journal of Applied Science & Technology, 12(2), 1.

[70] Ghavami, K., Toledo Filho, R. D., & Barbosa, N. P. (1999). Behaviour of composite soil reinforced with natural fibres. Cement and Concrete Composites, 21(1), 39-48. doi: https://doi.org/10.1016/S0958-9465(98)00033-X

[71] Laborel-Preneron, A., Aubert, J. E., Magniont, C., & Bertron, A. (2015). Influence of straw content on the mechanical and thermal properties of bio-based earth composites. Academic Journal of Civil Engineering, 33(2), 517-522.

[72] Farouki O. T. (1986). Thermal properties of soils. Trans Tech Publ

[73] Lertwattanaruk, P., & Choksiriwanna, J. (2011). The physical and thermal properties of adobe brick containing bagasse for earth construction. International Journal of Building, Urban, Interior and Landscape Technology (BUILT), 1, 57-6

[74] M. Rossi, V. M. Rocco,"External walls design: The role of periodic thermal transmittance and internal areal heat capacity", Energy and Buildings (2012). Vol. 68, pp. 732- 740.

[75] Asan, H. S. Y. S. (1998). Effects of Wall's thermophysical properties on time lag and decrement factor. ENERGY AND BUILDINGS, 28(2), 159-166. 034

ملخص

اليوم، يجب على مجتمعنا التعامل مع قضيتين رئيسيتين لهذا القرن: الاستنفاد التدريجي للوقود الأحفوري (الكربون والنفط والغاز والفحم)، والتي توفر حاليًا أكثر من 80٪ من الطاقات الأولية التي يتم تسويقها عالميًا، وتغير المناخ. التي تمثلها انبعاثات غازات الاحتباس الحراري التي تم تحديدها على أنها السبب الرئيسي للاحترار المناخي على مدار الخمسين عامًا الماضية، وكان هناك قلق متزايد بشأن هذه القضية. تمثل المباني 40-45٪ من استهلاك الطاقة في أوروبا والصين (وحوالي 30-40٪ على مستوى العالم). معظم هذه الطاقة مخصصة لتزويد الطاقة للإضاءة والتدفئة والتبريد والتهوية. يستهلك قطاع البناء الجزائري 34٪ من إجمالي استهلاك الطاقة النهائي في البلاد. وهو أكبر مستهلك للكهرباء في البلاد ويتناول هذا العمل للمساهمة في تقليل استهلاك الطاقة والوصول إلى الراحة الحرارية داخل المبنى ؛ أول طريقة لتقدير الطاقة الشمسية وإظهار طريقة مختلفة لدمجها في المبنى بالطريقة الثانية من خلال دراسة عينتين من التربة المستخدمة في البناء القديم ومعرفة أفضل موصلية حرارية عن طريق إضافة مادة محلية رخيصة ومتاحة

Abstract

Today, our society must deal with two major issues for this century: the progressive depletion of fossil fuels (carbon, oil, gas, and coal), which currently provide more than 80% of the primary energies marketed globally, and climate change. Which represent by Greenhouse gas emissions that have been identified as the primary cause of climatic warming over the last fifty years, and there has been a growing concern about this issue. Buildings account for 40– 45% of energy consumption in Europe and China (and about 30–40% world-wide). Most of this energy is for the supplying the energy for lighting, heating, cooling, and ventilation. Algeria's building sector consumes 34% of the country's total final energy consumption. It is the country's largest electricity consumer This work addresses to contribute to the reduce energy consumption and reach thermal comfort inside building; first way by estimating solar energy in Msila as exemple and show different way to integrate it in the building second way by studying two samples of soil used in old construction and figure out the best thermal conductivity by adding straw which is cheap, available local material

Résumé

Aujourd'hui, notre société doit faire face à deux enjeux majeurs pour ce siècle : l'épuisement progressif des combustibles fossiles (carbone, pétrole, gaz et charbon), qui fournissent actuellement plus de 80 % des énergies primaires commercialisées à l'échelle mondiale, et le changement climatique. Qui représentent par les émissions de gaz à effet de serre qui ont été identifiés comme la principale cause du réchauffement climatique au cours des cinquante dernières années, et il y a eu une préoccupation croissante à ce sujet. Les bâtiments représentent 40 à 45 % de la consommation d'énergie en Europe et en Chine (et environ 30 à 40 % à l'échelle mondiale). La majeure partie de cette énergie est destinée à la fourniture d'énergie pour l'éclairage, le chauffage, le refroidissement et la ventilation.Le secteur du bâtiment en Algérie consomme 34% de la consommation énergétique finale totale du pays. Il est le plus grand consommateur d'électricité du pays Ce travail vise à contribuer à la réduction de la consommation d'énergie et atteindre le confort thermique à l'intérieur du bâtiment; première voie par estimsting énergie solaire et montrer une manière différente de l'intégrer dans le bâtiment deuxième voie en étudiant deux échantillons de sol utilisés dans la construction ancienne et de comprendre la meilleure conductivité thermique en ajoutant de la paille qui est bon marché, matériel local disponible